

# The Halichondrins and E7389

Katrina L. Jackson, James A. Henderson, and Andrew J. Phillips\*

Department of Chemistry and Biochemistry, University of Colorado, Boulder, Colorado 80309-0215

Received January 15, 2009

## Contents

1. Introduction, Isolation, and Structure Elucidation of the Halichondrins	3044	9. Concluding Comments	3077
2. Biological Activity	3046	10. References	3077
3. Kishi's Total Syntheses of Halichondrin B and Norhalichondrin B	3046		
3.1. C1–C13 Subunit Synthesis	3048		
3.2. C14–C26 Subunit Synthesis	3048		
3.3. C27–C38 Subunit Synthesis	3049		
3.4. Halichondrin B C39–C54 Subunit Synthesis	3049		
3.5. Norhalichondrin B C39–C53 Subunit Synthesis	3051		
3.6. Subunit Couplings and Completion of the Syntheses	3051		
3.7. Subsequent Improvements by the Kishi Group	3052		
4. Total Synthesis of Norhalichondrin B by Phillips and Co-workers	3056		
4.1. C1–C13 Subunit Synthesis	3056		
4.2. C14–C26 Subunit Synthesis	3057		
4.3. C27–C38 and C40–C53 Subunit Syntheses	3057		
4.4. Subunit Couplings and Completion of the Synthesis	3058		
5. Synthetic Work toward Halichondrin B by Horita and Yonemitsu	3058		
5.1. C1–C13 and C1–C15 Subunit Synthesis	3059		
5.2. C16–C26 Subunit Synthesis	3060		
5.3. C27–C36 Subunit Synthesis	3061		
5.4. C37–C54 Subunit Synthesis	3062		
5.5. Subunit Couplings	3063		
6. Synthetic Work toward Halichondrin B by Salomon	3065		
6.1. C1–C15 Subunit Synthesis	3066		
6.2. C1–C21 Subunit Synthesis	3066		
6.3. C27–C35 Subunit Synthesis	3066		
6.4. C37–C51 Subunit Synthesis	3067		
7. Synthetic Work toward Halichondrin B by Burke	3068		
7.1. C1–C15 Subunit Synthesis	3068		
7.2. C14–C22 Subunit Synthesis	3069		
7.3. Synthesis of the C22–C34(36) Subunit	3070		
7.4. Synthesis of the C38–C54 Subunit	3072		
7.5. Subunit Couplings	3073		
8. The Discovery and Development of E7389	3073		
8.1. Preliminary SAR Studies	3074		
8.2. Synthesis and SAR of ER-076349, E7389, and Analogues	3075		
8.3. Preclinical Development	3076		
8.4. Progress toward the Clinic: Current Status of E7389	3077		

## 1. Introduction, Isolation, and Structure Elucidation of the Halichondrins

Since the initial report of norhalichondrin A in 1985, there has been substantial interest from chemists, biologists, and most recently the medical community in the halichondrin family of compounds. This interest is without doubt a combination of the chemical synthesis challenges posed by their structures, their remarkable *in vitro* and *in vivo* antitumor activities, and the potential for a therapeutic based on a halichondrin. While the area has been reviewed from several standpoints<sup>1–4</sup> over the past two decades, in this review, we endeavor to provide comprehensive coverage through the end of February, 2009.

In 1981, independent studies by Schueur and Schmitz culminated in the isolation of okadaic acid, **1** (Figure 1), the structure of which was elucidated in collaboration with Clardy.<sup>5,6</sup> This complicated polyether was isolated from two sponges, *Halichondria okadaei* Kadota, a black sponge commonly located along the Pacific coast of Japan, and *Halichondria melanodocia*, a Caribbean sponge collected from the Florida Keys.

Okadaic acid is remarkably toxic with intraperitoneal injections in mice showing the LC<sub>50</sub> to be 192 μg/kg; however, it displays no *in vivo* antitumor activity at subtoxic doses against P388 lymphocytic leukemia. In contemporaneous studies that were guided by the observation of potent *in vivo* activity of crude extracts from *Halichondria okadaei* Kadota (see Figure 4), Uemura isolated and identified norhalichondrin A (**2**) and demonstrated that this compound was the likely source of the cytotoxicity (IC<sub>50</sub> = 5 ng/mL vs B16 melanoma).<sup>7</sup>

Although a number of key features of the structure were obtained from methods such as mass spectrometry, IR, and NMR, the structure of norhalichondrin A was ultimately secured by X-ray analysis on the *p*-bromophenacyl ester (Figures 2 and 3, compound **3**). The absolute configuration determined as part of the crystallographic process was also consistent with the dibenzoate exciton chirality data for compound **4**, which showed a positive split CD. The determination of the structures of other halichondrins has subsequently been performed by careful comparison of data (especially NMR) to that for **2**.

Uemura and co-workers subsequently collected 600 kg of *H. okadaei*, and from this material, seven further halichondrins were identified.<sup>8</sup> All of the members of the halichondrin family possess an unusual 2,6,9-trioxatricyclo[3.3.2.0]decane ring system, as well as a 22-membered macrolactone ring, two exocyclic olefins, and an array of polyoxygenated pyran and furan rings that define three major classes of halichon-

\* E-mail: andrew.phillips@colorado.edu.



Katrina L. Jackson obtained her B.S. degree in biochemistry from Boston College in 2002, where she performed undergraduate research with Professor Shana O. Kelley. In 2007, she obtained her Ph.D. from the University of Colorado—Boulder under the direction of Professor Andrew J. Phillips for the total synthesis of norhalichondrin B. Currently, she is a postdoctoral researcher at Harvard University with Professor Yoshito Kishi.

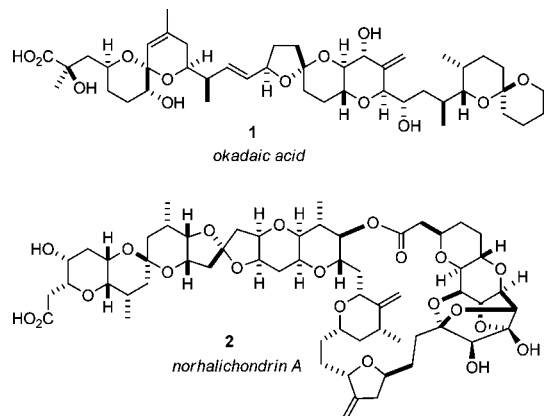


James A. Henderson received a B.Sc. in Biochemistry from Tennessee Technological University. After completing a M.S. degree in Chemistry at the same institution with Professor Jeffrey O. Boles, he moved to the University of Colorado at Boulder where he received his Ph.D. degree under the direction of Professor Andrew Phillips for the total synthesis of aburatubolactam A. In 2008, he moved to Harvard University where he is currently a postdoctoral researcher in the lab of Professor Yoshito Kishi.

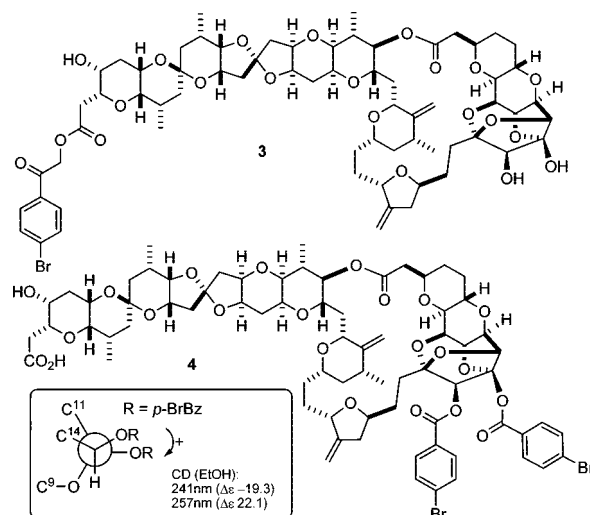


Andrew Phillips obtained his B.Sc. (Hons, 1st class) and Ph.D. degrees from the University of Canterbury in Christchurch, New Zealand. After a postdoctoral appointment with Professor Peter Wipf at the University of Pittsburgh, he joined the faculty at the University of Colorado in 2001, where he is currently an Associate Professor of Chemistry.

drins (Figure 5). The A, B, and C families differ in their degree of oxidation at C12 and C13, and within each family,



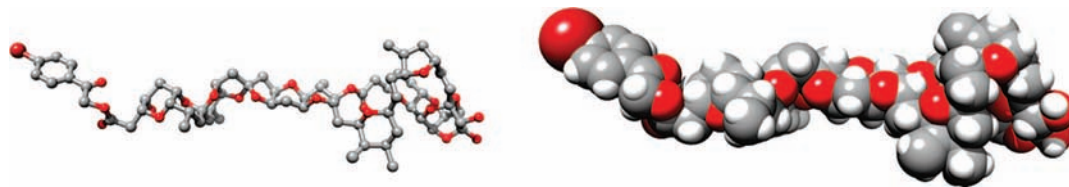
**Figure 1.** (+)-Okadaic Acid, **1**, and Norhalichondrin A, **2**.



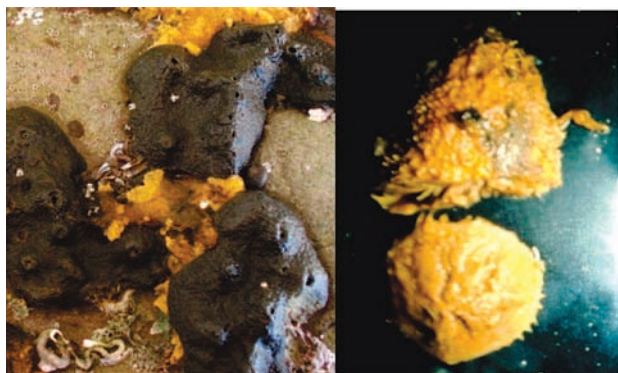
**Figure 2.** Norhalichondrin A *p*-bromophenacyl ester, **3**, and the C12–C13 bis-*p*-bromobenzoate, **4**, used for absolute stereochemical determination.

there are differences beyond the C45 position that are differentiated by the prefix, or lack thereof, before “halichondrin”.

In 1987, Blunt and Munro identified halichondrins in two unrelated New Zealand species of sponge: *Raspalia agminata* a black shallow-water sponge and *Lissodendoryx* sp. a deep water sponge.<sup>9</sup> Only trace amounts of halichondrins were detected in *Raspalia agminata*, but the *Lissodendoryx* sp. sponge, which was collected by benthic dredging at ~100 m, produced significant amounts of halichondrins. The yield from this sponge is typically 10-fold higher than any of the other halichondrin-producing sponges (~1 mg total halichondrins per kilogram of wet weight of sponge vs 0.1 mg/kg or less for other species). Bioassay-directed fractionation of the extract of *Lissodendoryx* sp. produced isohomohalichondrin B, **10**, as the major component, along with lesser amounts of halichondrin B and homohalichondrin B, **6**.<sup>10</sup> A large scale purification campaign from ~200 kg of sponge yielded three minor new compounds: neonorhalichondrin B (**8**), neohomohalichondrin B (**7**), and 55-methoxyisohomohalichondrin B (**11**).<sup>11</sup> In contemporaneous studies that were described in 1991, Pettit and co-workers reported the isolation of halichondrin B and homohalichondrin B from an *Axinella* sp. sponge that was collected in Palau.<sup>12</sup> Three new halichondrin compounds, halistatins 1, 2, and 3 (**13**, **14**, and **15**, respectively), were subsequently reported by Pettit.<sup>13</sup> These compounds are oxidized at C10 relative to other



**Figure 3.** Ball and stick (hydrogens omitted for clarity) and space-filling depictions of norhalichondrin A *p*-bromophenacyl ester, **3**.



**Figure 4.** Left image, *Halichondria okadai* (black sponge); right image, *Lissodendoryx* sp. sponges. Photos courtesy of Professor Daisuke Uemura and Professors J. W. Blunt and M. H. G. Munro.

halichondrins and were isolated from an east Indian Ocean sponge (*Phakellia carteri*), a western Indian Ocean sponge (*Axinella* sp.), and a Pacific Ocean *Phakellia* sp. sponge. The isolation of halichondrins from a variety of sponges lends credence to the possibility that these compounds are biosynthesized by sponge symbionts rather than the sponges themselves.

## 2. Biological Activity

Beyond their exquisitely complex molecular architectures, the most exciting feature of the halichondrins is the impressive biological activity that the class presents. With an  $IC_{50}$  of 0.093 ng/mL against B-16 melanoma cells, halichondrin B, **5**, was singled out as the most potent congener of the halichondrin family members isolated in Uemura studies (Table 1).

Initial biological evaluation of halichondrin B against B-16 melanoma cells, P-388 leukemia cells, and L-1210 leukemia cells resulted in dramatically increased survival times in mice. In the cases of B-16 melanoma and P-388 leukemia xenografts in mice, daily treatment with 5  $\mu$ g/kg of halichondrin B for 9 days resulted in a 2-fold improvement in the mean survival time (Tables 2 and 3). Several other dosing regimens provided comparable results, and similar results were observed with L-1210 leukemia (Table 4).

Later studies determined that halichondrin B behaves as a tubulin destabilizing agent with subtle differences in mechanism of action from those of other antimitotics such as the vinca alkaloids.<sup>14</sup> During *in vitro* studies, halichondrin blocked cells at G2/M phase of the cell cycle and disrupted normal mitotic spindle architecture through microtubule destabilization with few, if any, effects on other phases of the cell cycle. Halichondrin B, **5**, was also found to possess extraordinary *in vivo* activity against various chemoresistant human solid tumor xenografts, including LOX melanoma, KM20L colon, FEMX melanoma, OVCAR-3 ovarian, NCI H522 lung, and MDA-MB-435 breast cancers. On account of its impressive biological activity, halichondrin B, **5**, was

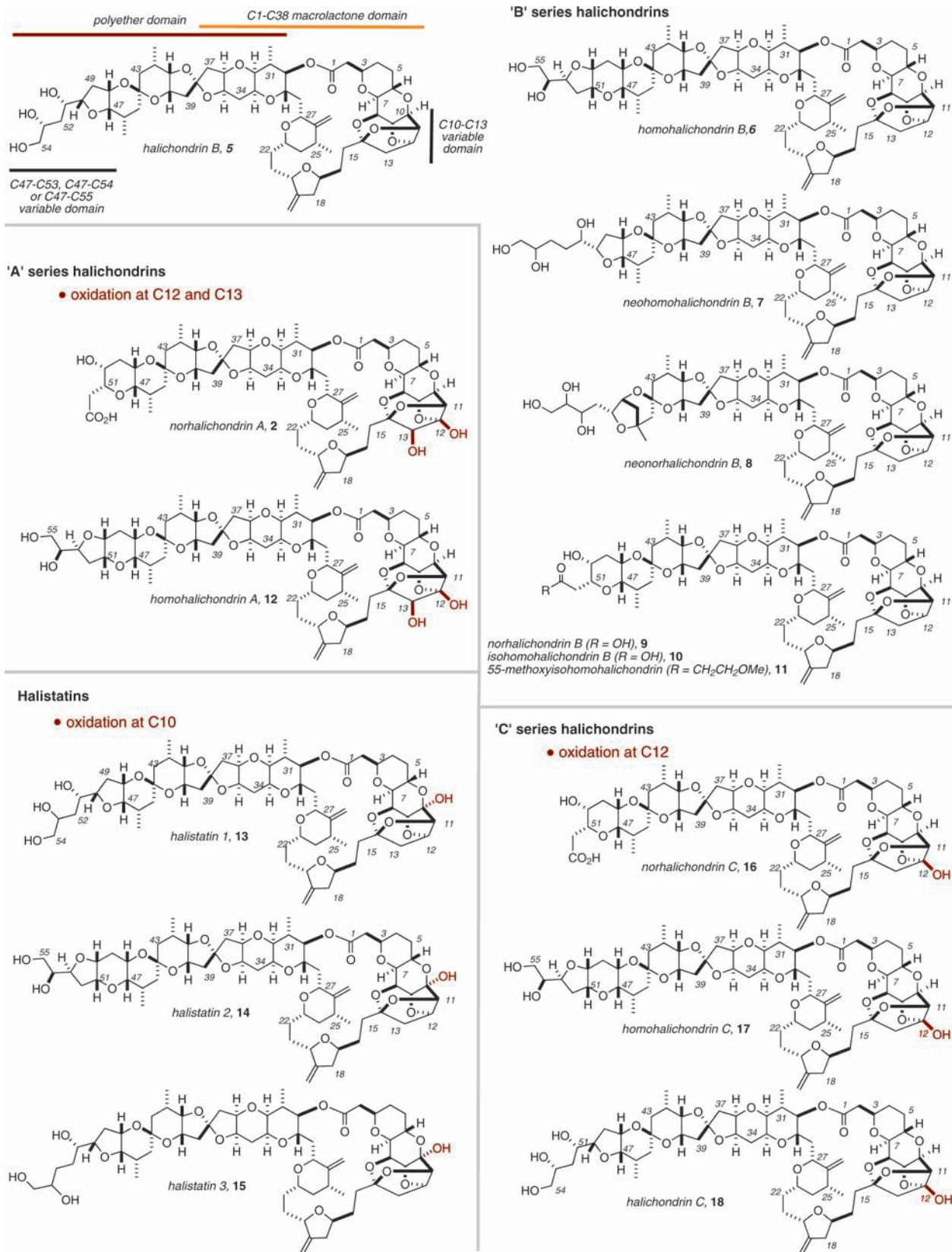
recommended by the National Cancer Institute (NCI) for preclinical trials in March 1992. However, the naturally low abundance of the molecule from natural sources rendered supply a seemingly difficult problem. From consideration of the potency of halichondrin B, **5**, *in vivo* and projection of the dose regimens for human use, the likely amount needed for preclinical trials and eventual clinical investigation would be on the order of 10 g.<sup>15</sup> Assuming success in clinical trials, the necessary commercial supply was estimated to be quite small, at around 1–5 kg/yr. Obtaining even this relatively small amount through collection from natural sources is unlikely. For example, the halichondrin-producing *Lissodendoryx* sp. sponge is a rare, deep water species found off the Kaikoura Peninsula of New Zealand. A survey of the region by remotely operated underwater vehicle (ROV) and a benthic camera gave an estimated total biomass of the *Lissodendoryx* sponge of just 200–380 t. A collection of 1 t was undertaken and from this material Blunt and Munro were able to isolate 310 mg of halichondrin B, **5**, and a comparable amount of isohomohalichondrin B, **10**. Although this campaign provided material that was sufficient for preclinical work at the NCI, it also underscored the fact that large-scale harvesting of deep sea sponges was unlikely to be a viable option for supply.

One potential source of halichondrin B, **5**, is aquaculture of the appropriate sponge genera. The New Zealand National Institute of Water and Atmospheric Research (NIWA) in collaboration with the University of Canterbury and the NCI have carried out aquaculture feasibility trials and found that the rate of production of halichondrin B, **5**, from cultured *Lissodendoryx* sp. is lower than that found in the wild sponge by approximately 30–60%. Additionally, it is estimated that approximately 1000–5000 tons of sponge/year would need to be harvested to fulfill the need should halichondrin become a marketed drug. Unfortunately, initial research in this area has produced only limited results on small-scale trials, making aquaculture a somewhat unlikely option for producing the necessary quantity of halichondrin B, **5**, at least in the near future.

At the current time, perhaps the most tractable option for a reliable source of the halichondrins is total synthesis. Nonetheless, the molecular architecture presents significant challenges to synthetic chemistry. Although three total syntheses of halichondrins have been reported, for any of them to become viable and cost-effective options, significant refinement is required. An alternative would be the identification of simplified analogues, an avenue that has received significant attention, and is discussed in section 8.

## 3. Kishi's Total Syntheses of Halichondrin B and Norhalichondrin B

In a ground-breaking piece of work, Kishi and co-workers were the first to describe total syntheses of halichondrin B, **5**, and norhalichondrin B, **9**, in 1992.<sup>16</sup> As was the case with the total synthesis of palytoxin, the Kishi syntheses of



**Figure 5.** The halichondrin–halistatin family of natural products. halichondrin B, **5**, and norhalichondrin B, **9**, underscored the utility of the Ni/Cr Nozaki–Hiyama–Kishi (NHK) reaction<sup>17,18</sup> to construct highly complex molecules. By the time the sequence was completed, this transformation had been used to forge five carbon–carbon bonds, several of which were the key bonds formed as part of subunit couplings, with good to excellent yields. Another overarching

feature of the Kishi synthesis was the use of readily accessible carbohydrate-based starting materials. The key overall strategy for halichondrin B, **5**, is shown in Figure 6. The endgame was based on the formation of the key C38–C39 bond by NHK reaction, followed by formation of the two final polyether-domain spiroketals. This analysis provided C39–C54 fragment **19**, which ultimately could be

**Table 1. Initial *in Vitro* Testing of Halichondrins Isolated by Uemura**

	IC <sub>50</sub> (ng/mL)	amount (mg) <sup>a</sup>
halichondrin B, <b>5</b>	0.0093	12.5
halichondrin C, <b>18</b>	0.35	7.2
norhalichondrin A, <b>2</b>	5.2	35.0
norhalichondrin B, <b>9</b>		4.2
norhalichondrin C, <b>16</b>		2.4
homohalichondrin A, <b>12</b>	0.26	17.2
homohalichondrin B, <b>6</b>	0.10	3.1
homohalichondrin C, <b>17</b>		2.1

<sup>a</sup> Amount isolated from 600 kg of wet sponge.

**Table 2. Halichondrin B Antitumor Activity against B-16 Melanoma *in Vivo***

dose (μg/kg)	regimen <sup>a</sup>	MST (days) <sup>b</sup>	T/C (%) <sup>c</sup>
0		16	
2.5	qd; 1–9; ip	32.5	203
5.0		39	244
0		19	
5	qod; 1, 3, 5, 7, 9; ip	37.5	197
10		39.5	208
0		18	
10	1, 5, 9; ip	36.5	203
20		39.5	219
0		17.5	
10	1, 4, 7, 10; iv	27.5	157

<sup>a</sup> Abbreviations: qd, every day; qod, every other day; ip, intraperitoneal; iv, intravenous. <sup>b</sup> Median survival time. <sup>c</sup> Test group/control group.

**Table 3. Halichondrin B Antitumor Activity against P-388 Leukemia *in Vivo***

dose (μg/kg)	regimen <sup>a</sup>	MST (days) <sup>b</sup>	T/C (%) <sup>c</sup>
0		11	
1.25	qd; 1–9; ip	15	136
2.5		16.5	150
5.0		26	236
10	qod; 1, 3, 5, 7, 9; ip	35.5	323

<sup>a</sup> Abbreviations: qd, every day; qod, every other day; ip, intraperitoneal. <sup>b</sup> Median survival time. <sup>c</sup> Test group/control group.

**Table 4. Halichondrin B Antitumor Activity against L-1210 Leukemia *in Vivo***

dose (μg/kg)	regimen <sup>a</sup>	MST (days) <sup>b</sup>	T/C (%) <sup>c</sup>
0		7	
30	qd; 1–5, 7–12; ip	10	143
50		14.5	207
70		14	200
0		8	
50	qod; 1, 3, 5, 7, 9, 11; ip	11	138
100		>30	>375

<sup>a</sup> Abbreviations: qd, every day; qod, every other day; ip, intraperitoneal. <sup>b</sup> Median survival time. <sup>c</sup> Test group/control group.

traced back to L-ascorbic acid, and macrolactone **21**. This macrolactone **21** is also common to the synthesis of norhalichondrin B, **9**. Analysis of **21** quickly leads to **22** as a key intermediate that should be readily assembled by the union of C1–C13 fragment **23**, C14–C26 fragment **25**, and C27–C38 fragment **27**. The starting materials for these three fragments are D-glucose acetonide (**24**), L-arabinose (**26**), and D-galactose glycol (**28**), respectively. A similar analysis for norhalichondrin B, **9** (Figure 7), reveals D-galactose glycol, **28**, as the starting material for C39–C53 subunit **29**.

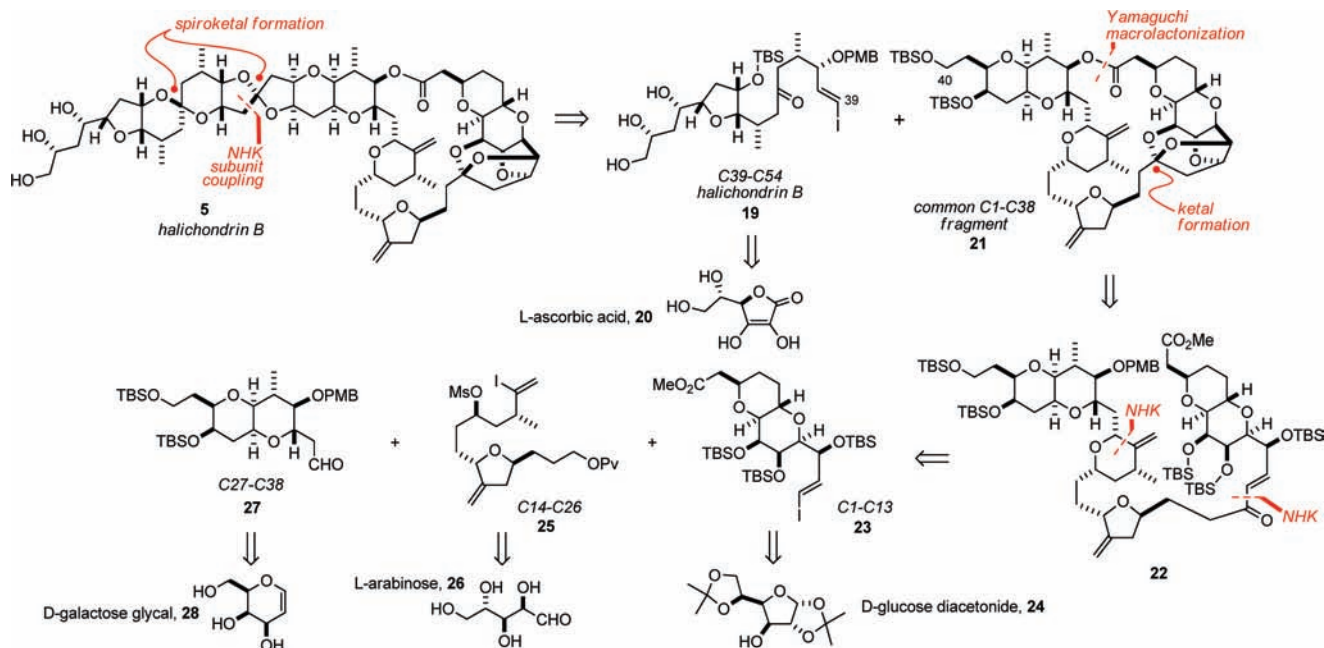
We note at the outset that since the total synthesis was published in 1992, Kishi and co-workers have continued their research and have published improved routes to several of these fragments. The first generation synthesis is presented below, and a discussion of the improved routes to various subunits is provided at the end of this section.

### 3.1. C1–C13 Subunit Synthesis<sup>19</sup>

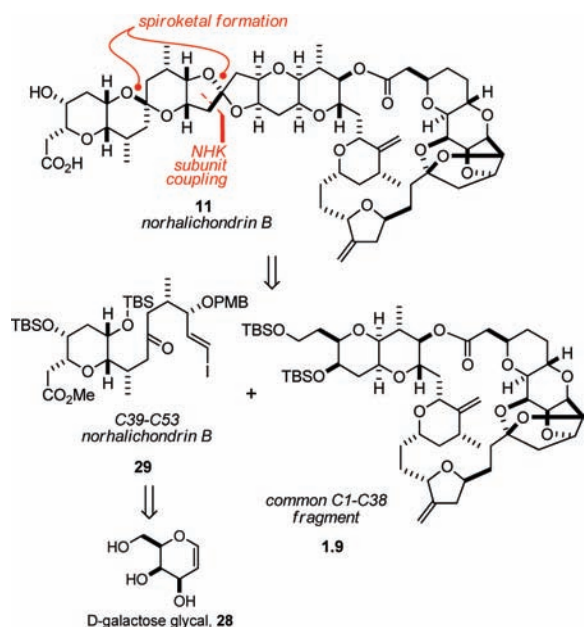
The synthesis of the C1–C13 segment commenced with D-glucose diacetonide (**24**, Scheme 1), which was oxidized to the ketone using the Omura–Swern protocol<sup>20</sup> and treated with sodium borohydride in order to provide **31**, which has the correct alcohol stereochemistry at C8. After benzyl protection, the C5–C6 acetonide was selectively removed with HCl in aqueous MeOH to give **32**. Mesylation of the diol and double displacement with KOAc, followed by acetate cleavage with sodium methoxide, provided diol **33**. Acid-catalyzed rearrangement to the pyranose and treatment with acetyl chloride and methanol provided the methyl talopyranoside **34**. After perbenzylation, exposure of **34** to allyltrimethylsilane and TMSOTf provided allyl glycoside **36**, presumably via the intermediacy of oxacarbenium ion **35**. A series of standard protecting group manipulations, oxidation reactions,<sup>21</sup> and a Wittig reaction produced α,β-unsaturated ester **37**. Removal of the acetates, followed by treatment with Triton-B methoxide, and finally benzylation of the C11 alcohol, provided the heteroconjugate addition product **38** as a 2.5:1 mixture of C3 diastereomers. This mixture of diastereoisomers could be consolidated to a single diastereoisomer, **39**, by a two-step process consisting of formation of the *p*-methoxyphenyl acetal and treatment with Triton B methoxide. After a four-step sequence of straightforward manipulations, aldehyde **40** was obtained, setting the stage for the first Ni(II)/Cr(II)-mediated reaction. When exposed to CrCl<sub>2</sub> and 0.01% NiCl<sub>2</sub> in THF, iodotrimethylsilylacetylene **41** added to the aldehyde to form **42** in 80% yield and with impressive diastereoselectivity (dr = 10:1). Kishi and Stamos have provided a rationale for this reaction that invokes a Cornforth-type model, for example, **44** → **42** compared with **45** → C11-epi-**42**.<sup>22</sup> Four additional steps were then employed to convert the TMS alkyne to vinyl iodide **23** via the intermediary of vinyl stannane **43**.

### 3.2. C14–C26 Subunit Synthesis

The synthesis of the C14–C26 segment **25** was a convergent approach based on the key union of **55** and **62** via a Horner–Wadsworth–Emmons reaction (Scheme 2). Thioacetal **46**, readily accessible in two steps from L-arabinose (**26**), was converted to **47** by removal of the acetonide and protection of the primary alcohol as the *tert*-butyldiphenylsilyl (TBDPS) ether. Treatment with I<sub>2</sub> in buffered wet acetone resulted in cleavage of the dithiane to give an intermediate tetrahydrofuran hemiacetal that was acetylated to yield **48**. A highly stereoselective oxacarbenium ion allylation with allyltrimethylsilane mediated by BF<sub>3</sub>·OEt<sub>2</sub> installed the three carbons needed for C12–C14 (**48** → **49**). Hydroboration–oxidation, protection of the resulting alcohol as the methoxytrityl ether, and removal of the acetate gave **50**. Swern oxidation, followed by removal of the monomethoxytrityl (MMTr) ether, produced hydroxyketone **51**, which was readily olefinated using the Tebbe reagent **52** to give **53**. Protecting group exchange and Dess–Martin oxidation<sup>23</sup> advanced this compound to the key aldehyde **55** via **54**.



**Figure 6.** An overview of the retrosynthesis for halichondrin B, **5**, by Kishi and co-workers.



**Figure 7.** An overview of the retrosynthesis for norhalichondrin B, **9**, by Kishi and co-workers.

The synthesis of  $\beta$ -ketophosphonate **62** commenced with pyroglutamic acid, **56**, which was reduced to the primary alcohol and protected to yield **57**. Enolate alkylation with lithium diisopropylamide (LDA)/MeI provided lactone **58**, which conveniently crystallizes from hexanes. Lactone opening with methyllithium and protection (**58**  $\rightarrow$  **59**) was followed by a Shapiro reaction with  $\text{Bu}_3\text{SnCl}$  as the electrophile. Subsequent iododestannylation gave vinyl iodide **60**. A five-step sequence produced **62**.

Fragments **55** and **62** were coupled by Horner–Wadsworth–Emmons reaction in the presence of sodium hydride, and subsequent Stryker reduction<sup>24</sup> provided saturated ketone **63**. Ketone reduction gave a 2:1 mixture of secondary alcohols **64** and **65** favoring the undesired diastereoisomer. Inversion of **64** to **65** under Mitsunobu conditions and then

ester hydrolysis allowed material of the correct stereochemistry to be pooled, and then mesylation completed the sequence.

### 3.3. C27–C38 Subunit Synthesis<sup>25</sup>

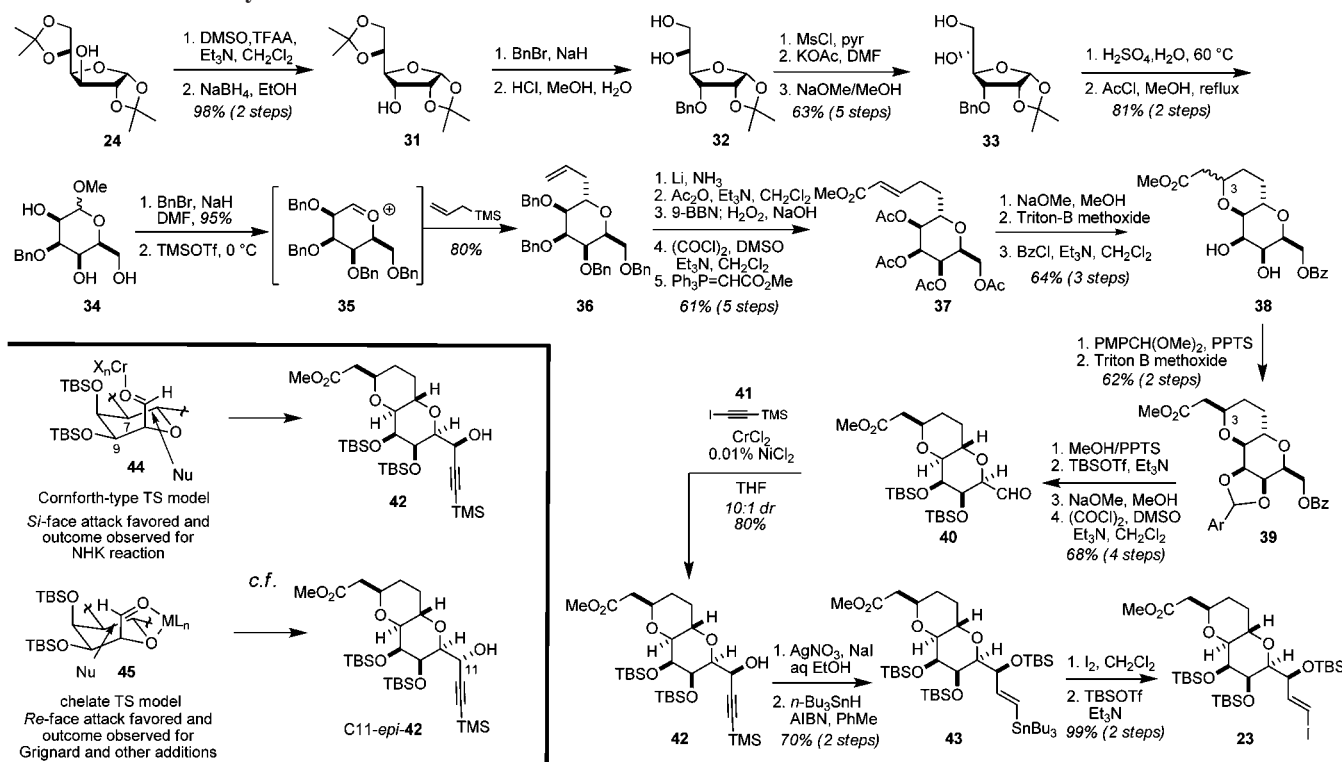
The synthesis of the C27–C38 domain began with D-galactose glycal, **28**, which was converted in a four steps to the 4-*O*-benzyl-3,6-*O*-dipropionate, **66** (Scheme 3). An Ireland–Claisen rearrangement via the intermediacy of the silylketene acetal produced **67** as an approximately 8:1 mixture of diastereoisomers. This mixture was subjected to iodolactonization followed by reductive removal of the iodide to produce  $\gamma$ -lactone **68**. At this stage, the minor isomer from the Ireland–Claisen rearrangement was removable by recrystallization. By a 10-step sequence of routine transformations, including a one-carbon homologation (**69**  $\rightarrow$  **70**),  $\gamma$ -lactone **68** was then converted into aldehyde **72**.

At this juncture, a Nozaki–Hiyama–Kishi reaction between aldehyde **72** and methyl-(*E*)-3-iodoacrylate, **73**, with  $\text{CrCl}_2$  containing 1%  $\text{NiCl}_2$  in THF was employed to form *trans*- $\gamma$ -hydroxy-acrylate, **75**, in an excellent 84% yield and with a d.r. of 2:1 (favoring the desired diastereoisomer) (Scheme 4). The diastereoisomers could be separated by repeated chromatography, and the undesired diastereoisomer **74** was easily inverted to the desired alcohol **75** by a two-step process consisting of Mitsunobu reaction with *p*-nitrobenzoic acid and methanolysis of the nitrobenzoate. Protecting group manipulations produced **76**, which, upon treatment with tetra-*n*-butylammonium fluoride (TBAF), underwent heteroconjugate addition to provide the desired pyran **77** with excellent diastereoselectivity. Four further steps were required to convert **77** into the C27–C38 aldehyde-containing **27**.

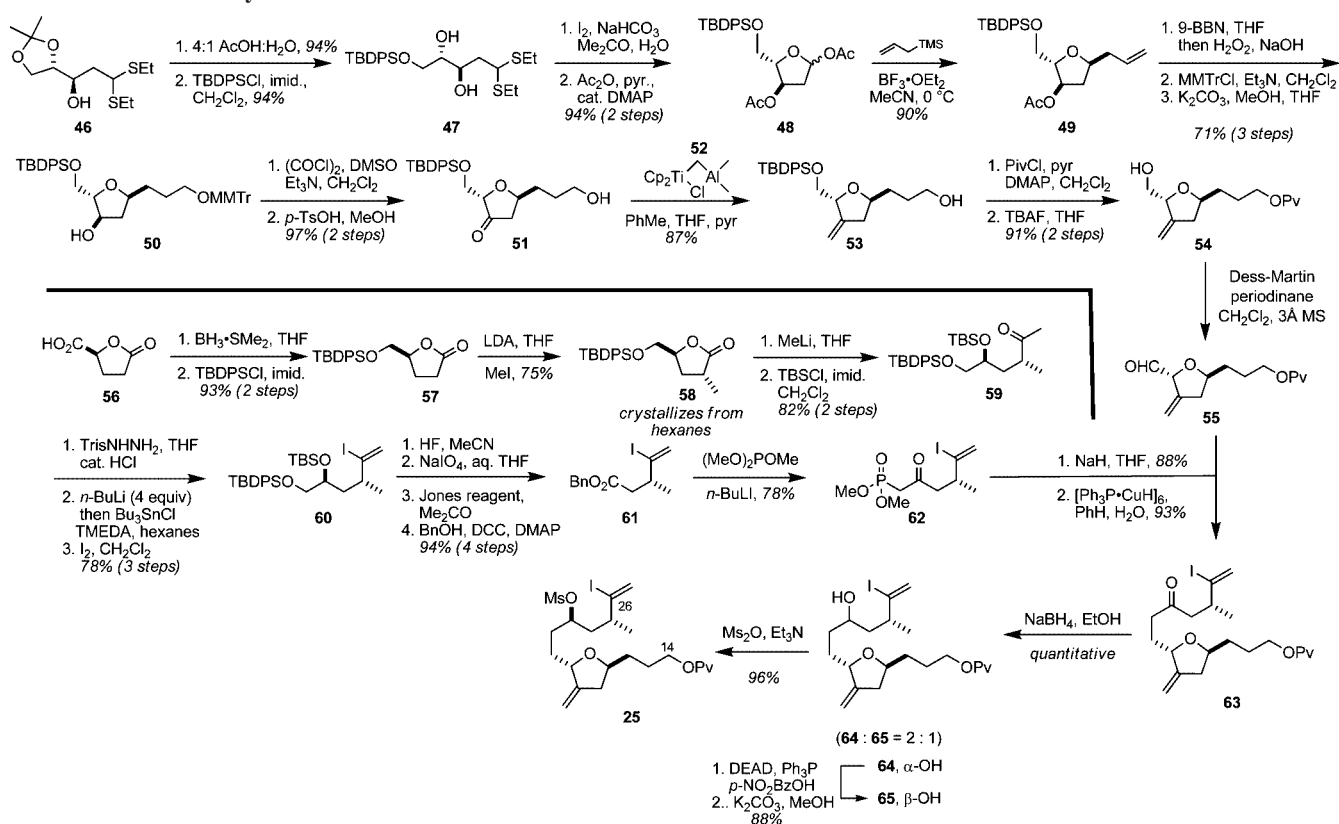
### 3.4. Halichondrin B C39–C54 Subunit Synthesis<sup>26</sup>

The C<sub>39</sub>–C<sub>54</sub> segment of halichondrin B was synthesized as shown in Scheme 5. At the time that this work was being done, there was a significant amount of ambiguity regarding

## Scheme 1. The Kishi Synthesis of the C1–C13 Subunit



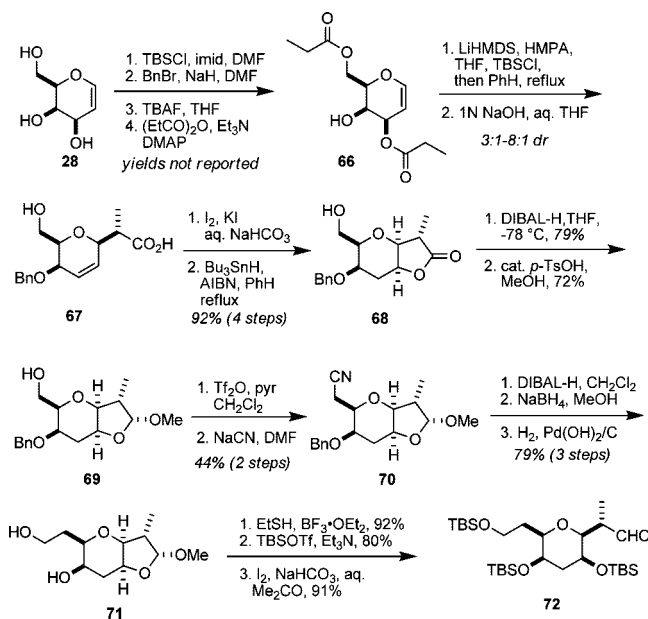
## Scheme 2. The Kishi Synthesis of the C14–C26 Subunit



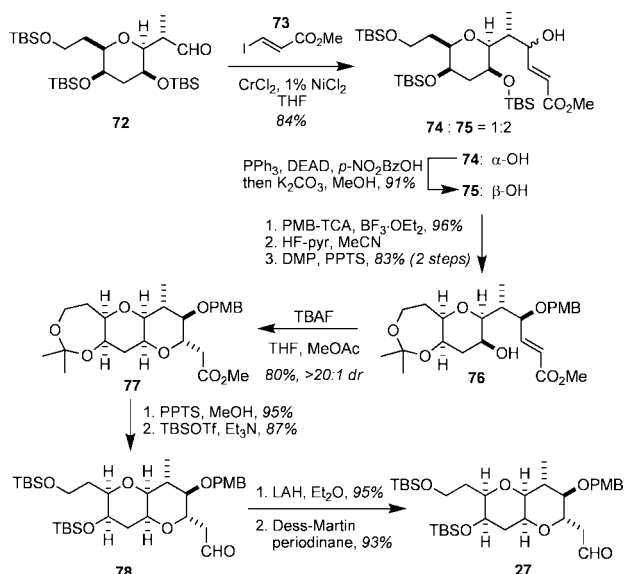
the stereochemistry of the C50, C51, and C53 centers, all of which had been assigned based on  $^1\text{H}-^1\text{H}$  vicinal couplings as well as biogenetic considerations. Therefore, the Kishi synthesis was designed specifically to address whether the assigned stereochemistry was correct and to be able to easily synthesize all possible permutations of the triol should the data not match the natural product.

Conjugate addition of methylcuprate to the  $\alpha,\beta$ -unsaturated  $\gamma$ -lactone **79** (readily available from L-ascorbic acid, **20**, in five steps<sup>27</sup>) provided **80** as a single stereoisomer in 95% yield. A standard sequence of seven steps advanced **80** to the epoxide **83**. This epoxide was coupled under Yamaguchi's conditions<sup>28</sup> with the alkynylborane derived from acetylide **84** and reduced under Lindlar conditions to provide

### Scheme 3. The Initial Stages of the Kishi Synthesis of the C27–C38 Subunit



### Scheme 4. Completion of the Kishi Synthesis of the C27–C38 Subunit

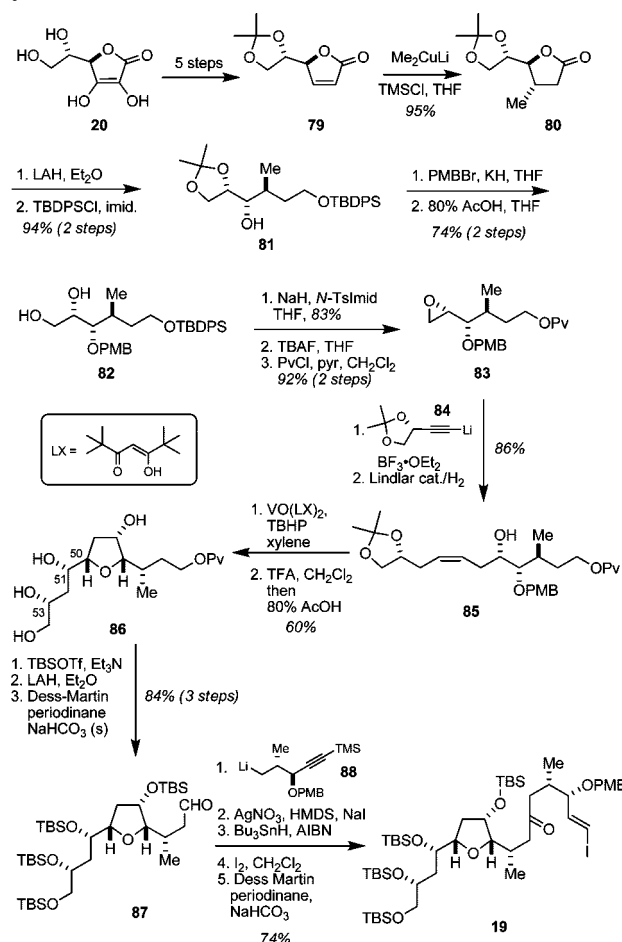


*cis*-olefin **85**. Subsequent vanadium-mediated directed epoxidation using Sharpless' protocol,<sup>29</sup> followed by acidification, furnished tetrahydrofuran **86**. Importantly, all of the other possible stereochemical combinations of C50, C51, and C53 could be accessed in similar fashion by using epoxidations of the corresponding *cis*- and *trans*-olefins prepared from acetylide **84** and its antipode. To complete the sequence, **86** was converted to aldehyde **87** in three steps, and organolithium **88** was added to the aldehyde. Removal of the silicon with AgNO<sub>3</sub>, hexamethyldisilazane (HMDS), and NaI was followed by conversion to the vinyl stannane under radical conditions. Iododesilylation and oxidation gave **19**.

### 3.5. Norhalichondrin B C39–C53 Subunit Synthesis<sup>30</sup>

The synthesis of the C39–C53 fragment of norhalichondrin B, **29**, began in a similar vein to the synthesis of the C27–C38 segment, with D-galactose glycal being converted

### Scheme 5. The Kishi Halichondrin B C39–C54 Subunit Synthesis



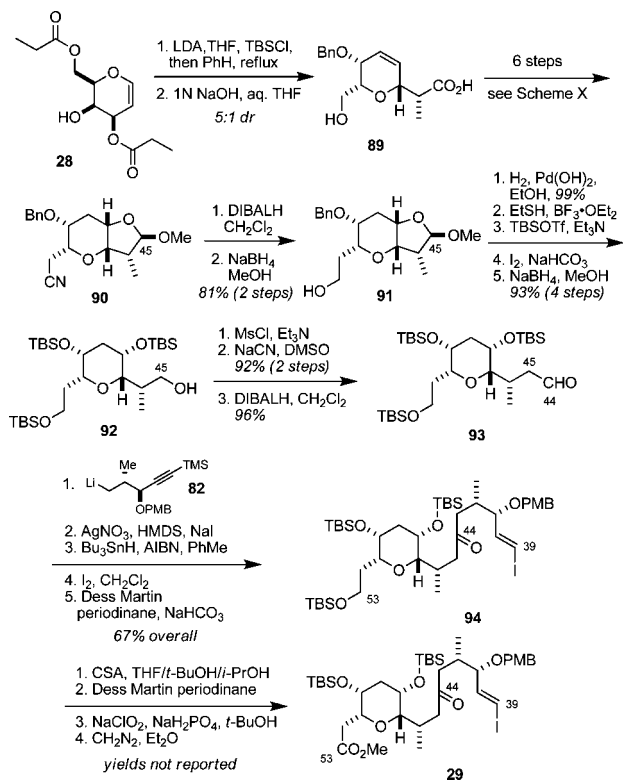
to 4-*O*-benzyl-3,6-*O*-dipropionate, **66** (Scheme 6). Ireland–Claisen rearrangement of the silylketene acetal generated in the absence of hexamethylphosphoramide (HMPA) gave **89** as the major product with 5:1 diastereoselectivity. Compound **89** was advanced to **90** by the same sequence as was used earlier (see Scheme 3). From **90**, reductions and protecting group changes gave **92**. Mesylation, homologation with cyanide, and reduction gave **93**. The same five-step sequence employed to complete the C39–C54 segment was then employed to form **94**. Lastly, the TBS-protected C53 alcohol was converted to the methyl ester in a three-step process (**94** → **29**) to complete the C39–C53 segment of norhalichondrin B.

### 3.6. Subunit Couplings and Completion of the Syntheses

The assembly of the segments of halichondrin B and norhalichondrin B to complete the total syntheses is shown in Schemes 7 and 8. In the case of halichondrin B, the first fragment coupling between **26** and **27** relied upon the use of the Ni(II)/Cr(II)-mediated coupling reaction to give **95** (d.r. = 6:1 in favor of the desired stereochemistry). Base-induced cyclization with inversion furnished tetrahydropyran **96** in 50–60% overall yield for the two steps, along with a small amount of the undesired diastereoisomer. Subsequent treatment with LiAlH<sub>4</sub> and then Dess–Martin periodinane converted the pivaloyl ester into aldehyde **97**. To effect the union of **97** and **23**, another Ni(II)/Cr(II)-mediated coupling was employed, this time resulting in an 80% yield of **98**.



### Scheme 6. Kishi's Norhalichondrin B C39–C53 Subunit Synthesis



Oxidation to the enone and treatment with 2,3-dichloro-5,6-dicyanobenzoquinone (DDQ),<sup>31</sup> followed by lithium hydroxide, cleaved the *p*-methoxybenzyl (PMB) ether and hydrolyzed the methyl ester. Subjection of the resultant seco-acid **99** to Yamaguchi conditions<sup>32</sup> allowed lactonization to form **21** in 81% yield. Formation of the trioxatricyclo-[3.3.2.0<sup>3,7</sup>]decane ring system was initiated by treatment of **21** with TBAF. Under these conditions, the TBS groups were cleaved, and the liberated C9 alcohol added the C12–C13 enone in Michael fashion to form the five-membered ring with approximately 5–6:1 diastereoselectivity in favor of the desired stereochemistry. Treatment with pyridinium *p*-toluenesulfonate (PPTS) resulted in formation of the desired polycyclic ketal **100** in an impressive 64% yield after *p*-nitrobenzoyl protection of the C38 primary alcohol. It is worth noting that the undesired Michael adduct, which did not undergo ketalization, could be separated and recycled by treatment with TBAF (equilibration to a ~5–6:1 ratio of C12 diastereoisomers occurs) and PPTS to produce further **100**. Silylation of the secondary alcohol, followed by removal of the *p*-nitrobenzoate, gave **101**.

Coupling of the common right half aldehyde with either the left portion of halichondrin B or the left portion of norhalichondrin B was accomplished with the Ni(II)/Cr(II)-mediated coupling reaction (Scheme 8). After Dess–Martin oxidation, a 50–60% yield was obtained for the coupled products **102** and **103**. In the case of halichondrin B, the synthesis was completed by treatment of **102** with TBAF to remove the TBS groups and form the hemiketal between the C48 alcohol and C44 ketone. At this point, exposure to DDQ resulted in cleavage of the PMB ether, and finally treatment with (±)-camphorsulfonic acid (CSA) resulted in spiroketal formation at C38 to give halichondrin B in 50–60% yield. An overview of the presumed intermediates in the sequence of **102** → **5** is also provided in Scheme 8. In summary,

Kishi's ground-breaking B synthesis of halichondrin B was completed by a 47-step longest linear sequence (from D-galactose gycal via **27**).

The norhalichondrin B synthesis paralleled the final steps of the halichondrin synthesis and required only one further step to complete the synthesis, the hydrolysis of the C53 methyl ester, which was readily achieved with LiOH.

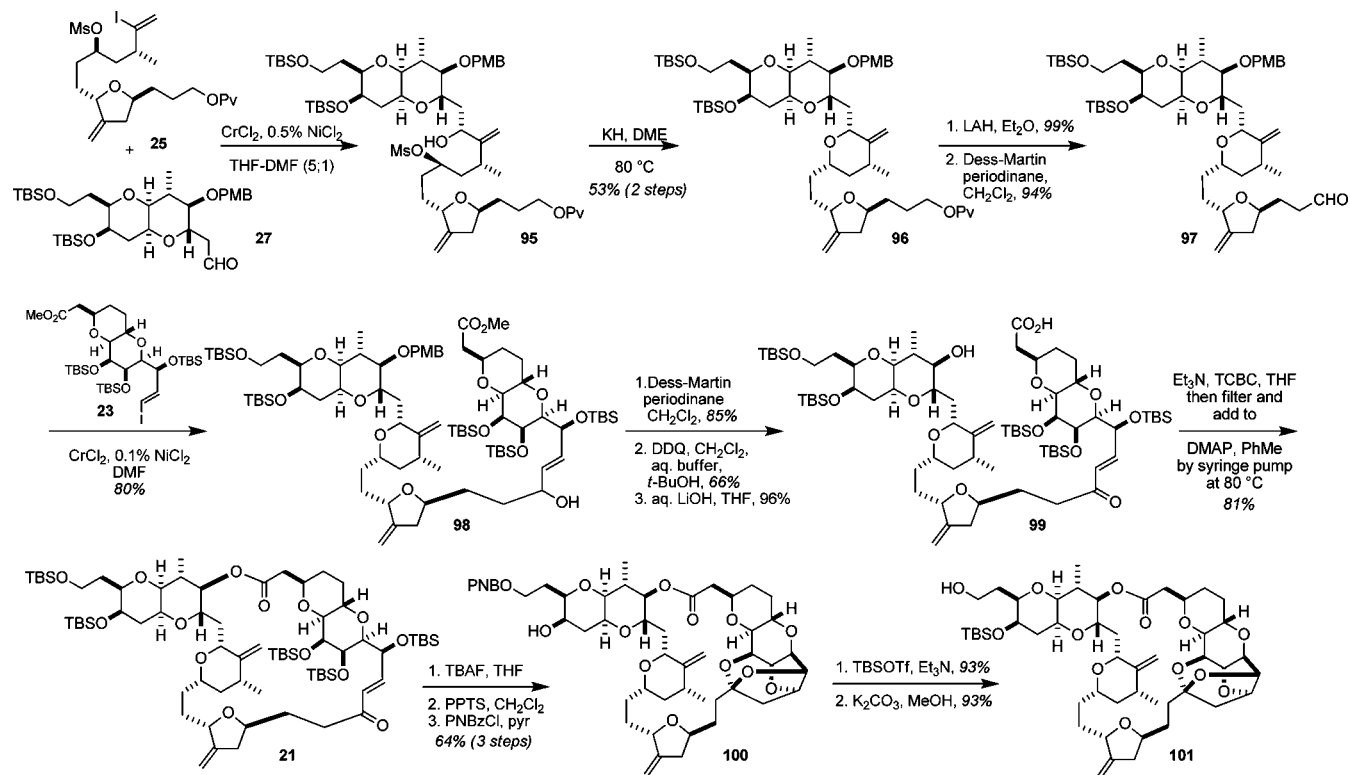
### 3.7. Subsequent Improvements by the Kishi Group

Although the chemistry by Kishi and co-workers delineated in the previous sections led to total syntheses of halichondrin B and norhalichondrin B, they have continued to refine the approach to a number of the fragments in the period since. These improvements are described below.

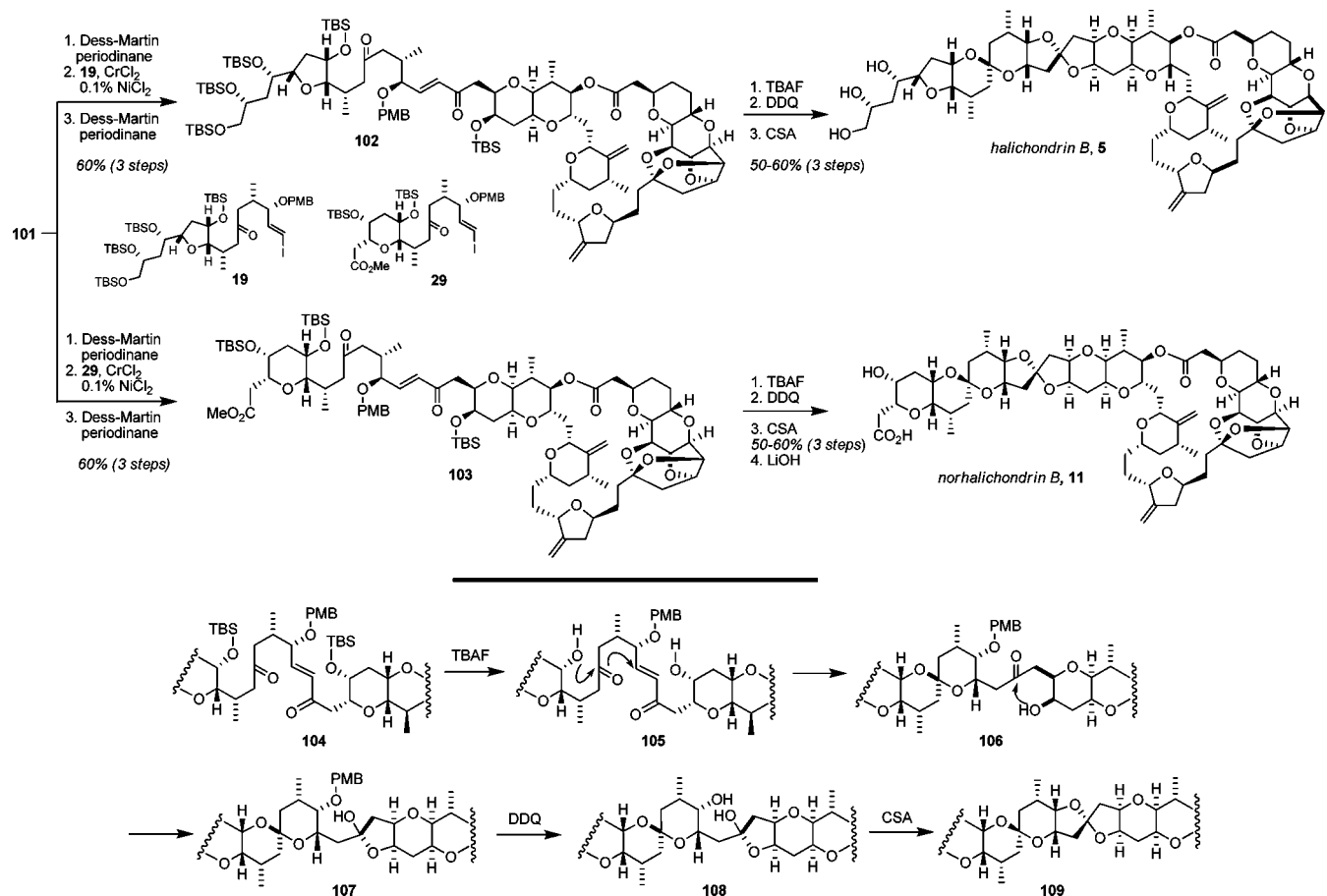
While the route to the C1–C13 subunit **23** described in Scheme 1 was relatively efficient (31 steps, 4% overall yield), a more succinct approach is shown in Scheme 9a.<sup>33</sup> This sequence commenced with L-mannonic- $\gamma$ -lactone, which possessed the appropriate stereochemistry for the C8–C11 stereocenters of halichondrin. Acetonide formation, reduction of the lactone to the C7 aldehyde with diisobutylaluminum hydride (DIBAL-H), and Wittig olefination led to methyl vinyl ether **111**. Upon treatment with osmium tetroxide followed by acetic anhydride, enol ether **111** was converted to **112** with a 16:1 preference for the desired stereoisomer. C-Allylation with allyltrimethylsilane provided exclusively the expected axial allyl glycoside **113** with a C6 configuration matching that of the natural product. Rh-catalyzed hydroboration of **113**, followed by a PCC oxidation<sup>34</sup> led to hemiacetal **114**. Subsequent Wittig olefination furnished the unsaturated ester, which underwent *in situ* heteroconjugate addition reaction to generate a 1:1 mixture of C3 epimers, which was readily equilibrated upon exposure to Triton B methoxide to yield **115**. Selective cleavage of the less hindered acetonide liberated diol **116**. Oxidative cleavage with NaIO<sub>4</sub> was followed by a Ni(II)/Cr(II)-mediated addition reaction with vinyl iodide **117** and removal of the TBS groups with FeCl<sub>3</sub>/SiO<sub>2</sub> to give **118**. Silylation, ozonolysis, and Takai reaction completed the C1–C13 domain **23**.

Due to difficulties performing the last five steps in Scheme 9a in an acceptable efficiency on large scale, an alternate route was developed. After an extensive study of the Ni(II)/Cr(II)-mediated coupling as well as some refinement throughout the sequence, a 12-step synthesis of the C<sub>1</sub>–C<sub>13</sub> segment was achieved (Scheme 9b).<sup>35</sup> L-Mannonic- $\gamma$ -lactone was again used as the starting material for the sequence, and protection of the two vicinal diols as cyclohexylidene ketals gave **119**. Reduction of **119** to the lactol followed by Wittig homologation yielded methyl vinyl ether **120**. Catalytic osmylation with the chiral ligand dihydroquinidine (DHDQ) as described by Sharpless,<sup>36</sup> followed by acetylation, provided **121** as a 4–5:1 ratio at C7. In effort to improve material throughput, functionalized allylic silane **122** was used as an allylating reagent for the C6 position and provided **123** as a single diastereoisomer. When **123** was treated with Triton B methoxide, a four-step sequence ensued that consisted of (i) cleavage of the acetate, (ii) isomerization of the olefin into conjugation, (iii) cyclization by heteroconjugate addition, and (iv) equilibration at C3 diastereoisomers. This sequence provided the desired product, **124**, in an impressive 87% overall yield. Selective hydrolysis of the cyclohexylidene ketal protecting the alcohols at C11 and C12, followed by oxidative cleavage, generated the C11 aldehyde. Ni(II)/Cr(II)-

## Scheme 7. Initial Subunit Couplings from the Kishi Synthesis of Halichondrin B and Norhalichondrin B



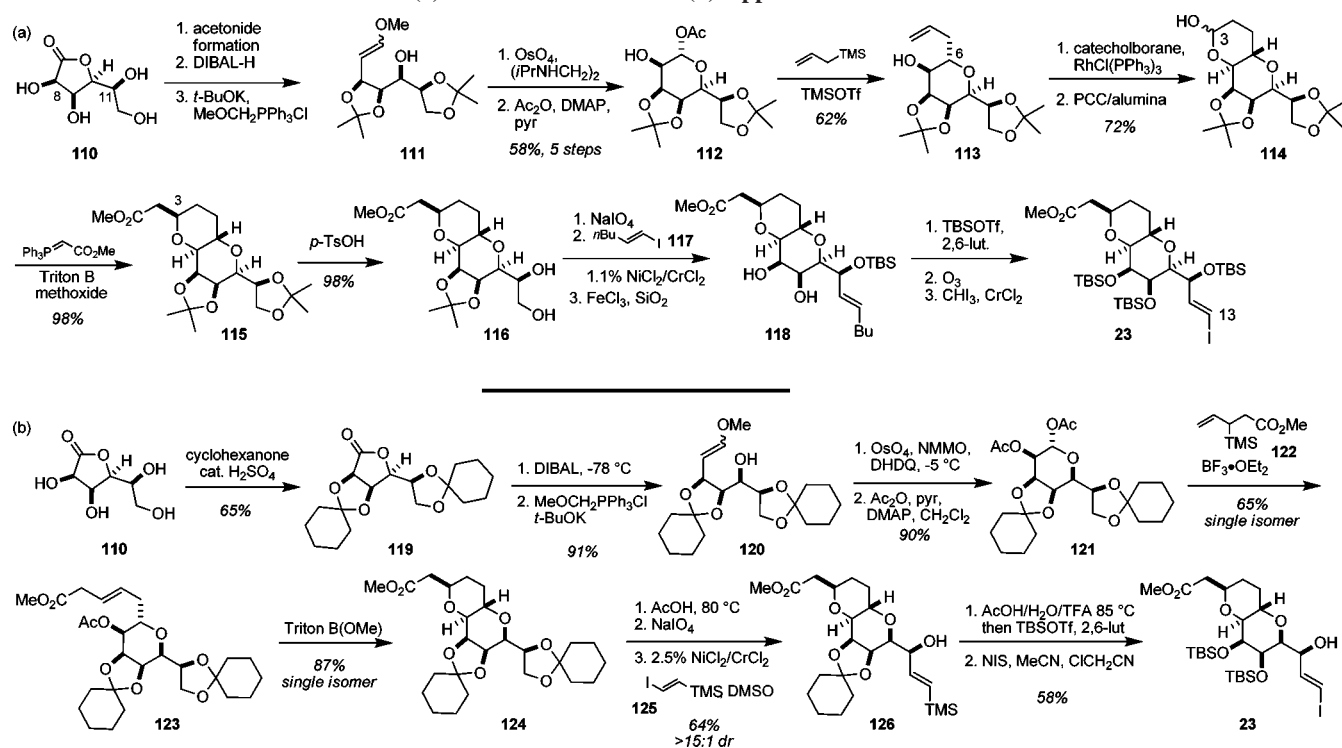
## Scheme 8. Completion of the Kishi Syntheses of Halichondrin B and Norhalichondrin B



mediated coupling using *trans*-ICH=CHTMS then produced **126** in good overall yield and with better than 15:1 diastereoselectivity at C11. It is also worth mentioning that

an improved workup for Ni(II)/Cr(II)-mediated couplings was also developed by Stamos and Kishi while optimizing this reaction.<sup>37</sup> Rather than using the commonly employed

## Scheme 9. Kishi's Second Generation (a) and Third Generation (b) Approaches to the C1–C13 Subunit



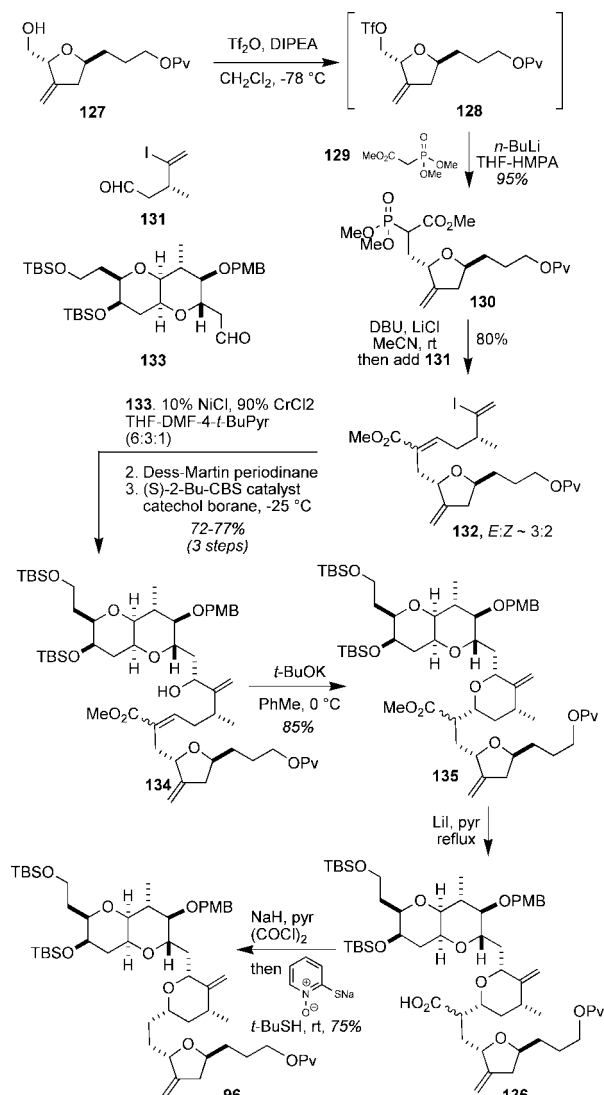
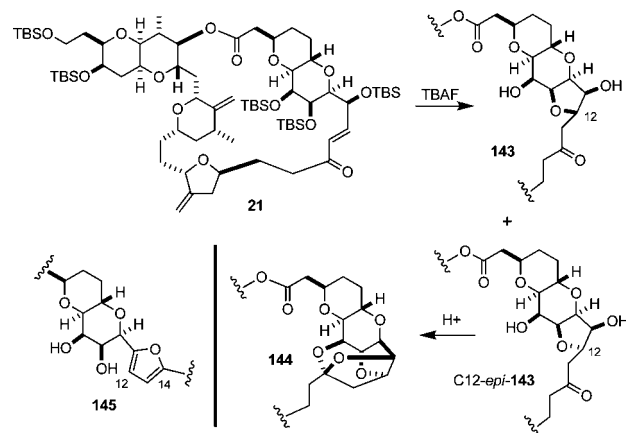
aqueous  $\text{NH}_4\text{Cl}$ , the more potent metal sequestering agent ethylenediamine was utilized, improving the yield of recovered material from 45% to 75%. Related studies also revealed the utility of 4-*tert*-butyl pyridine as a beneficial cosolvent that reduces homocoupling of the halide and also that the Na or K salts of serine can be used to facilitate workup of Ni/Cr reactions. Finally, in a one-pot reaction, the cyclohexylidene ketal of **126** was cleaved, and the resultant triol was TBS-protected. Iododesilylation with *N*-iodosuccinimide provided **23** with an 11% overall yield for the 12-step sequence.

An alternative approach to the coupling of the C14–C26 and C27–C38 domains that involves a heteroconjugate addition to establish stereochemistry at C23 has been reported (Scheme 10).<sup>38</sup> Tetrahydrofuran **127** could be activated to triflate **128** and in the same pot reacted with the anion of **129** to produce **130**. Horner–Wadsworth–Emmons reaction with **131** using the Roush–Masamune conditions<sup>39</sup> yielded enoate **132** as an inconsequential mixture of diastereoisomers. NHK reaction between **132** and **133** gave an ~4:1 mixture of diastereoisomers in 85–90% yield, and this material was converted to a 17:1 mixture of diastereoisomers by oxidation and reduction using the Corey–Itsuno system<sup>40</sup> to finally produce **134**. Conjugate addition under basic conditions gave **135**, and removal of the ester by radical decarboxylation in two further steps produced the final compound, **96**. Although slightly longer than the original approach, this route has some significant advantages with regard to stereocontrol around the C23–C27 pyran ring.

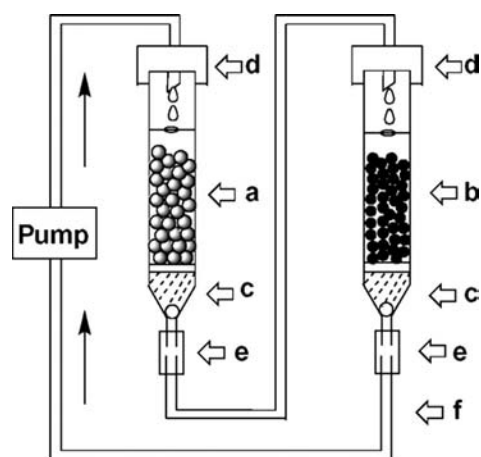
The latest synthesis of the C14–C26 segment is a concise and impressive display of the catalytic asymmetric Ni(II)/Cr(II)-mediated reaction and Co(I)/Cr(II)-mediated reaction methodology developed recently in the Kishi lab (Scheme 11). The sulfonamide ligands **139** and **142** were designed to effectively control the stereochemical course of the two reactions. Additionally, using a strategy first described by Fürstner, the NHK reaction was rendered catalytic with the

use of  $\text{TMSCl}$  (to facilitate turnover from the chromium alkoxide product) and  $\text{Mn(0)}$  (as a reducing agent for chromium).<sup>41</sup> The first bond formation of the scheme was achieved via the catalytic asymmetric Ni(II)/Cr(II)-mediated coupling of **137** and **138** in the presence of **139**. Treatment of the crude coupled product with PPTS/pyridine/isopropanol removed the resultant TMS ether formed as part of the reaction and also resulted in cyclization to form the tetrahydrofuran ring. Following debenzoylation, **140** was isolated in 80% yield. The primary alcohol was then oxidized to the aldehyde with Dess–Martin periodinane, and subsequently an asymmetric Co(II)/Cr(II)-mediated coupling was used to forge the C23–C24 bond with **141** in the presence of ligand **142**. It is noteworthy that the cobalt reaction selects for the alkyl iodide over the vinyl iodide.

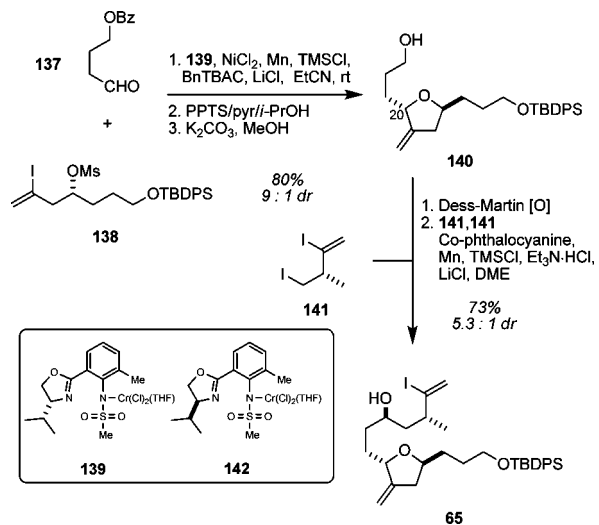
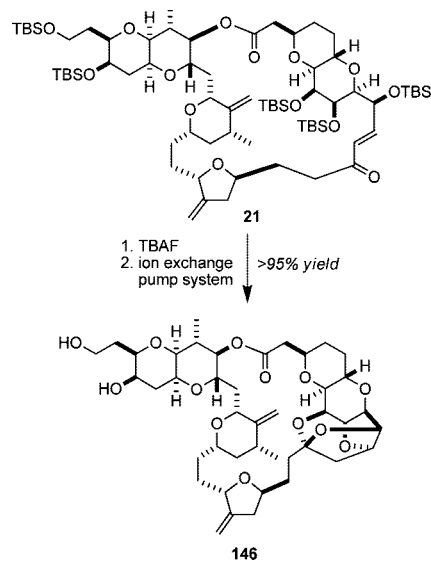
One of the key steps of the halichondrin synthesis and also the synthesis of E7389 is formation of the trioxatricyclo[3.3.2.0<sup>3,7</sup>]decane (Scheme 12). As noted earlier, treatment of **21** with TBAF results in removal of the TBS groups and heteroconjugate addition to give **143** and C12-*epi*-**143**. Subsequent acid-catalyzed ketalization provided the desired compound **144**, along with the undesired heteroconjugate addition product C12-*epi*-**143** in ratios of ~5–6:1. Separation is possible, and C12-*epi*-**143** can be recycled by treatment with TBAF and then PPTS to produce more material. In order to facilitate this process, an automated system was fabricated in which two columns were placed in sequence and connected to a pump.<sup>42</sup> The first was an Amberlite IRA 400 methoxide column, which was expected to facilitate the retro-heteroconjugate addition process, followed by a Rexyn 101 acid column, which was expected to facilitate ketal formation (Figure 8). When this system was loaded with the crude material obtained by desilylation of **21** with TBAF and circulated for a period of ~12 h, an excellent 95% yield of the desired compound **146** was obtained (Scheme 13). It is also worth noting the practical aspects of the system: for a 40 mg scale experiment,

**Scheme 10. Kishi's Heteroconjugate Addition Approach to the C14–C38 Domain**

**Scheme 12. Intermediates and Side Products in the Formation of the Trioxatricyclo[3.3.2.0<sup>3,7</sup>]decane**


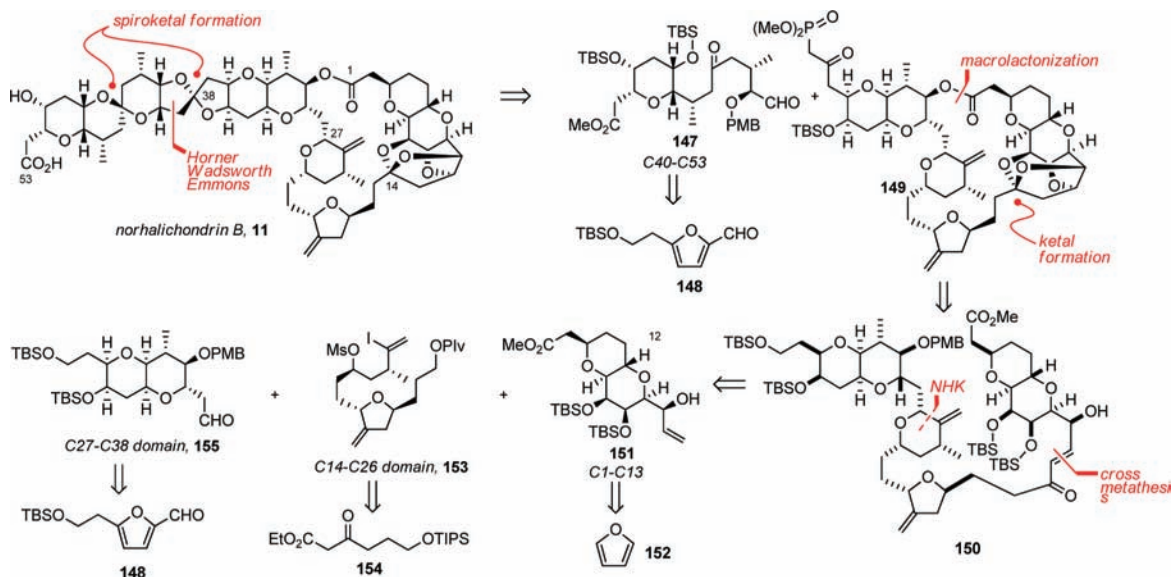
Kishi has also described an operationally simple nonaqueous workup for TBAF-mediated desilylation in the context of the formation of the polycyclic acetal.<sup>43</sup> Although framed



**Figure 8.** The Kishi ion-exchange system for formation of the polycyclic acetal: (a) Amberlite IRA 400 (OMe) column; (b) Rexyn 101 (H<sup>+</sup>) column; (c) basic Al<sub>2</sub>O<sub>3</sub> (Baker) filter with glass wool dividers; (d) septum; (e) Teflon connector tube; (f) Teflon tubing. Pump = FMI QG50. Figure taken from ref 42. Copyright 2004 American Chemical Society.

**Scheme 11. Kishi's Catalytic Asymmetric NHK and Alkyl Co Addition Reaction Approach to the C14–C26 Subunit**

**Scheme 13. Application of the Kishi Ion-Exchange System for Formation of the Polycyclic Acetal**


approximately 0.4 cm<sup>3</sup> of Amberlite IRA 400, 0.4 cm<sup>3</sup> of Rexyn 101, and 0.1 cm<sup>3</sup> of alumina were placed in each column. The total volume of solvent was ca. 4 mL (*c* = ca. 0.01 M) and the flow-rate was ca. 2 mL/min.



**Figure 9.** The Phillips strategy for norhalichondrin B with key disconnections.

in the context of halichondrin synthesis, there is no doubt that this protocol should be of much broader application. Many of the Kishi group's developments in the context of catalytic asymmetric Nozaki–Hiyama–Kishi reactions have also been framed in the context of halichondrin synthesis, and although not exhaustively covered here beyond the examples given, there is no doubt that they will have broader applications.<sup>44</sup>

Although the improvements described in this section would not affect the synthesis by the metric of longest linear sequence, they have made significant inroads into the total step count and also with regard to efficiency. Perhaps most importantly, these developments are of direct relevance to the important question of brevity in the context of E7389 (see section 8).

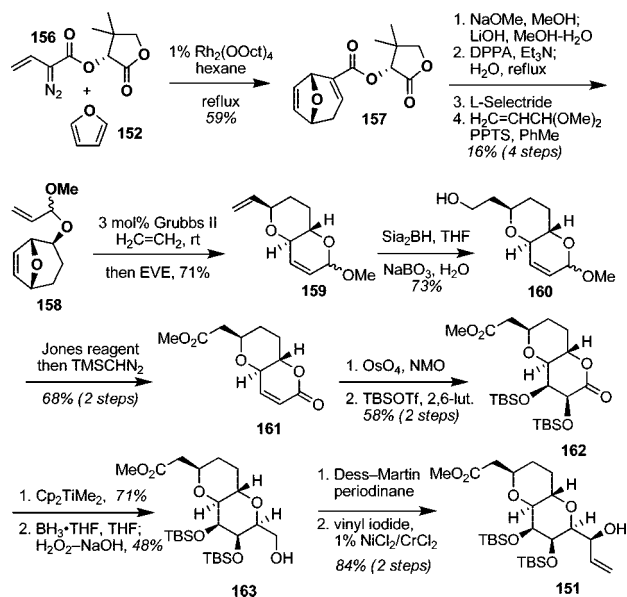
#### 4. Total Synthesis of Norhalichondrin B by Phillips and Co-workers

A second total synthesis of norhalichondrin B was reported in 2009 by Phillips and co-workers.<sup>45</sup> The overall plans for the synthesis are summarized in Figure 9. The completion of the synthesis was planned around a late-stage Horner–Wadsworth–Emmons coupling of C1–C39-containing phosphonate **149** with the C40–C53 domain aldehyde **147**, followed by spiroketal formation. The C40–C53 domain could be traced back to furfural derivative **148**. Further deconstruction of **149** via **150** yielded C1–C13 domain **151**, C14–C26 domain **153**, and C27–C38 domain **155**. The C1–C13 domain could be traced back to furan (**152**), the C14–C26 domain to  $\beta$ -keto ester **154**, and the C27–C38 domain to furfural derivative **148**.

##### 4.1. C1–C13 Subunit Synthesis

The synthesis of the C1–C13 domain commenced with the Davies Rh-catalyzed addition of diazo ester **156** to furan **152** to give oxabicyclo[3.2.1]octene **157** (Scheme 14).<sup>46</sup> This ester was advanced by a four-step sequence to **158**, and when **158** was exposed to 3 mol % of Grubbs' second generation catalyst<sup>47</sup> conversion of the bridged bicyclic structure to pyranopyran **159** readily occurred in 71% yield. Selective hydroboration of the terminal olefin with  $\text{Si}_2\text{BH}$  gave **160** and was followed by simultaneous oxidation of the acetal

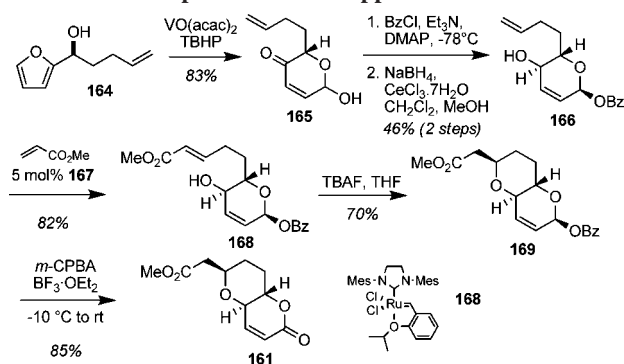
##### Scheme 14. Phillips' C1–C13 Subunit Synthesis



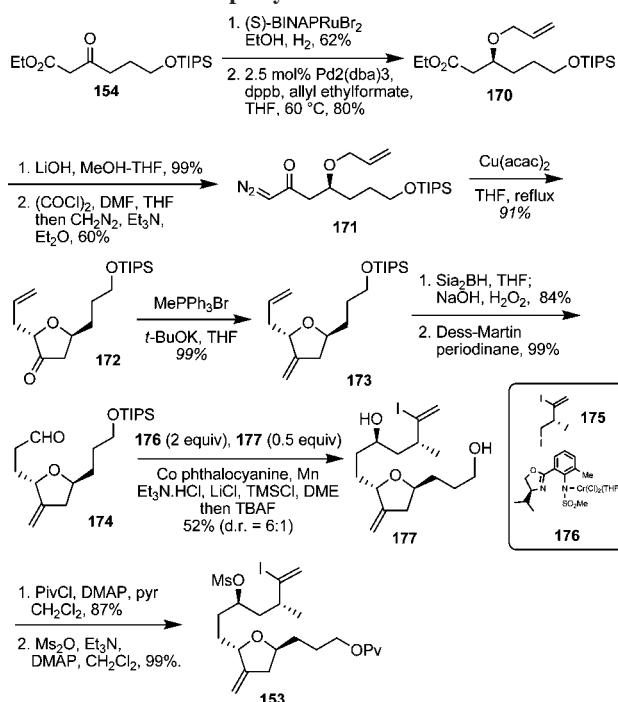
to the lactone and the alcohol to the acid, which was methylated with  $\text{TMSCHN}_2$ , producing **161**. Introduction of the C8 and C9 alcohols was achieved by dihydroxylation, and subsequent protection produced **162**. The remaining three carbons were introduced by a four-step sequence that began with selective olefination of the lactone with the Petasis reagent. Hydroboration–oxidation of the enol ether provided **163**, which was oxidized to the aldehyde and subjected to a Nozaki–Hiyama–Kishi reaction with vinyl iodide to give **151**.

An alternative sequence to this subunit that bisects the route above at compound **161** has also been described.<sup>48</sup> Furfuryl alcohol **164** (readily obtained in two steps from furfural by addition of butenylmagnesium bromide followed by Sato's kinetic resolution<sup>49</sup>) was subjected to Achmatowicz oxidation to give pyranone **165** (Scheme 15). Benzoylation, reduction, and cross metathesis with methyl acrylate in the presence of the Hoveyda–Grubbs catalyst **167** yielded **168**. The second pyran ring was formed by TBAF-induced heteroconjugate addition, and the sequence was completed by a Grieco type oxidation<sup>50</sup> to yield lactone **161**.

## Scheme 15. Phillips' Alternative Approach to Lactone 161



## Scheme 16. The Phillips Synthesis of the C14–C26 Domain



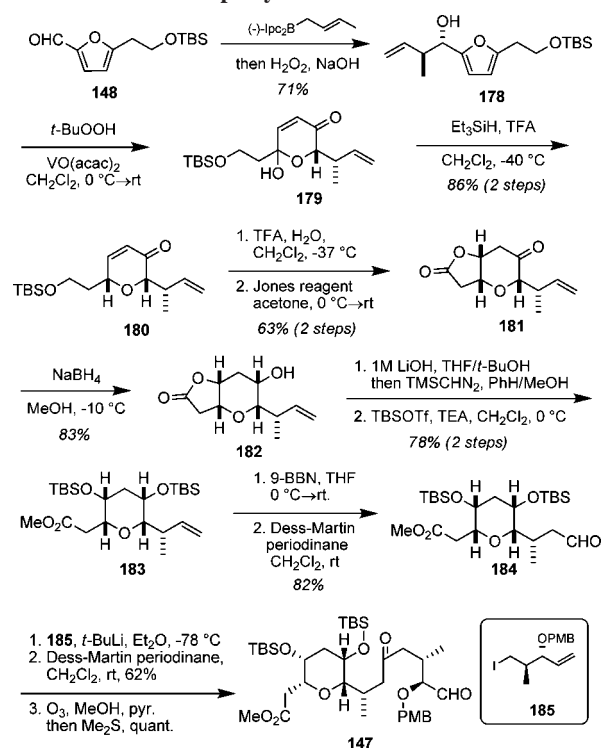
## 4.2. C14–C26 Subunit Synthesis

The C14–C26 subunit was prepared by a sequence that began with Noyori hydrogenation of  $\beta$ -keto ester **154** and subsequent Pd-mediated allylation to give *O*-allyl ester **170** (Scheme 16). This ester was readily converted to diazoketone **171** and when exposed to  $\text{Cu}(\text{acac})_2$  in THF under reflux, the expected [2,3]-rearrangement occurred to yield 2,5-*anti*-tetrahydrofuran **172**.<sup>51</sup> Wittig olefination led to diene **173**, which was selectively hydroborated with  $\text{Sia}_2\text{BH}$  at the terminal olefin. Oxidation gave aldehyde **174** and the balance of the carbons required for this subunit were introduced by the Kishi asymmetric Co/Cr addition process with **175** in the presence of **176**, which after desilylation of the product produced diol **177**.<sup>52</sup> Selective acylation of the primary alcohol with pivaloyl chloride and formation of the mesylate completed the synthesis of the C14–C26 fragment.

## 4.3. C27–C38 and C40–C53 Subunit Syntheses

The syntheses of both the C27–C38 domain and the C40–C53 domain were based around the earlier reported process for the conversion of furans to 2,6-*syn*-pyranones.<sup>53</sup> In the case of the C40–C53 domain **147**, the synthesis began with furfural **148**, which was subjected to Brown crotylation using  $(-)\text{-Ipc}_2\text{-}(E)\text{-crotylborane}$  to produce **178** (Scheme 17).

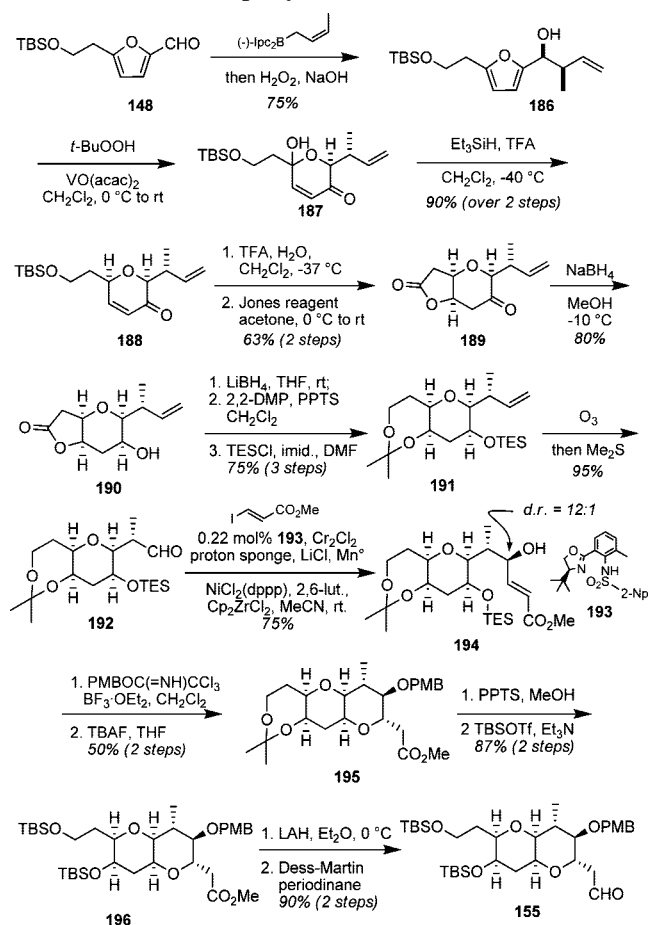
## Scheme 17. The Phillips Synthesis of the C14–C26 Domain



Achmatowicz oxidation<sup>54</sup> produced an intermediate pyranone hemiacetal **179**, which was immediately subjected to trifluoroacetic acid-mediated ionic hydrogenation using  $\text{Et}_3\text{SiH}$  to give pyranone **180** in 86% yield and as a single diastereomer.<sup>55</sup> Removal of the TBS protecting groups under acidic conditions was followed by a Jones oxidation and *in situ* heteroconjugate addition of the acid to the enone to produce pyranolactone **181**. The final pyran stereocenter was introduced by reduction of the ketone with  $\text{NaBH}_4$  to arrive at **182** and a straightforward four-step sequence advanced material to aldehyde **184**. Addition of the lithium anion derived from iodide **185**, followed by Dess–Martin oxidation, and ozonolysis of the olefin gave the fully functionalized C40–C53 domain, **147**.

Furfural **148** also served as the starting material for the C27–C38 domain **155** (Scheme 18). In this case, Brown crotylation of **148** with  $(-)\text{-Ipc}_2\text{-}(Z)\text{-crotylborane}$  gave **186** and was followed by the same general process of Achmatowicz oxidation and ionic hydrogenation to give pyranone **188** as a single diastereomer. This material was taken forward by an analogous three-step process to that employed above to produce alcohol **190**. Reduction to the triol, selective formation of the seven-membered ketal, and protection of the secondary alcohol as the TES ether gave **191**. Ozonolysis of the olefin gave aldehyde **192**, which was subjected to an asymmetric Nozaki–Hiyama–Kishi reaction with methyl-*trans*-3-iodoacrylate in the presence of Kishi's oxazoline-sulfonamide ligand **193** to give **194** in 75% yield (d.r. = 12:1). The impressive diastereoselectivity of this process meant that the tedious separation of the alcohol diastereoisomers was minimized. Protection of the alcohol as the PMB ether was followed by a one-pot, two-step process that involved removal of the TES group with TBAF and heteroconjugate addition of the liberated alcohol to produce pyranopyran **195**. Four standard transformations produced the fully functionalized C27–C38 domain, **155**.

## Scheme 18. The Phillips Synthesis of the C27–C38 Domain

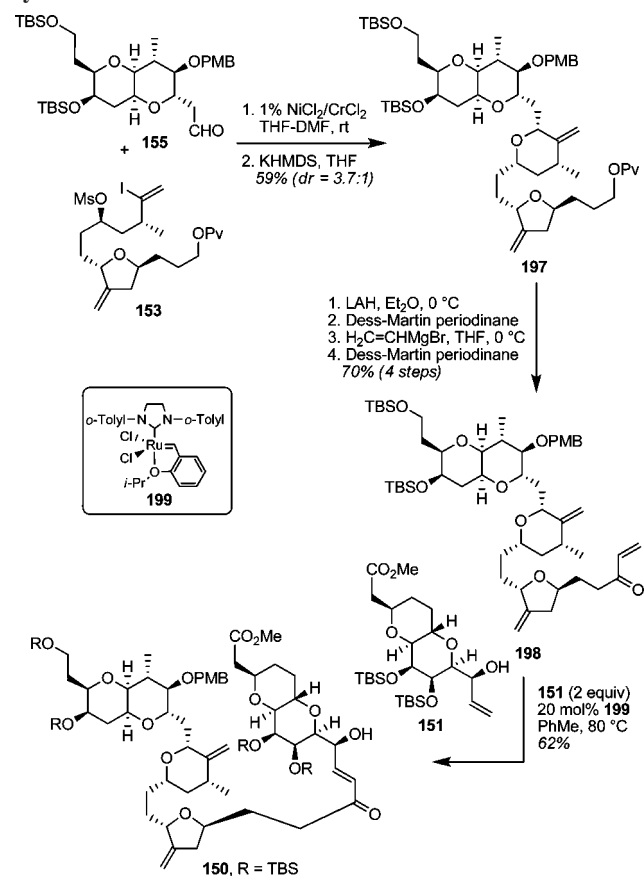


## 4.4. Subunit Couplings and Completion of the Synthesis

The first subunit coupling was the connection of pyranopyran **155** and tetrahydrofuran **153**, which were unified by the well-established combination of Nozaki–Hiyama–Kishi reaction and pyran ring formation by  $S_N2$  reaction (see Scheme 19)<sup>56</sup> to give **197** in 59% yield. The diastereoselectivity of this process was  $\sim 3.7:1$ , and although the diastereoisomers could not be separated at this point, separation was possible at the point of **202**  $\rightarrow$  **203** (see Scheme 20). A four-step sequence of (i)  $\text{LiAlH}_4$ -mediated pivalate removal, (ii) Dess–Martin periodinane oxidation, (iii) addition of vinylmagnesium bromide, and (iv) Dess–Martin periodinane oxidation provided enone **198**. At this juncture, it was possible to introduce the C1–C13 domain **151** by cross metathesis using 20 mol % of catalyst **199**<sup>57</sup> to give **150** in 62% yield.

Steps toward the completion of the total synthesis commenced with treatment of cross metathesis product **150** with AcOH buffered TBAF (Scheme 20). Removal of the silyl protecting groups and heteroconjugate addition under these conditions produced intermediate tetrahydrofuran **200**. When the reaction mixture was subjected to nonaqueous workup conditions ( $\text{CaCO}_3$ , DOWEX 50WX8-400, MeOH)<sup>58</sup> ketal formation also occurred to form the desired 2,6,9-trioxatricyclo-[3.3.2.0<sup>3,7</sup>]decane ring system directly, providing **201** in 64% yield, along with 26% of the intermediate tetrahydrofuran **200** in which the C12 stereocenter is epimeric to the desired stereochemistry. A three-step sequence of protecting group chemistry provided *seco*-acid **204**, which readily lactonized under standard Yamaguchi conditions<sup>5</sup> to give macrolactone

## Scheme 19. Initial Subunit Couplings of the Phillips Synthesis of Norhalichondrin B



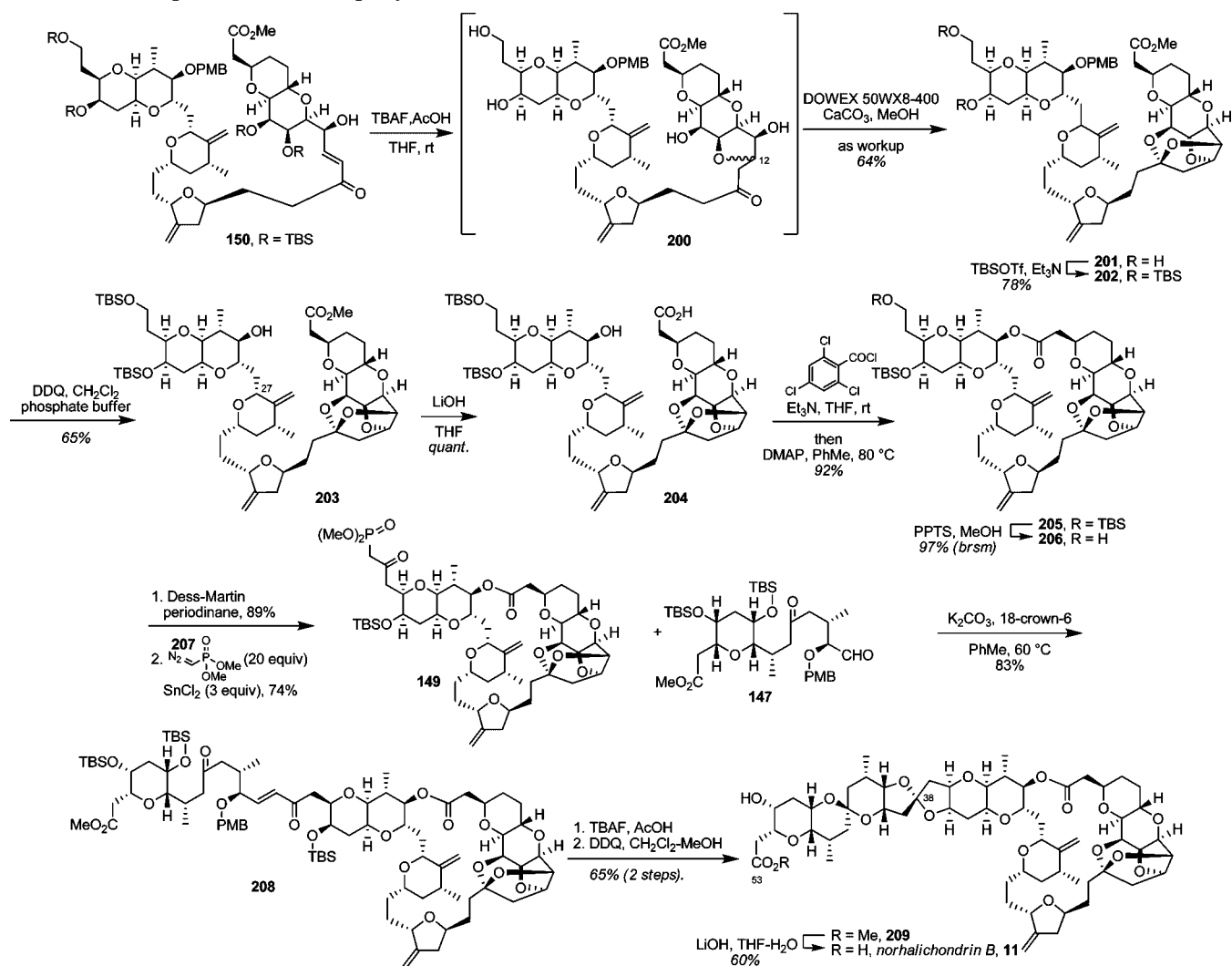
**205**. After removal of the primary TBS group (**205**  $\rightarrow$  **206**) and oxidation of the alcohol to the aldehyde,  $\beta$ -ketophosphonate **149** was formed by Roskamp reaction with dimethyl(diazomethyl)phosphonate **207** in the presence of  $\text{SnCl}_2$ .<sup>59</sup> The final subunit was then introduced by Horner–Wadsworth–Emmons coupling between **147** and **149** using  $\text{K}_2\text{CO}_3$  and 18-crown-6 in warm toluene to yield enone **208** in 83% yield. Treatment of enone **208** with TBAF resulted in removal of the silyl protecting groups to give an intermediate that contained the C44 spiroketal. In contrast to Kishi's two-step DDQ then CSA approach, the removal of the PMB ether with DDQ in  $\text{CH}_2\text{Cl}_2$ –MeOH (10:1) also resulted in direct formation of the spiroketal, yielding norhalichondrin B methyl ester, **209**. The synthesis was then completed by hydrolysis of the methyl ester to yield norhalichondrin B.

In summary, the Phillips synthesis of norhalichondrin B proceeds in 37 steps longest linear sequence from commercially available  $\beta$ -furylethanol (converted in two steps to **148**). Noteworthy features of the synthesis include the furan–pyranone and tandem metathesis strategies for the synthesis of pyranopyrans and the application of cross metathesis and Roskamp reactions on highly complex substrates.

## 5. Synthetic Work toward Halichondrin B by Horita and Yonemitsu

Along with the Kishi and Salomon groups, Horita and Yonemitsu were among the early investigators with respect to halichondrin synthesis. To date they have completed syntheses of the two advanced models that are directed

## Scheme 20. Completion of the Phillips Synthesis of Norhalichondrin B



toward halichondrin B (the macrolactone domain **210**, Figure 10, and the polyether domain **217**, Figure 11). Although a total synthesis has not been completed, the ordering of subunit assembly based on intermediates available from these studies has been proposed.

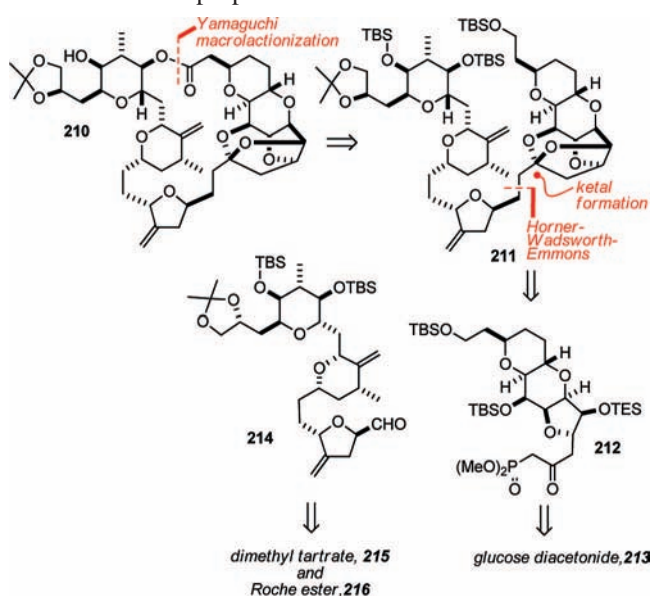


Figure 10. An overview of the Horita and Yonemitsu plans for the macrolactone domain of the halichondrins.

## 5.1. C1–C13 and C1–C15 Subunit Synthesis

The initial Horita–Yonemitsu synthesis of the C1–C13 segment was centered around the construction of pyran rings via heteroconjugate addition reactions.<sup>60</sup> The synthesis commenced with *D*-glucose diacetonide (**213**, Scheme 21), which was readily advanced by standard transformations to epoxide **223**. When **223** was exposed to acetic acid, 5-*exo* cyclization with loss of the PMP acetal occurred to provide tetrahydrofuran **224**. A series of manipulations was then used to differentially protect the C13 and C11 hydroxyl groups,

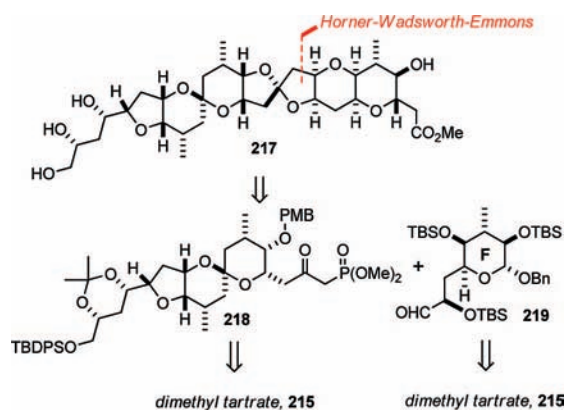
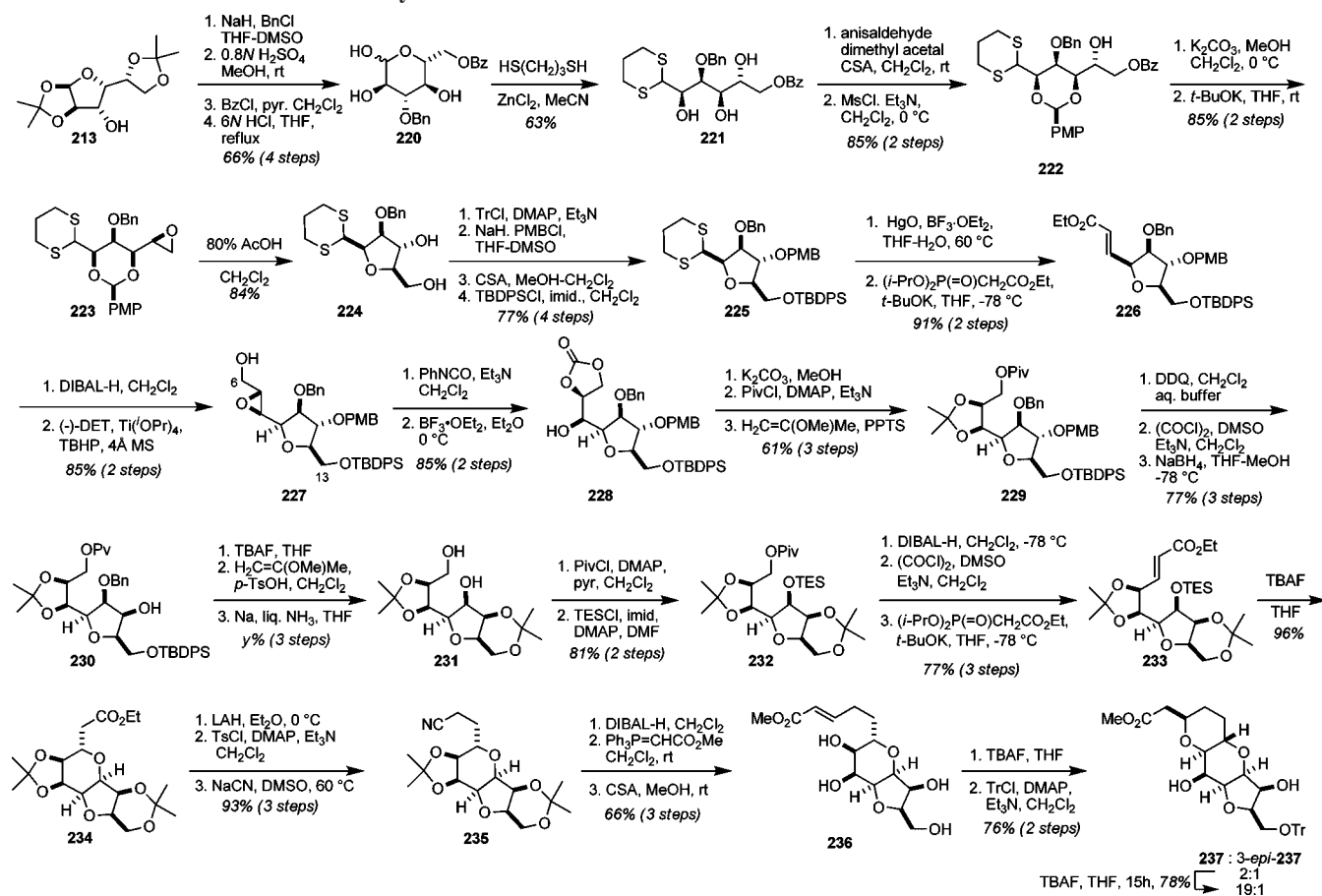


Figure 11. Horita and Yonemitsu's plans for the polyether domain of halichondrin B.



## Scheme 21. The Horita–Yonemitsu Synthesis of the C1–C13 Domain



unmask the C8 aldehyde via dithiane hydrolysis, and generate the  $\alpha,\beta$ -unsaturated enoate **226** by Horner–Wadsworth–Emmons reaction. Subsequent DIBAL reduction and Sharpless asymmetric epoxidation provided epoxide **227**, which could be ring-opened (via the carbamate using Roush’s method<sup>61</sup>) to provide **228**. A 14-step sequence of largely protecting group manipulations produced **233**, the precursor for the first pyran-forming heteroconjugate addition reaction. Treatment of **233** with TBAF resulted in TES deprotection and subsequent cyclization to form **234**. Six further steps produced **236**, which cyclized upon treatment with TBAF. After protection of the primary alcohol as the trityl ether, **237** and 3-*epi*-**237** were obtained in a 2:1 ratio. Exposure to TBAF for extended periods allowed for equilibration and produced a 19:1 ratio of the desired 2,3-*cis*- to the undesired 2,3-*trans*-disubstituted tetrahydropyrans.

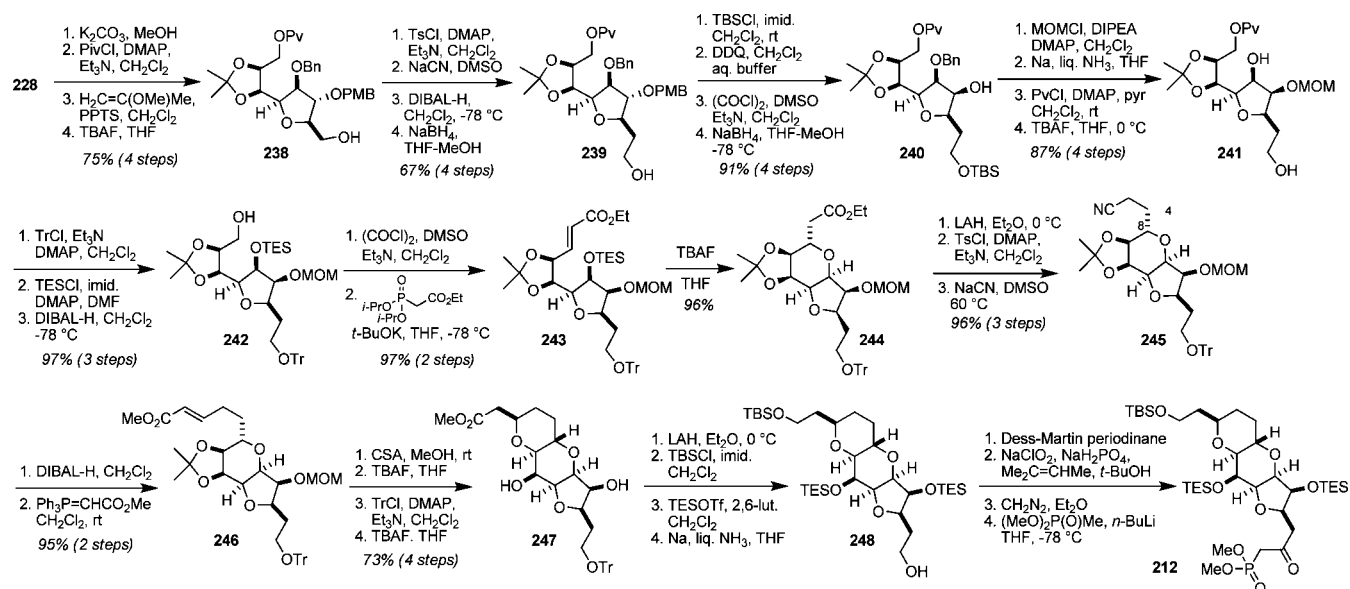
An alternative synthesis of this domain, plus a further two carbons has also been reported (Scheme 22).<sup>62</sup> It commences with tetrahydrofuran **228**, an intermediate prepared by the previous route. Protecting group manipulations provide **238** in four steps, and this allows for homologation of the primary alcohol, which is achieved by tosylation/cyanide displacement of the tosylate, and then a two-step reduction to yield **239**. A sequence of nine steps, which includes the inversion of the C7 stereochemistry by a standard oxidation–reduction protocol, led to enoate **243**, the precursor for formation of the pyran ring by conjugate addition. Desilylation with TBAF was accompanied by the desired addition, yielding **244** in close to quantitative yield. Reduction of the ester and homologation of the primary alcohol (again by tosylate formation and displacement with cyanide) provided nitrile **245**. Reduction and Wittig olefination advanced material to

**246**, which was readily cyclized to the pyranopyran by removal of the acetonides with CSA and then treatment with TBAF. Reprotection of the C14 primary alcohol as the trityl ether, and equilibration of C3 stereochemistry by treatment with TBAF gave **247**. After reduction of the ester to the alcohol and protection as the TBS ether, the introduction of the  $\beta$ -ketophosphonate was achieved by standard methods, providing **212** in six further steps.

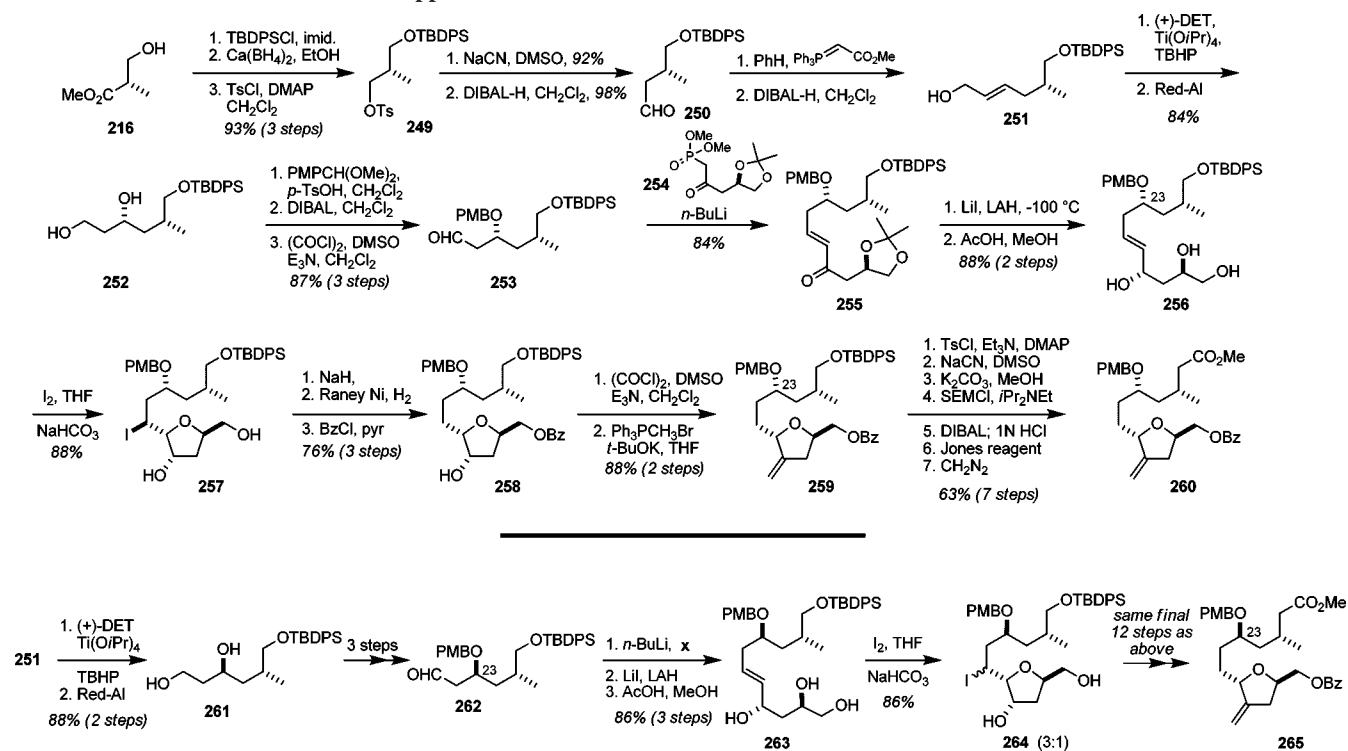
## 5.2. C16–C26 Subunit Synthesis

Because their plans for subunit coupling in the C26–C28 region centered around an aldol reaction and then pyran formation, Yonemitsu and Horita chose to prepare two C16–C26 segments, **260** and **265**, epimeric at C23 (Scheme 23).<sup>63,64</sup> This approach allowed flexibility of planning for formation of the pyran ring in either direction by either S<sub>N</sub>2-type inversion at C23 or reduction of an acetal at C27, which would be expected to provide 2,6-*syn* stereoinduction. The syntheses of both **260** and **265** began with allylic alcohol **251**, obtained in seven steps from the Roche ester, **216**. Use of Sharpless epoxidation conditions followed by Red-Al reductive epoxide opening allowed access to both C23 epimers, **252** and **261**. In the case of final target **260**, **252** was advanced by PMP-acetal formation, regioselective reductive cleavage to the C21 alcohol, and Swern oxidation to provide aldehyde **253**. Horner–Wadsworth–Emmons reaction between **253** and phosphonate **254** (derived from (*R*)-malic acid in four steps<sup>65</sup>) gave **255**. Reduction of **255** with lithium aluminum hydride in the presence of lithium iodide at –100 °C under chelation-controlled conditions<sup>66</sup> proceeded stereoselectively to give the allyl alcohol in near

## Scheme 22. Horita and Yonemitsu's Second Generation Approach to the C1–C13 Domain and Homologation to the C1–C15 Domain



## Scheme 23. Horita and Yonemitsu's Approach to the C16–C26 Subunit

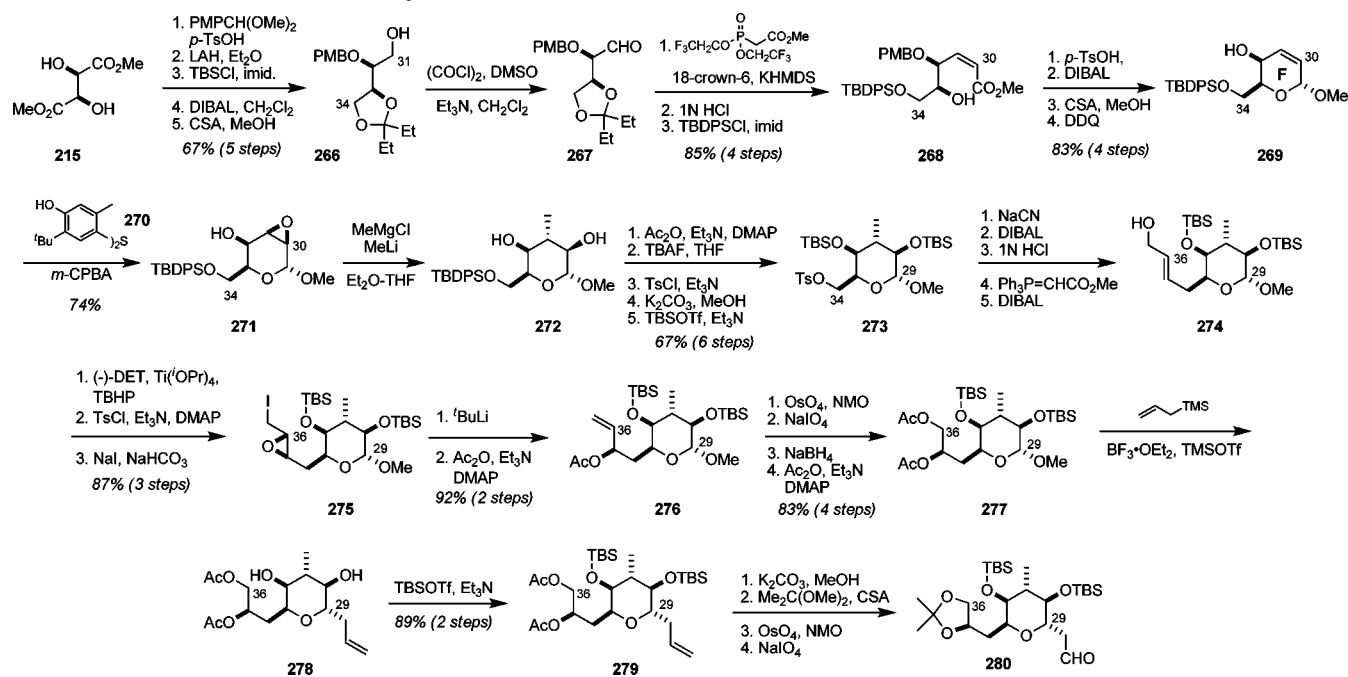


quantitative yield, and removal of the acetonide provided triol **256**. The tetrahydrofuran ring was introduced by an iodoetherification process, whereby the treatment of **256** with iodine effected a completely stereoselective iodoetherification to form **257**. Removal of the iodide by elimination to the olefin and treatment with Raney Ni/H<sub>2</sub>(g), followed by benzoyl protection of the primary alcohol, provided **258**. Swern oxidation and methylenation under Wittig conditions provided **259**, which was converted in seven further steps to the C16–C26 subunit **260**. In a similar vein, the Horner–Wadsworth–Emmons coupling between **254** and the C23 epimeric aldehyde **262** gave **263**, which was processed on via iodoetherification to the C23-epimeric C16–C26 subunit **265**.

## 5.3. C27–C36 Subunit Synthesis

The synthetic route to the C27–C36 fragment is presented in Scheme 24 and features a stereoselective C-glycosidation at C29.<sup>67,68</sup> The sequence begins with the conversion of dimethyl tartrate **215** in five standard steps to alcohol **266**.<sup>69</sup> Swern oxidation of **266**, Z-selective Horner–Wadsworth–Emmons reaction following the procedure of Still and Gennari,<sup>70</sup> removal of the ketal, and protection of the primary alcohol as the TBDPS ether furnished **268**. Exposure of **268** to *p*-TsOH provided an intermediate lactone, which was reduced with DIBAL and immediately methylated to give the methyl glycoside. Oxidative removal of the PMB ether afforded allylic alcohol

## Scheme 24. The Horita–Yonemitsu Synthesis of the C27–C36 Subunit



**269.** Epoxidation of **269** with *m*-CPBA directed by the C32 alcohol gave epoxide **271**. No epoxidation occurred in the absence of the radical scavenger **270**. Selective *trans*-diaxial opening of epoxide was achieved with a supernatant mixture of methylmagnesium chloride and salt-free methyl lithium in Et<sub>2</sub>O–THF (presumed to be “Me<sub>2</sub>Mg”<sup>71</sup>) to produce **272**. Protecting group manipulations and formation of the C34 tosylate led to **273**. C-Glycosidation with allyltrimethylsilane in the presence of boron trifluoride etherate was attempted with **273** but gave a mixture of  $\alpha$  and  $\beta$  diastereomers, necessitating postponement of the C-glycosidation for a number of steps. Conversion of **273** to allylic alcohol **274** was achieved by cyanide displacement of the tosylate and then a reduction–Wittig reaction–reduction sequence. Sharpless epoxidation, followed by opening of the epoxide by  $\beta$ -elimination and acylation introduced the C37 stereocenter (**274** → **275** → **276**), and four further steps were employed to arrive at **277**. In contrast to **273**, allylation<sup>72</sup> of **277** was completely  $\alpha$ -stereoselective and high-yielding, although it was accompanied by loss of the TBS groups, which were readily reintroduced to provide **279**. In four further steps, the protecting groups at C35 and C36 were exchanged, and the olefin was oxidatively cleaved to provide aldehyde **280**. Interestingly, Horita and Yonemitsu have reported that **280** has *in vitro* activity against KB and L1210 cells, with IC<sub>50</sub> values of 3.9 and 3.1 nM respectively.<sup>73</sup>

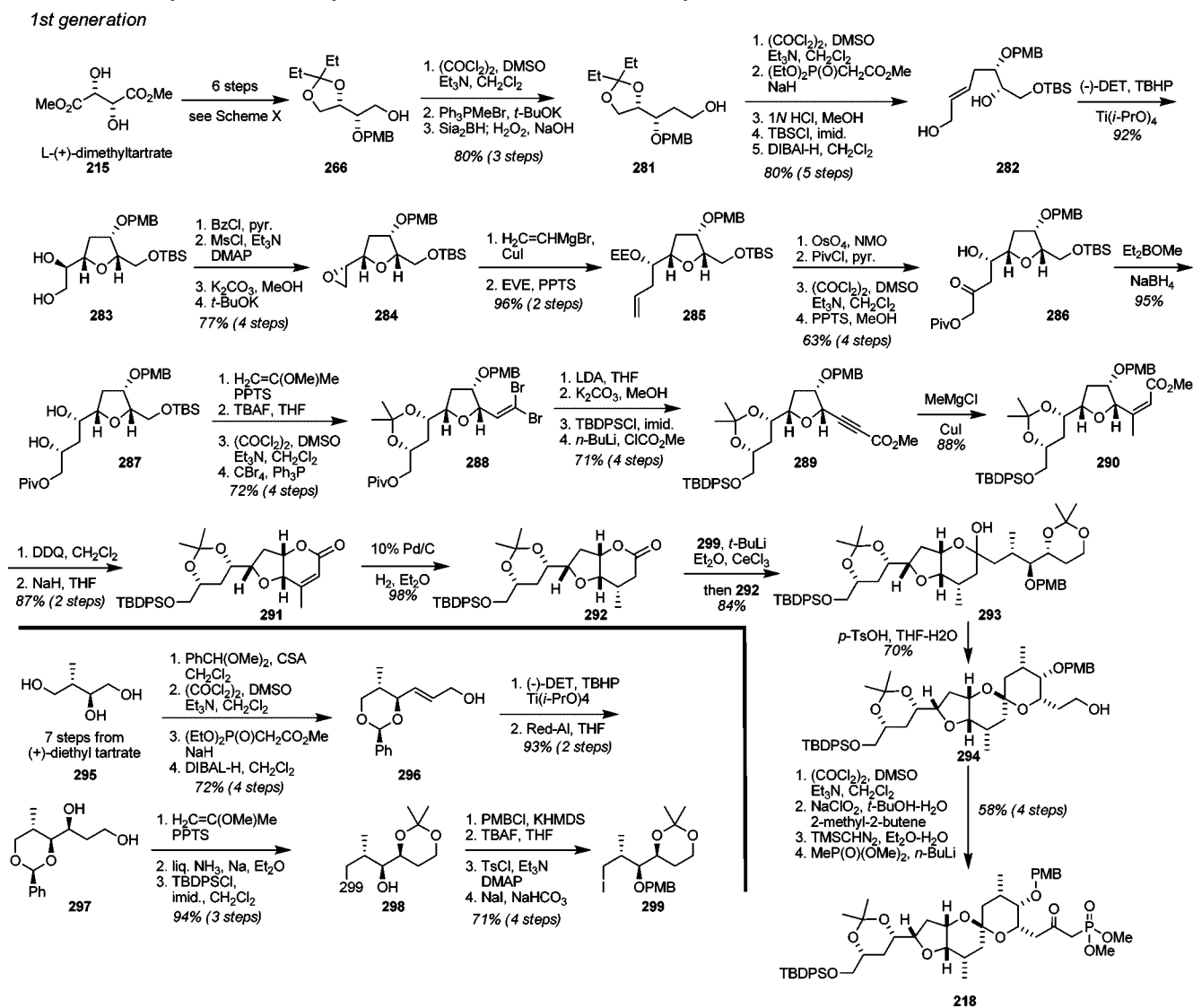
## 5.4. C37–C54 Subunit Synthesis

Two separate syntheses for the C37–C54 subunit have been reported by Horita and Yonemitsu.<sup>74,75</sup> The first synthesis began with L-(+)-dimethyltartrate, which was converted to **266** in the same fashion as was employed for the C27–C36 domain (Scheme 25). One carbon homologation produced **281**, and a sequence of five steps provided diol **282**. When **282** was subjected to Sharpless asymmetric epoxidation with (-)-DET, Ti(*i*-PrO)<sub>4</sub>, and TBHP, epoxidation with *in situ* opening of the epoxide occurred to yield tetrahydrofuran **283**. Manipulation of the diol by protection of the primary alcohol and activation

of the secondary alcohol as the mesylate allowed for conversion of **283** to epoxide **284**. Opening of the epoxide with vinylmagnesium bromide in the presence of CuI provided homoallylic alcohol **285**, which was readily converted to the C51–C54 triol domain **287** by a sequence of five steps that concluded with a Prasad reduction (**286** → **287**). Four steps advanced **287** to the germinal dibromide **288**, which was readily converted to the acetylene by treatment with LDA. Exchange of the C54 pivalate ester for a TBDPS group and formation of the alkynoic ester produced **289**. A further four steps, which included introduction of the C46 methyl group by heterogeneous hydrogenation from the *exo* face of **291**, led to key lactone **292**. This lactone was reacted with the organolithium derived from **299** (synthesized in 20 steps from (+)-diethyl tartrate as shown) in the presence of CeCl<sub>3</sub> to yield hemiacetal **293**. Simultaneous removal of the acetonide and formation of the C44 ketal was possible upon treatment with *p*-TsOH and gave alcohol **294**. Four standard transformations completed the synthesis of a C37–C54 domain that is appropriately functionalized for coupling with a C1–C36 domain.

The second synthesis of the C37–C54 domain is shown in Scheme 26 and leverages the observation that there is local symmetry in the C38–C50 region of the molecule. The starting material was again **266**, which was converted to the  $\gamma$ -alkoxy- $\alpha,\beta$ -unsaturated ester **300** by oxidation and olefination. Following Hanessian’s protocol,<sup>76</sup> lithium dimethylcuprate was used to stereoselectively afford **301** with 3,4-*anti*-stereochemistry (d.r. = 14:1). After conversion to the  $\beta$ -ketophosphonate **302**, a second enone was then installed by Horner–Emmons coupling to form **303**. The second conjugate addition of lithium dimethylcuprate without TMSCl cleanly provided the desired ketone **304** in excellent yield and with better than 25:1 diastereoselectivity. When **304** was exposed to 6 N H<sub>2</sub>SO<sub>4</sub> in THF, removal of the pentyldiene acetals and subsequent spiroketalization proceeded gradually to yield the C<sub>2</sub>-symmetrical spiroketal **305** as a single diastereoisomer in 75% yield. Three further steps

## Scheme 25. The Synthesis of a Fully Functionalized C37–C54 Domain by Horita and Yonemitsu



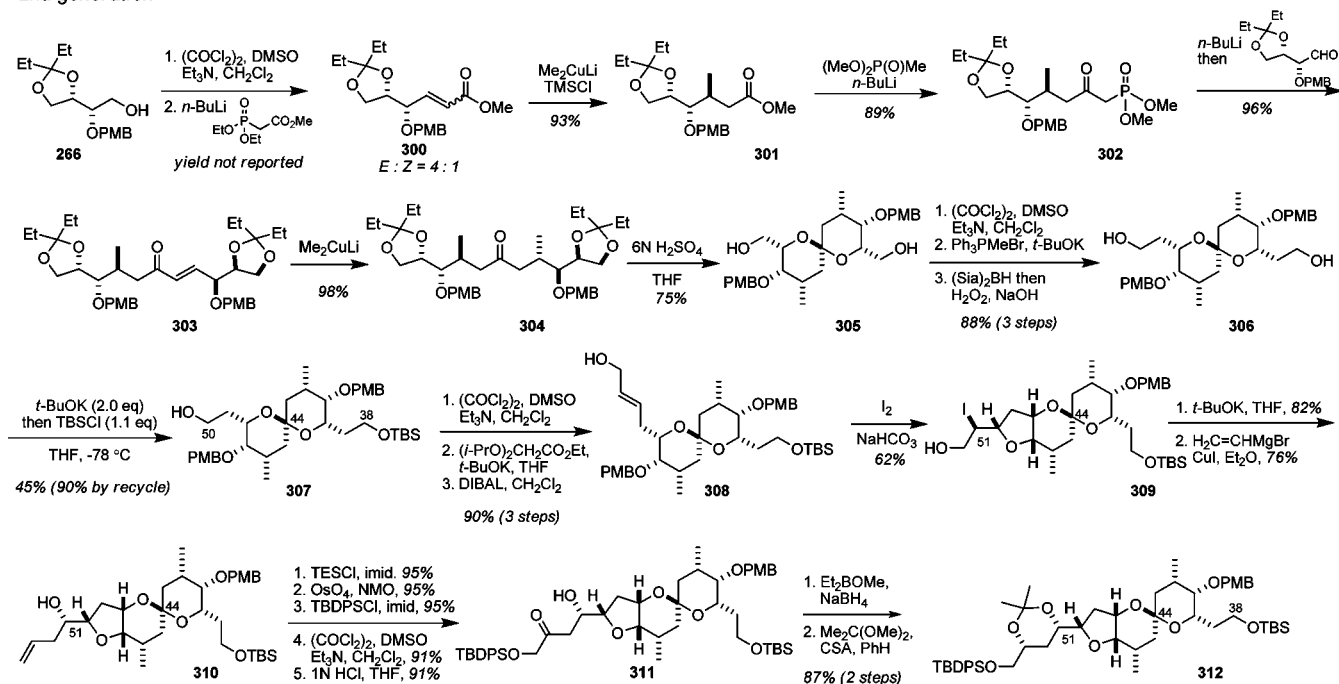
were required to effect the one-carbon homologation of the primary alcohols to yield **306**. At this juncture, desymmetrization was necessary; however all attempts to monoprotect **306** with  $\text{TBSCl}$  following known literature procedures met with failure. However, when the dipotassium salt of **306** (generated with 2.0 equiv of  $t\text{-BuOK}$  in  $\text{THF}$  at  $-78^\circ\text{C}$ ) was trapped with 1.1 equiv of  $\text{TBSCl}$ , the desired mono-protected silyl ether **307** was obtained in 45% yield with only a trace of the disilyl ether. Furthermore, the unreacted diol could be recovered chromatographically and resubjected to the reaction conditions to give 90% yield of **307** through three recycles. Three further steps converted alcohol **307** to allylic alcohol **308**, and when treated with iodine in the presence of  $\text{NaHCO}_3$ , **308** underwent iodoetherification to provide the tricyclic iodohydrin **309** as a single diastereoisomer. Subsequent exposure to potassium *tert*-butoxide afforded the epoxide, which was then opened with vinylmagnesium bromide in the presence of copper(I) iodide to give **310**. In five conventional steps, **310** was converted to  $\beta$ -hydroxy ketone **311**, which was reduced under Prasad conditions<sup>77</sup> and protected to form **312**. Five more steps were required to form phosphonate **218** from **312** (see Scheme 25).

## 5.5. Subunit Couplings

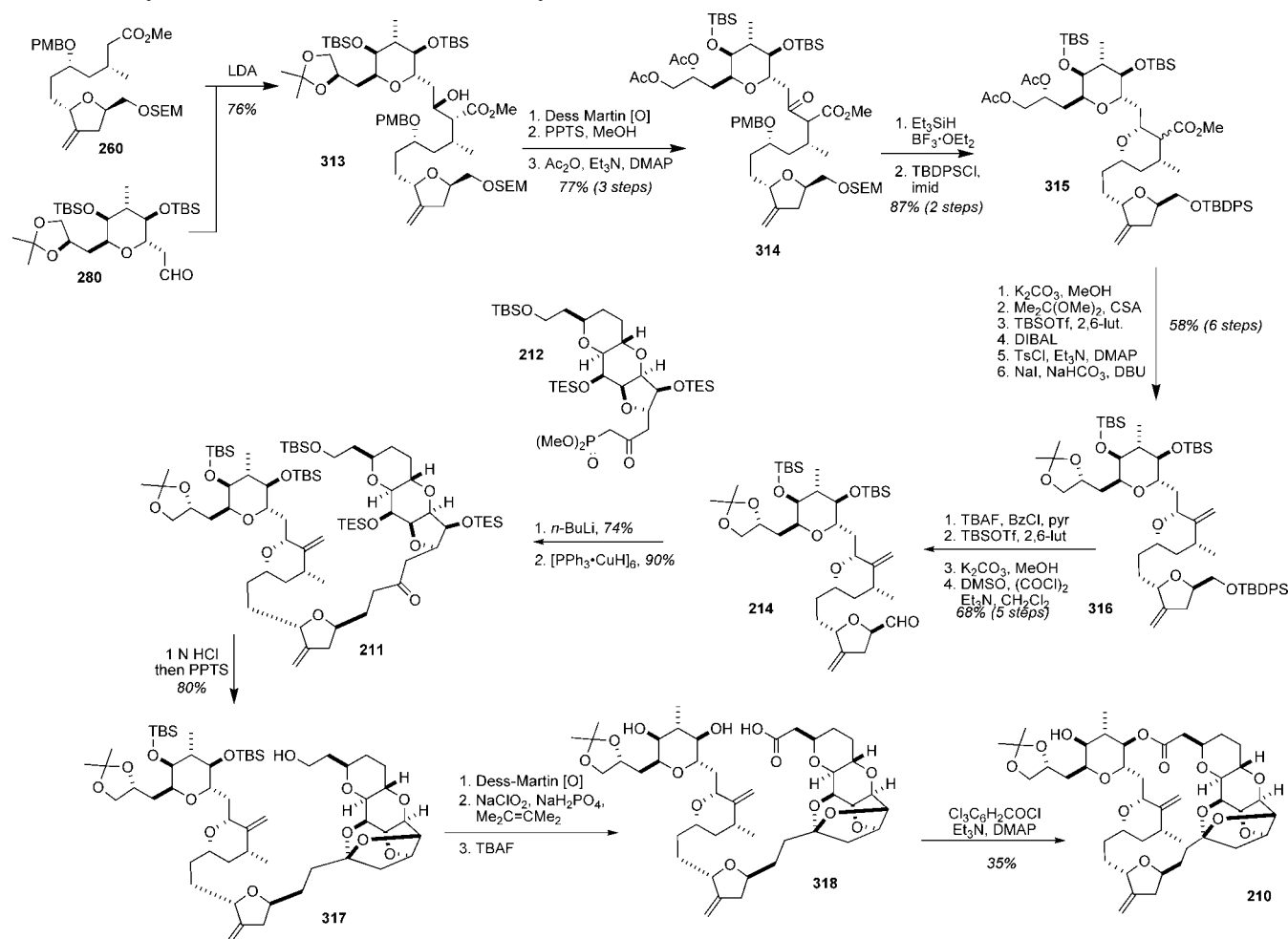
Although a total synthesis has not been reported, Horita and Yonemitsu have undertaken studies on key subunit couplings, and the products of these studies are completed syntheses of both the right-hand macrolactone **210** and the left-hand polyether **217**. In the context of the synthesis of the macrolactone, the first subunit coupling examined was the connection of the C27–C36 and C16–C26 subunits.<sup>78</sup> Deprotonation of **260** with  $\text{LDA}$  and aldol reaction with **280** proceeded smoothly and stereoselectively to afford adduct **313** (Scheme 27). Dess–Martin oxidation of the resultant secondary alcohol and protecting group exchange at the C35/C36 1,2-diol (acetone  $\rightarrow$  acetates) provided **314**. Treatment of **314** with  $\text{Et}_3\text{SiH}$  in the presence of  $\text{BF}_3 \cdot \text{OEt}_2$  resulted in a sequence of events that included removal of the  $\text{PMB}$  ether, oxocarbenium ion formation and reduction, and also removal of the  $\text{SEM}$  ether. After protection of the primary alcohol as the  $\text{TBDPS}$  ether, **315** was obtained in an excellent 87% yield. After the C35 and C36 acetates were replaced by an acetonide, the ester at C26 was converted to the olefin in three routine steps (**315**  $\rightarrow$  **316**). In five additional steps, the  $\text{TBDPS}$  protected alcohol **316** was converted to aldehyde **214**. Horner–Wadsworth–

## Scheme 26. Horita and Yonemitsu's Second Generation Synthesis of the ~C37–C54 Domain

2nd generation



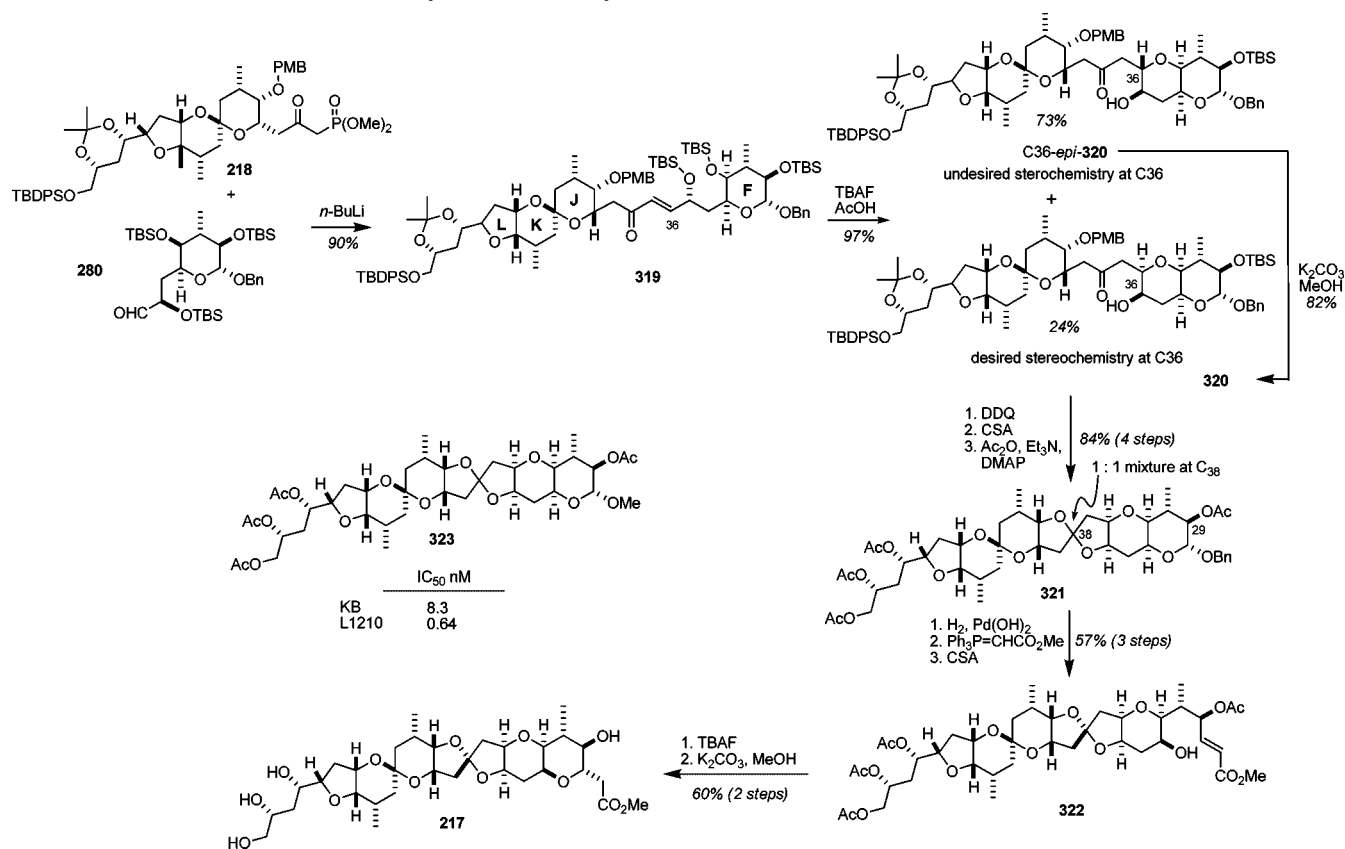
## Scheme 27. Synthesis of the Macrolactone Domain by Horita and Yonemitsu



Emmons reaction between **212** and **214**, followed by Stryker reduction of the resultant enone, provided **211**. Careful treatment of **211** with 1 N HCl deprotected selectively the

C8 and C11 TES groups and the C1 primary TBS group. Under these conditions, the C28 and C30 secondary alcohols remained TBS protected. Exposure of the resultant triol to

## Scheme 28. Horita and Yonemitsu's Polyether Domain Synthesis



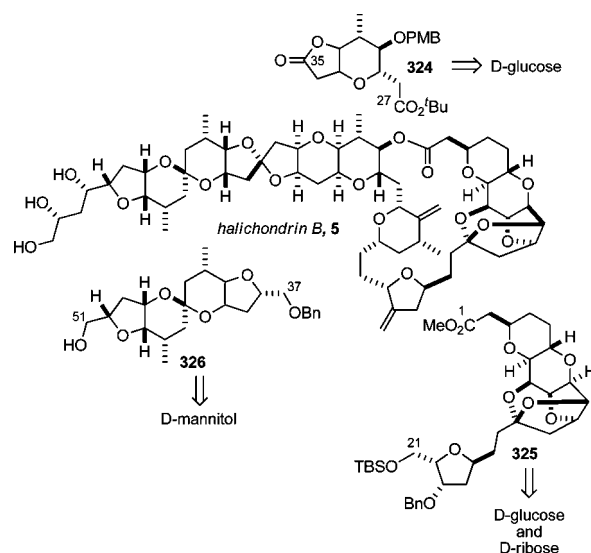
pyridinium *p*-toluenesulfonate prompted intramolecular ketal ring formation between the C8 and C11 hydroxyl groups and the C14 carbonyl to provide **317** in 80% yield. In a two-step procedure, the primary alcohol was converted to the acid by treatment with Dess–Martin periodinane and exposure to Lindgren–Pinnick conditions.<sup>79</sup> Treatment with TBAF then deprotected the two secondary TBS groups to reveal *seco*-acid **318**, which could be cyclized under standard Yamaguchi conditions to give macrolactone **210**, albeit in somewhat modest 35% yield. It is, however, noteworthy that the macrolactonization can occur in the presence of a free alcohol at C32.

The construction of the left-hand polyether domain began with a Horner–Wadsworth–Emmons reaction between aldehyde **280** and the lithium anion of phosphonate **218** to provide **319** (Scheme 28).<sup>80</sup> On treatment with TBAF, **319** underwent an intramolecular cyclization to give a 3:1 mixture of diastereoisomers that unfortunately favored the undesired product, 36-*epi*-**320**. Thankfully, this mixture could be converted to **320** by treatment with potassium carbonate in methanol at 80 °C. Removal of the PMB ether was achieved with DDQ, and the resultant triol underwent intramolecular spiroketalization when treated with camphor-sulfonic acid. The spiroketal formation was not diastereoselective (d.r. = 1:1) and after acetylation **321** was obtained. In order to elongate the C29 position by two carbons, the benzyl ether was deprotected by hydrogenation, and the resultant hemiacetal was homologated using a Wittig reaction. At this juncture, the C38 stereocenter was still a 1:1 mixture, but it was discovered that treatment with CSA at this point converted the mixture to a single diastereoisomer, **322**. In two final steps, **322** was treated with TBAF to promote the heteroconjugate addition, and the resultant

polyether ring system was deprotected with potassium carbonate in methanol to yield **217**.

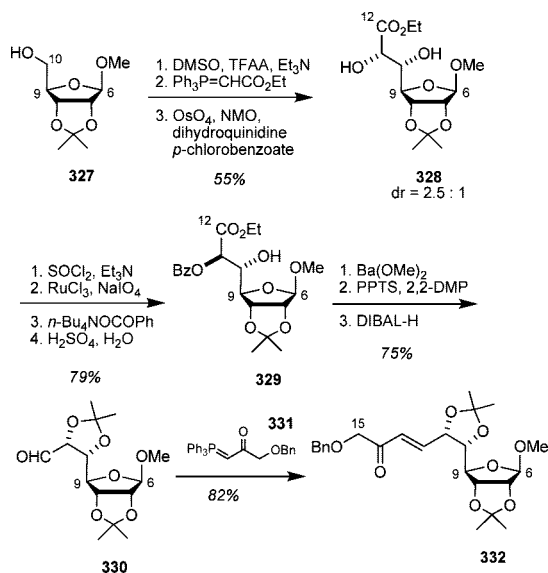
## 6. Synthetic Work toward Halichondrin B by Salomon

Salomon and co-workers have synthesized several segments of halichondrin B from a variety of inexpensive and commercially available starting materials: a C1–C15 segment from D-ribose, a C1–C21 segment, **325**, from D-ribose and D-glucose, a C27–C35 segment, **324**, from D-glucose, and a C37–C51 segment, **326**, from D-mannitol (Figure 12).



**Figure 12.** Key subunits and starting materials of the Salomon synthetic studies.

### Scheme 29. The Initial Stages of Salomon's Synthesis of the C1–C15 Domain

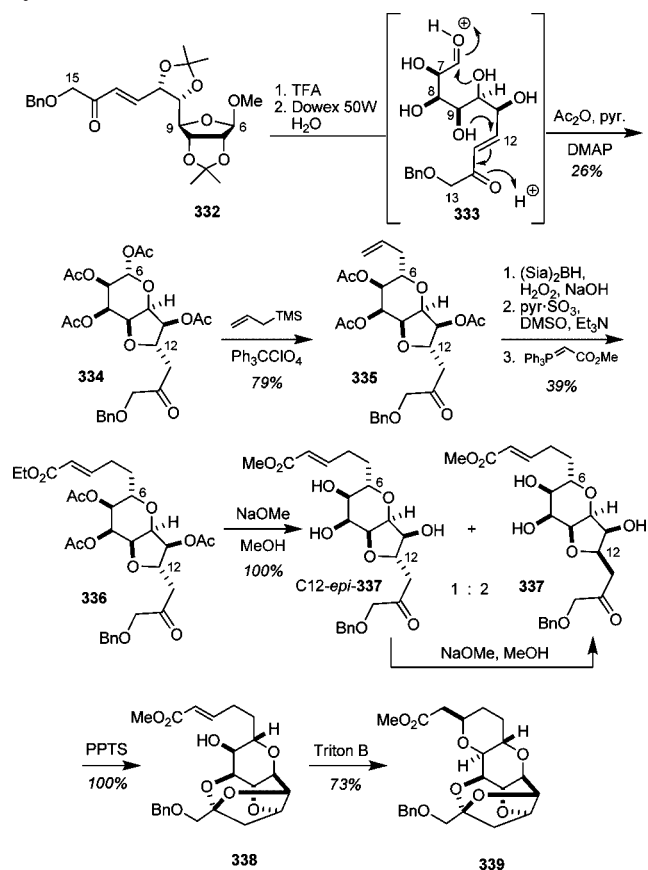


#### 6.1. C1–C15 Subunit Synthesis<sup>81</sup>

The starting material for Salomon's synthesis of the C1–C15 segment was D-ribose, which possesses the correct stereochemistry for the C7, C8, and C9 positions of halichondrin, as well as an appropriately positioned aldehyde for construction of one of the pyrans. Oxidation of ribofuranoside **327** at the C10 position and Wittig olefination provided access to the unsaturated ester. An early variant of the Sharpless asymmetric dihydroxylation was then used to provide **328** with 2.5:1 diastereoselectivity (Scheme 29).<sup>82</sup> At this point, it was necessary to invert the stereochemistry at the C11 position, and this was accomplished by conversion to the cyclic sulfate followed by a regioselective nucleophilic substitution with tetrabutylammonium benzoate.<sup>83</sup> Debenzoylation, acetonide formation, and partial reduction of the ester with DIBAL then provided the C12 aldehyde **330**. Subsequent Wittig olefination with phosphorane **331** afforded the  $\alpha,\beta$ -unsaturated enone **332**.

Trifluoroacetic acid-mediated acetonide hydrolysis and treatment of the resulting tetraol with Dowex 50W (a stronger acid) generated the highly functionalized acyclic **333** via opening of the furanoside (Scheme 30). Subsequent formation of the furopyran ring system ensued, and after acetylation, **334** was obtained, albeit with the incorrect stereochemistry at C12. All attempts to epimerize the C12 stereochemistry at this point met with failure, and it was reasoned that epimerization might be possible at a later stage in the synthesis. To continue the sequence, tetraacetate **334** was allylated selectively by a trityl perchlorate-catalyzed axial addition reaction with allyltrimethylsilane<sup>84</sup> to give **335**. Three further steps then converted **335** to the  $\alpha,\beta$ -unsaturated ester **336**. Treatment of **336** with sodium methoxide resulted in transesterification and partial epimerization of the C12 stereocenter to a 2:1 mixture favoring the desired compound, **337**. Upon treatment of the mixture with PPTS, ketalization of **337** gave the polycyclic acetal **338**. Fortunately, **338** was readily separable from C12-*epi*-**337**, which upon reexposure to sodium methoxide provided more **337** by epimerization. Finally, when **338** was subjected to Triton-B methoxide, intramolecular heteroconjugate addition occurred to close the final pyran ring and complete the synthesis of the C1–C15 domain, **339**.

### Scheme 30. Completion of Salomon's C1–C15 Subunit Synthesis



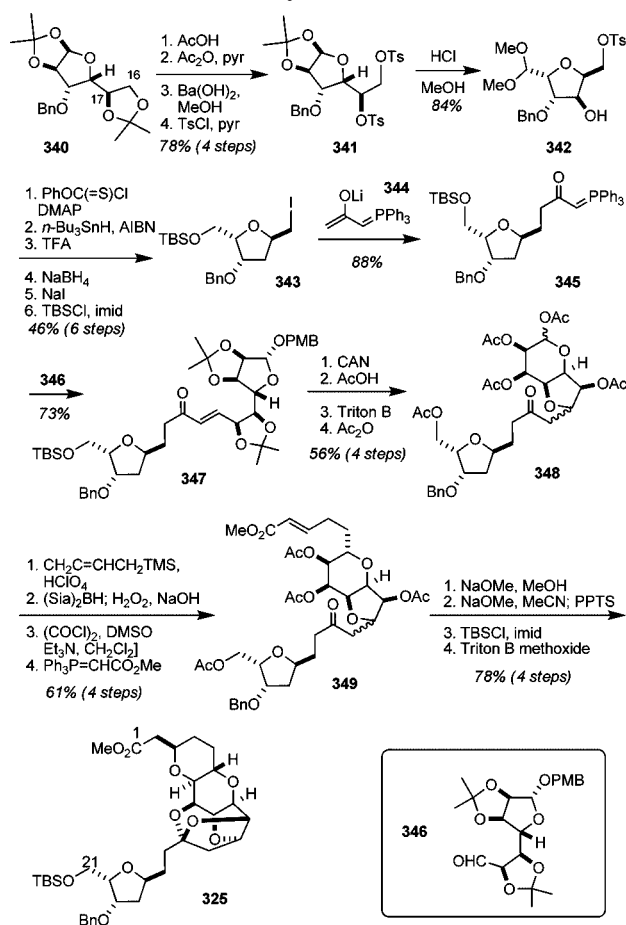
#### 6.2. C1–C21 Subunit Synthesis<sup>85</sup>

The C1–C21 fragment of halichondrin B was prepared as shown in Scheme 31. The sequence began with **340**, readily accessed from D-glucose in three high-yielding steps on molar scale. Selective deprotection of the C16–C17 acetonide and tosylation of the resulting diol gave **341**. Acid-catalyzed transketalization and tetrahydrofuran formation then provided **342**. Deoxygenation was then carried out under Barton conditions,<sup>86</sup> and four further steps provided intermediate **343**. Reaction of **343** with enolate **344** and subsequent Wittig reaction with **346** gave C16–C21 segment **347**. Selective removal of the PMB group was accomplished with ceric ammonium nitrate, and subsequent exposure to mild acid resulted in acetonide and silyl group cleavage. Treatment with Triton B followed by acylation of the crude product gave **348**. Conversion of **348** to **325** was carried out in similar fashion to the analogous conversion of **334** to **339** in the C1–C15 synthesis (Scheme 30), involving axial allylation and reaction of **349** with sodium methoxide to form a tetraol. However, the ordering of steps had to be modified to perform the heteroconjugate addition in advance of the C14 ketalization. When done in the opposite order, a significant amount of the known furan derivative was formed. After silylation of the remaining C21 hydroxy group, exposure to Triton B methoxide resulted in C3 equilibration to yield the desired C1–C21 segment **325**.

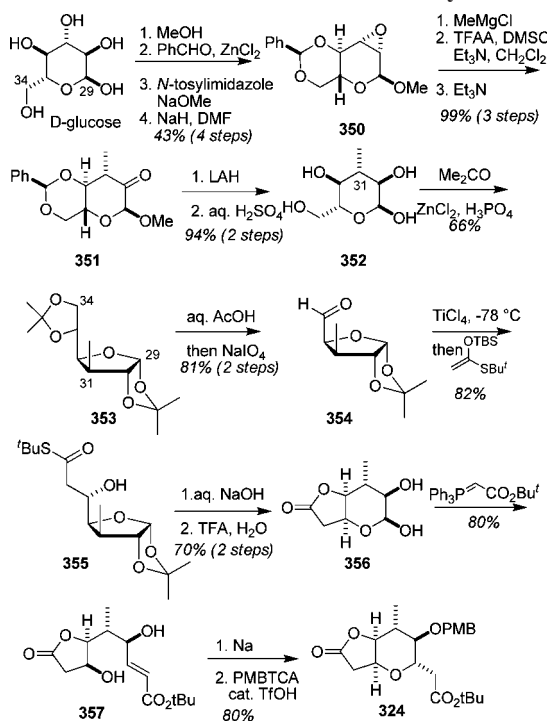
#### 6.3. C27–C35 Subunit Synthesis<sup>87</sup>

Scheme 32 outlines the synthesis of the C27–C35 segment **324**, for which D-glucose was used to provide much of the framework of the key pyran ring. Selective masking of

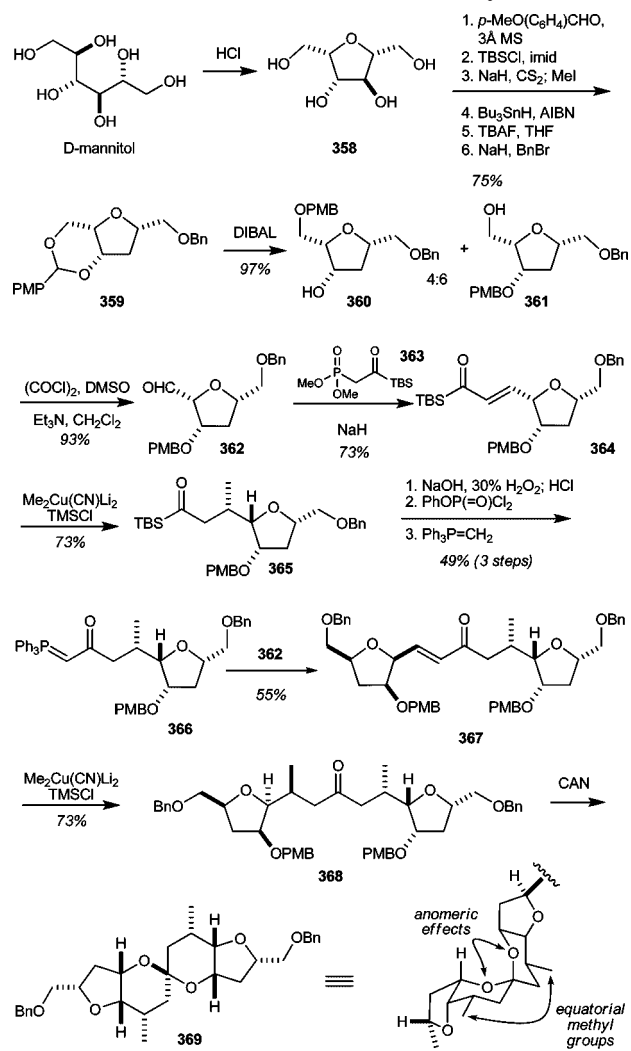
## Scheme 31. The Salomon Synthesis of the C1–C21 Domain



## Scheme 32. The Salomon C27–C35 Subunit Synthesis



## Scheme 33. The Salomon C37–C51 Subunit Synthesis



group and subsequent C31 epimerization via the enol provided the thermodynamically more favored (>99:1) equatorial methyl group (**350** → **351**). Axial reduction at C30 and hydrolysis of the protecting groups provided **352**, which was reprotected as the furanose bis-acetonide to give **353**. Deprotection of the C33–C34 acetonide and oxidative cleavage of the diol destroyed the incorrect C33 stereochemistry, providing aldehyde **354**. TiCl<sub>4</sub>-mediated and chelation-controlled reaction of aldehyde **354** and a silylketene thioacetal proceeded stereoselectively (>99:1) to afford thioester **355**. Base-induced hydrolysis of the thioester and acid-mediated acetonide cleavage was accompanied by conversion of furanose back to pyranose as well as *in situ* lactonization, yielding **356**. Finally, Wittig olefination produced **357**, and heteroconjugate addition reaction of the intermediate  $\alpha,\beta$ -unsaturated ester followed by protection of the secondary alcohol with *p*-methoxybenzyl trichloroacetimidate under acidic conditions delivered the target lactone **324**.

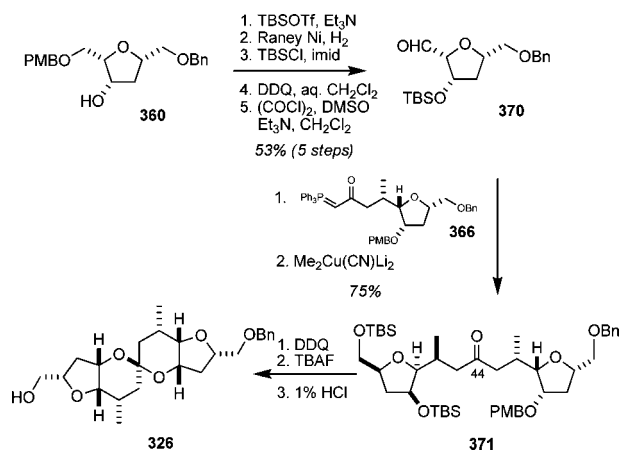
6.4. C37–C51 Subunit Synthesis<sup>88</sup>

The Salomon synthesis of the C37–C51 segment is shown in Schemes 33 and 34. In designing a synthesis of this domain, Salomon and co-workers noted the C<sub>2</sub> symmetry of the C37–C51 fragment and predicted that a thermodynamically controlled stereoselective spiroketalization could

all but the *trans* alcohols at C30 and C31 followed by tosylation and sodium hydride-mediated epoxide formation provided **350**. Regioselective opening of the epoxide by axial attack of MeMgCl provided the undesired methyl group stereochemistry. However, oxidation of the C30 hydroxyl



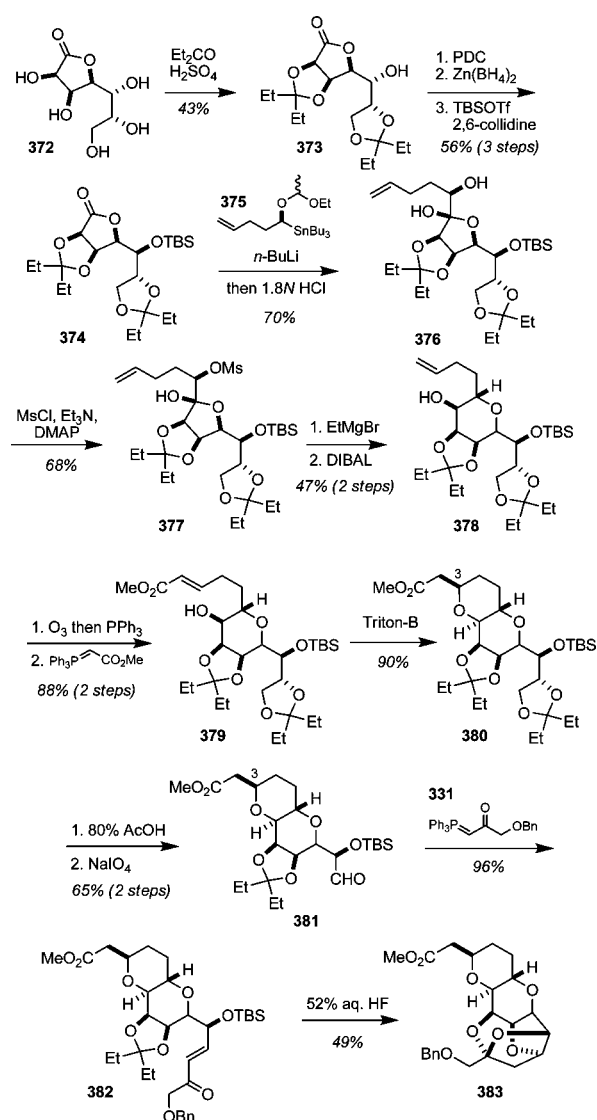
### Scheme 34. The Salomon C37–C51 Subunit Synthesis, With Terminus Differentiation



be used as the final synthetic step. Both the presence of two anomeric effects and the preference of the C42 and C46 methyl groups for equatorial disposition were invoked as rationale for the expected course of the reaction. Beginning with *D*-mannitol, acid-catalyzed cyclization gave tetraol **358** (Scheme 33). In six steps, **358** was converted to **359**. Reductive cleavage of **359** with DIBAL generated a 6:4 regioisomeric mixture of **360** and **361**, and either could be quantitatively recycled back to the starting acetal **359** by treatment with DDQ under anhydrous conditions. Compound **361** was then oxidized under Swern conditions to provide aldehyde **362**, and Horner–Wadsworth–Emmons reaction furnished the  $\alpha,\beta$ -unsaturated acyl silane **364**, which was diastereoselectively methylated in 1,4 fashion on treatment with Me<sub>2</sub>Cu(CN)Li<sub>2</sub> in the presence of TMSCl<sup>89</sup> to provide **365**. In three further steps, acyl silane **365** was converted into the corresponding phosphorane **366**, which was then condensed with aldehyde **362** to form enone **367**. A second diastereoselective methyl addition was subsequently used to form the key C<sub>2</sub>-symmetric ketone. It is of particular note that (i) the  $\alpha,\beta$ -unsaturated acyl silane **364** was required, because no reaction was observed with the corresponding  $\alpha,\beta$ -unsaturated ester, (ii) although the corresponding  $\alpha,\beta$ -unsaturated methyl ketone underwent conjugate addition, the aldol addition of the product ketone with aldehyde **362** did not generate enone **367**, and (iii) the stepwise approach was necessary, because dienones in this series tended to be unreactive toward cuprates. To conclude the sequence, ceric ammonium nitrate was used to oxidatively cleave the PMB ethers with concomitant spiroacetalization to afford the targeted compound **369**.

Despite the development of a route to the C<sub>2</sub>-symmetric subunit of C37–C51, it was of pivotal importance to break the symmetry of the system in order to incorporate the fragment into a synthesis of halichondrin B (Scheme 34). For the terminus differentiation of the C37–C51 segment, Salomon and co-workers returned to both regioisomers **360** and **361** obtained from the reductive cleavage of **359**. Thus **360** was converted into differentially protected aldehyde **370** through a five-step sequence involving selective hydrogenolysis of a benzyl ether in the presence of a *p*-methoxybenzyl ether with Raney nickel. Wittig coupling of the silyl protected aldehyde **370** with previously prepared phosphorus ylide **366** provided the enone, and subsequent conjugate methylation afforded ketone **371**, now terminus differentiated. Deprotection of the *p*-methoxybenzyl ether with DDQ and subsequent TBAF-mediated TBS deprotection

### Scheme 35. The Burke Pinacol Rearrangement Approach to the C1–C15 Domain



delivered a triol that afforded diastereoisomerically pure spiroketal **326** upon treatment with 1% HCl in THF.

Despite the significant progress made in the period 1989–1993, no further work has been published by the Salomon group.

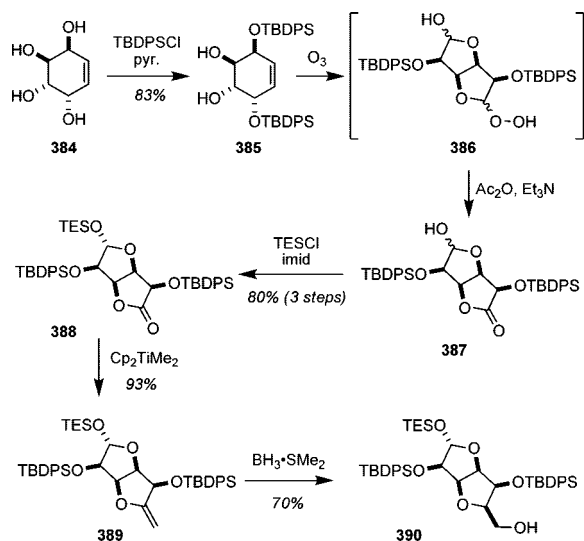
## 7. Synthetic Work toward Halichondrin B by Burke

Burke and co-workers have synthesized a variety of halichondrin B fragments and have also examined some subunit couplings. A key feature of their studies has been to exploit elements of local symmetry within the molecule.

### 7.1. C1–C15 Subunit Synthesis

The synthetic route to the C1–C15 segment, which began with commercially available carbohydrate *D*-glycero-*D*-glucoheptono- $\gamma$ -lactone, **372**, is shown in Scheme 35.<sup>90</sup> With the correct stereochemistry for the C8, C9, and C10 positions, lactone **372** would require only inversion at C11. Regioselective bis(ketalization)<sup>91</sup> of **372** with 3-pentanone provided **373**; this result is in contrast with bis(acetonide) formation, which is known to proceed with different regioselectivity.<sup>92</sup>

## Scheme 36. Burke's Ozonolytic Desymmetrization Approach to the C15–C15 Domain

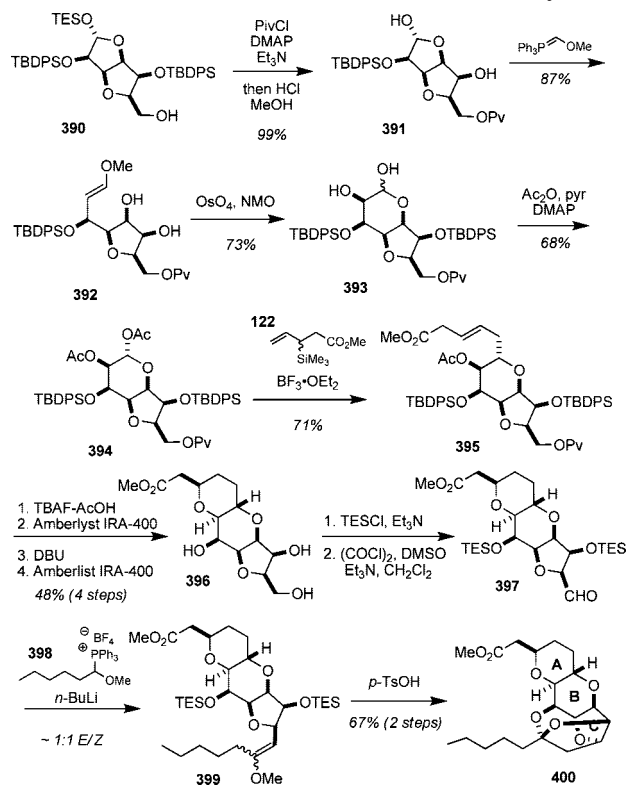


Oxidation to the C11 ketone and chelation-controlled reduction<sup>93</sup> with  $\text{Zn}(\text{BH}_4)_2$  gave the epimeric C11 alcohol, which now had the correct stereochemistry for the halichondrins and was subsequently protected as the TBS ether to provide **374**. The  $\alpha$ -alkoxyorganolithium reagent derived from tin–lithium exchange on stannane **375** was then added to lactone **374** to generate diol **376**. The secondary alcohol of **376** was converted to the mesylate **377**, which underwent a pinacol-type rearrangement<sup>94</sup> on exposure to ethylmagnesium bromide under heating conditions. Stereoselective reduction of the resultant pyranone with DIBAL led to alcohol **378**. Ozonolysis followed by reductive workup and *in situ* Wittig olefination provided the (*E*)-enoate **379** and exposure to Triton B methoxide converted **379** exclusively to **380** via a heteroconjugate addition/equilibration process. Removal of the terminal acetal and oxidative cleavage gave aldehyde **381**, which could be olefinated with phosphorane **331** to furnish enone **382**. Spiroketalization with aqueous HF then provided **383**.

A second synthesis of a model of the C1–C15 segment of halichondrin B has also been reported by the Burke group and features a novel ozonolytic desymmetrization of a  $C_2$ -symmetric diol and the use of a C14–C15 enol ether as a precursor to the trioxatricyclodecane.<sup>95</sup> The starting material for the second synthesis was (+)-conduritol E, **384**, which was silylated to produce **385** (Scheme 36). Exposure of **385** to ozone resulted in the generation of dioxabicyclo[3.3.0]octane bearing a peroxyacetal at C12, which readily underwent elimination [with concomitant oxidation of the adjacent carbon] upon treatment with acetic anhydride and triethylamine to furnish hemiacetal **387** as a 2:1 mixture of anomers. Of particular mention in this desymmetrization protocol is the combination of Criegee's tactic of trapping carbonyl oxides with internal nucleophiles and Schreiber's ozonolytic desymmetrization of simple cycloalkenes.<sup>96</sup> Protection of **387** with TESCl yielded the lactone **388** as a single diastereoisomer, and subsequent treatment of **388** with the Petasis reagent resulted in olefination to provide **389**. Hydroboration of the resultant *exo*-olefin gave primary alcohol **390** in 70% yield.

Alcohol **390** was protected with a pivalate group, and the TES ethers were cleaved in a one-pot procedure to form hemiacetal **391** (Scheme 37). At this point, the Kishi strategy

## Scheme 37. Burke's C1–C15 Halichondrin Model System

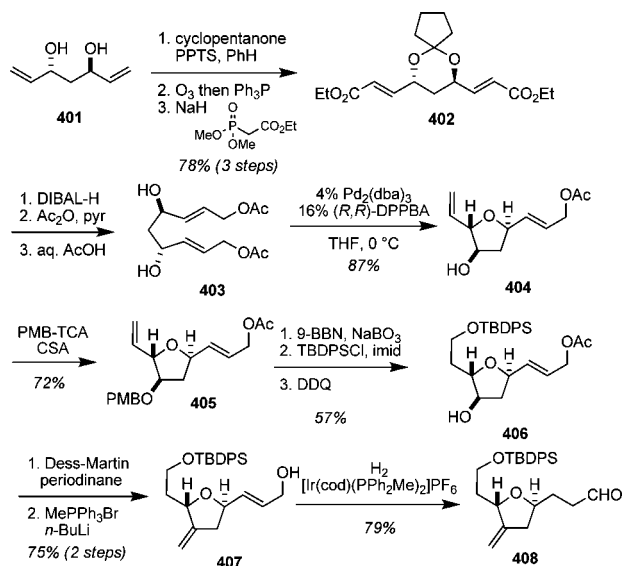


of olefination and then dihydroxylation was employed for the introduction of the C8 stereocenter. Acetylation and allylation with silane **122** gave **395**. At this point, treatment with Triton B methoxide was attempted to effect olefin isomerization, acetate cleavage, and heteroconjugate addition as has been done previously by the Kishi group. However, due to the TBDPS ethers, this series of transformations was prohibitively sluggish, and an alternative strategy had to be devised. To this end, treatment with TBAF/AcOH cleaved the TBDPS ethers, and subsequent exposure to basic resin (Amberlyst IRA-400) in methanol resulted in acetate cleavage to provide the triol. Upon treatment with 10 equiv of DBU in refluxing toluene, heteroconjugate addition occurred to provide a single diastereomer. As a side note, when the same transformation was conducted in benzene, a 2.9:1 mixture of C3 stereoisomers was obtained in 94% yield, leading to the speculation that high reaction temperatures are necessary for equilibration via the retro-Michael/Michael addition process. Exposure of the resultant pyranopyran to Amberlyst IRA-400 then cleaved the pivalate ester to provide triol **396**. Global protection of the alcohols as TES ethers was achieved with TESCl and  $\text{Et}_3\text{N}$ , and subsequent chemoselective oxidation of the primary TES ether under Swern conditions then provided aldehyde **397**.<sup>97</sup> Phosphonium tetrafluoroborate salt **398** was deprotonated with *n*-BuLi, and the resultant phosphorane was allowed to react with the aldehyde to yield the enol ether **399** as an inconsequential *E/Z* mixture, which when treated with *p*-TsOH formed the trioxatricyclodecane **400**.

7.2. C14–C22 Subunit Synthesis<sup>98</sup>

The first synthesis of the C14–C22 segment from the Burke group features a palladium-mediated, ligand-controlled, desymmetrization of a  $C_2$ -symmetric diol synthesized via a two-directional chain elongation strategy (Scheme 38). The sequence began with  $C_2$ -symmetric diol **401**, which was

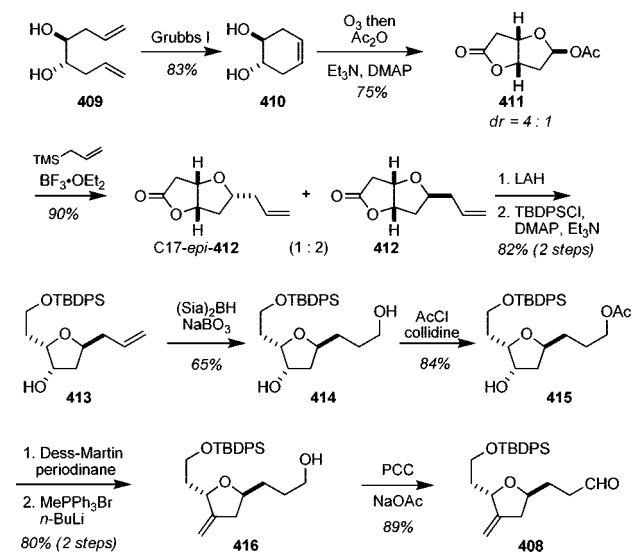
## Scheme 38. Burke's First Generation Synthesis of the C14–C22 Domain



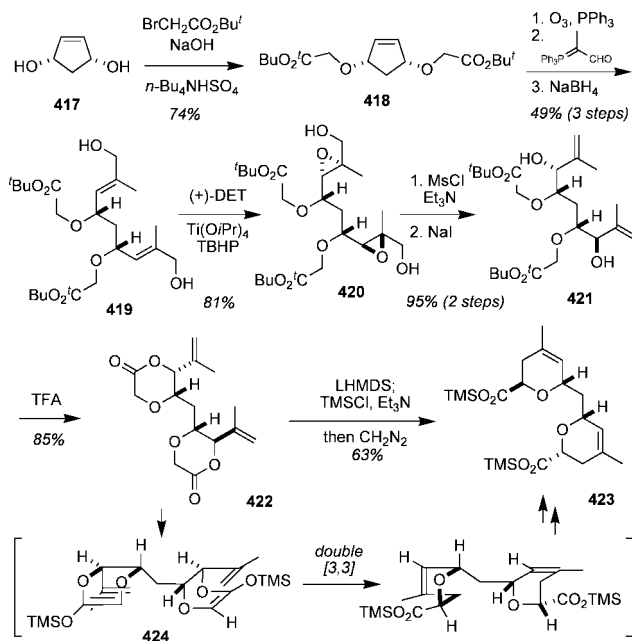
converted via two-directional synthesis in six steps to diacetate **403**. Treatment of **403** to desymmetrization conditions using Trost's (*R,R*)-diphenylphosphino benzoic acid (DPPBA) ligand<sup>99</sup> and Pd(0) at 0 °C smoothly provided **404** (d.r. = 5:1). When the desymmetrization reaction was attempted at room temperature, the products also included the double cyclization product as well as the desired compound. Protection of the secondary alcohol as the PMB ether furnished **405**, which could be separated at this point from the minor diastereoisomer formed in the preceding cyclization. Selective hydroboration of the terminal olefin provided an alcohol that could be used for subunit coupling, and after protection of this alcohol, treatment with DDQ then cleaved the PMB ether to provide **406**. Oxidation of the secondary alcohol was effected with Dess–Martin periodinane, and the installation of the *exo*-methylene and concomitant deacylation was achieved with methylenetriphenylphosphorane to provide allylic alcohol **407**. Lastly, the allylic alcohol was isomerized with a cationic iridium catalyst to generate aldehyde **408**.<sup>100</sup>

In addition to the route shown above, a second synthesis of the C14–C22 segment **408** was devised by the Burke group.<sup>101</sup> The principle highlight of the second synthesis is an ozonolytic desymmetrization of a C<sub>2</sub>-symmetric dihydroxycyclohexene, as shown in Scheme 39. The sequence began with (*S,S*)-dihydroxycyclohexene **410** (synthesized from known **409** via ring-closing metathesis with Grubbs first generation catalyst). Ozonolysis under Schreiber's conditions (modified by addition of excess acetic anhydride and DMAP) provided **411** as a separable 4:1 mixture in 75% yield. Subjecting the mixture to Lewis acid promoted allylation resulted in a 2:1 mixture of products **412** and C17-*epi*-**412**, with **412** being the desired isomer. Complete reduction to the diol with lithium aluminum hydride (LAH), and subsequent selective protection of the primary alcohol provided **413**. Subsequent hydroboration (**413** → **414**) and selective monoacylation led to **415**. In two further steps, the secondary alcohol was converted to the *exo*-olefin **416**, which was treated with NaOAc-buffered PCC to provide **408**.

## Scheme 39. Burke's Second Generation Synthesis of the C14–C22 Domain

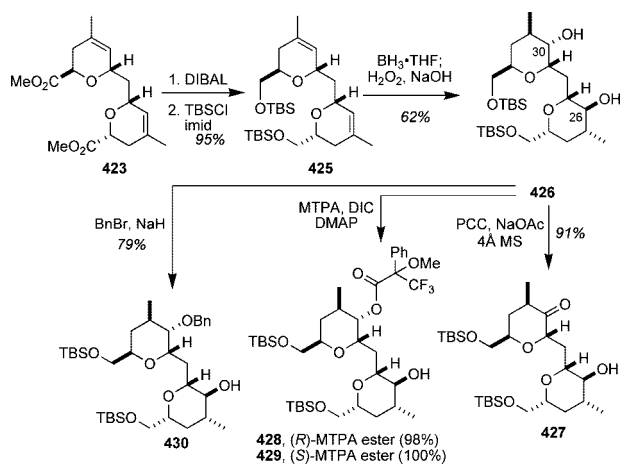


## Scheme 40. Burke's [3,3]-Sigmatropic Rearrangement Approach to the C20–C36 Domain

7.3. Synthesis of the C22–C34(36) Subunit<sup>102</sup>

In their analysis of the challenges posed by the C22–C34 domain of the halichondrins, Burke and co-workers noted that this section was only a single epimerization away from being an achiral *meso* compound. In light of this, a strategy was adopted involving the asymmetric desymmetrization of the *meso* bis(allylic alcohol) **419** (Scheme 40). The *meso* diol **419** was converted to the requisite bis(allylic alcohol) **419** via a four-step sequence of (i) bis(O-alkylation) with *t*-butyl bromoacetate under phase-transfer conditions, (ii) ozonolytic ring cleavage, (iii) Wittig homologation, and (iv) sodium borohydride reduction. Desymmetrization of **419** was achieved with the Sharpless catalytic asymmetric epoxidation,<sup>103</sup> resulting in the formation of bis(epoxy alcohol) **420**. Conversion of **420** to the dimesylate was followed by iodide displacement with concomitant iodide-mediated reductive opening of the epoxide to provide **421**. Treatment of **421** with trifluoroacetic acid effected lactonization to form

## Scheme 41. Functionalization of the Diol 426



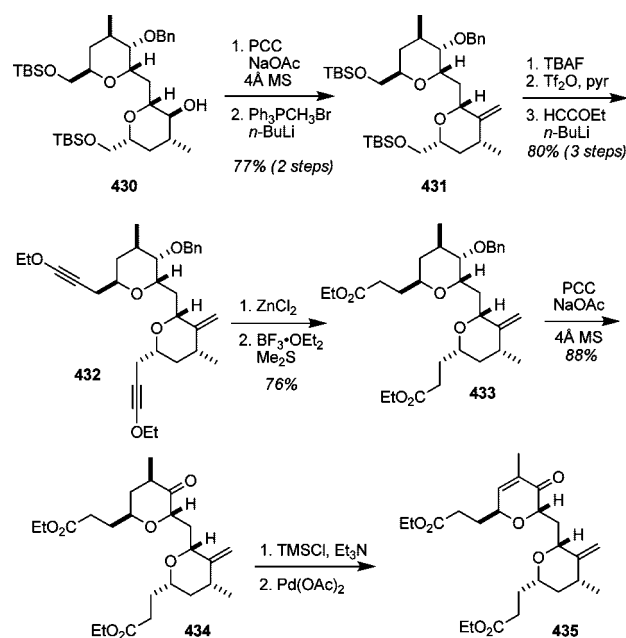
bis(dioxanone) **422**. Upon exposure to LHMDS and TMSCl, **422** underwent kinetic enolization to form the bis(silylketene acetal) **424**, and two Ireland–Claisen [3,3]-sigmatropic rearrangements subsequently occurred upon heating in toluene, thus forming bis(dihydropyran) **423**.

To elaborate **423** on to a C20–C36 halichondrin fragment, differential functionalization of the nearly symmetrical bis(dihydropyran) was required.<sup>104</sup> Toward this end, both esters were reduced, and the alcohols formed were protected to form the bis(TBS ether) **425** (Scheme 41). Subsequent regio- and stereoselective hydroboration gave diol **426**, also setting the C25 stereocenter. At this point, it was observed that the C30 and C26 possessed differential reactivity toward oxidation, acylation, and benzylation. For example, PCC oxidation proceeded with complete regioselectivity to give the C30 ketone **427**. Similarly, acylation under Steglich conditions<sup>105</sup> also occurred solely at the C30 alcohol to give the diastereomeric Mosher esters **428** and **429** in high yield. Although the C30 and C26 alcohols can be distinguished by the respective equatorial, axial, and diequatorial flanking substituents, it remains unclear why such a large reactivity preference exists for the C30 alcohol. Nonetheless, this preference was crucial for the differential functionalization of bis(dihydropyran) **426** and completion of the synthesis of the C22–C36 fragment. Though oxidation and acylation gave almost exclusively the C30 functionalized product, benzylation was found to occur with slightly less selective regiochemistry, as a 4:1 mixture was obtained favoring the desired **430**.

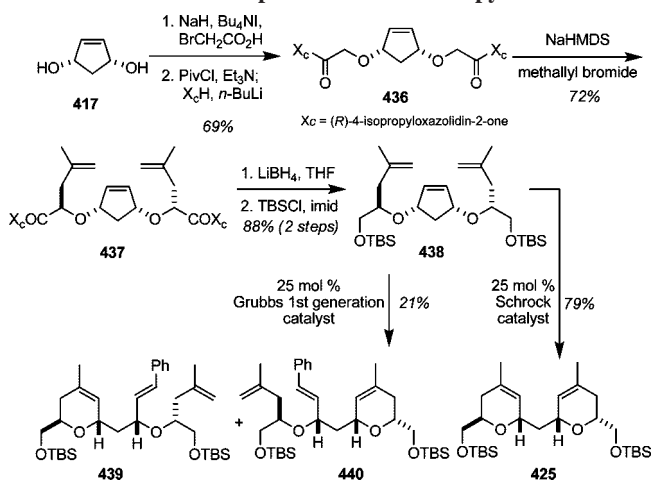
Progressing forward from **430**, oxidation and methylenation provided olefin **431** (Scheme 42). Next, simultaneous two-carbon chain extensions were performed at C22 and C34 via displacement of the bis(triflate) formed from **431** with lithio ethoxyacetylide to provide bis(alkyne) **432**. Alkyne hydration was then carried out under mild Lewis acidic conditions<sup>106</sup> with ZnCl<sub>2</sub> and was followed by cleavage of the benzyl ester, which proved to be somewhat difficult, although satisfactory results were seen with boron trifluoride etherate in the presence of dimethylsulfide, as described by Fuji,<sup>107</sup> to provide bis(ester) **433**. To complete the sequence, the unmasked secondary alcohol was oxidized with PCC and subjected to a Saegusa oxidation,<sup>108</sup> yielding the  $\alpha,\beta$ -unsaturated ketone **435** designed to serve as a precursor to the fully elaborated C20–C36 halichondrin B subunit.

In a later publication, Burke disclosed a more efficient synthesis of a bis(dihydropyran) intermediate **425** (Scheme 43).<sup>109</sup> The new strategy exploited the power of ring-opening

## Scheme 42. Burke's Second Generation Approach to the C20–C36 Halichondrin Subunit

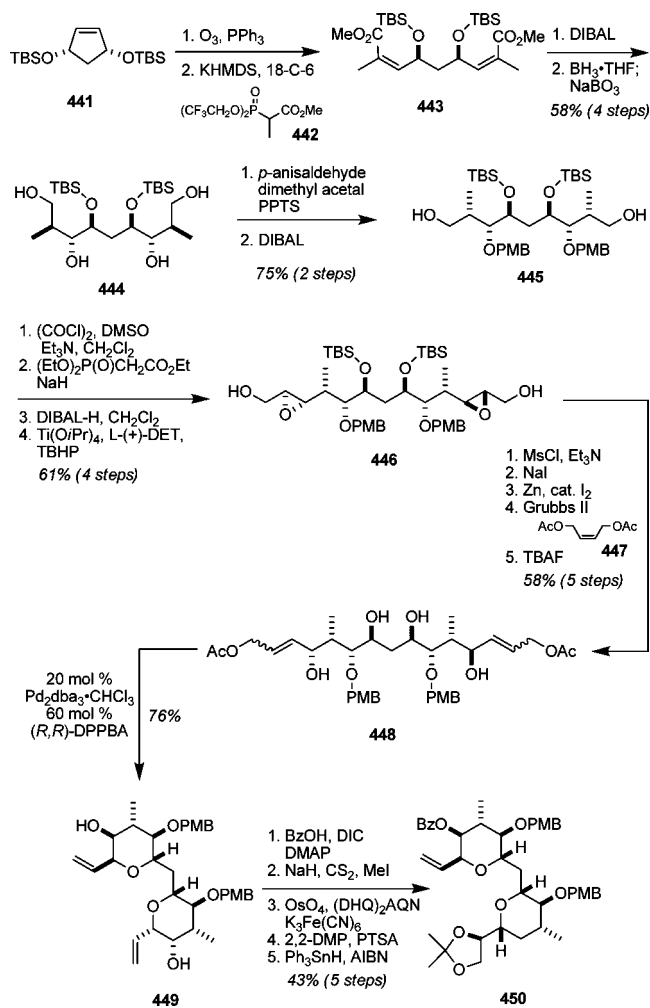


## Scheme 43. Burke's Improved Route to Bis-pyran 425



and ring-closing metathesis as a method for the rapid and facile assembly of functionalized rings. The sequence began with the same starting material, **417**, as was used for the double Ireland–Claisen route (see Scheme 40). Although conversion of **417** to the desymmetrized bis(imide) **436** could be achieved in one step by bis(O-alkylation) with (4*S*)-3-(bromoacetyl)-4-isopropyl-2-oxazolidinone and silver oxide, the best conversion was observed with a two-step protocol entailing (i) formation of the *meso* diacid with NaH, tetrabutylammonium iodide (TBAI), and sodium bromoacetate and (ii) formation of the bis(pivalic anhydride) followed by reaction with *N*-lithio-(4*S*)-4-isopropyl-2-oxazolidinone. Subsequent stereoselective double methallylation was achieved with the *Z*-enolate of **436** (formed using NaHMDS) and methallyl bromide to give **437** by virtue of the valine-derived Evans chiral auxiliaries.<sup>110</sup> Reductive cleavage of the auxiliaries and TBS protection provided **438**. At this point, the key ring-opening/ring-closing metathesis was investigated. Treatment of **438** with Grubbs first generation catalyst furnished an inseparable mixture of diastereomeric dihydropyrans **439** and **440** in which only one ring-closing metathesis occurred. Fortunately, however, exposure of **438** to the

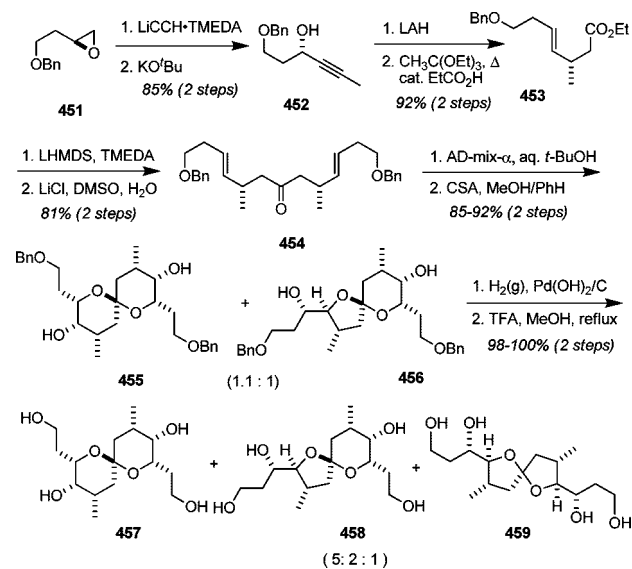
## Scheme 44. Burke's Third Generation Approach to the C22–C35 Domain



more reactive Schrock molybdenum-based catalyst smoothly produced the desired **425** in 79% yield.

The most recent work from the Burke group toward the C22–C36 segment is shown in Scheme 44.<sup>111</sup> The key goals of this synthesis were (i) to introduce the C19 and C26 *exo*-methylene units simultaneously and at a late stage, (ii) to synthesize the structure bidirectionally utilizing both substrate- and reagent-controlled reactions, and (iii) to use the Pd(0)-mediated asymmetric double cycloetherification previously developed. The sequence began with bis-silyl-protected cyclopentenediol **441**, which was oxidatively cleaved and treated with the Still–Gennari reagent **442** to give **443**. Reduction and hydroboration following Kishi's empirical rule<sup>112</sup> allowed the generation of four stereocenters via substrate-controlled asymmetric induction to produce **444**. Selective protection of the C30 and C26 secondary alcohols in **444** was achieved by formation of a PMP-acetal and DIBAL reduction to provide **445**. Using a two-directional strategy, **445** was elongated via oxidation, Horner–Wadsworth–Emmons olefination, and subsequent reduction to the *meso*-bis(allylic alcohol). At this point, the symmetry of the system was interrupted with Sharpless asymmetric epoxidation at the allylic alcohols to provide **446**. In five further routine steps, **446** was converted to the Pd(0)-mediated asymmetric double cycloetherification precursor **448**. Treatment of the tetraol **448** with  $\text{Pd}_2\text{dba}_3\cdot\text{CHCl}_3$  and the Trost (*R,R*)- $\text{DPPBA}$  ligand established the bis(tetrahy-

## Scheme 45. Burke's Symmetry-Based Approach to the C38–C54 Domain



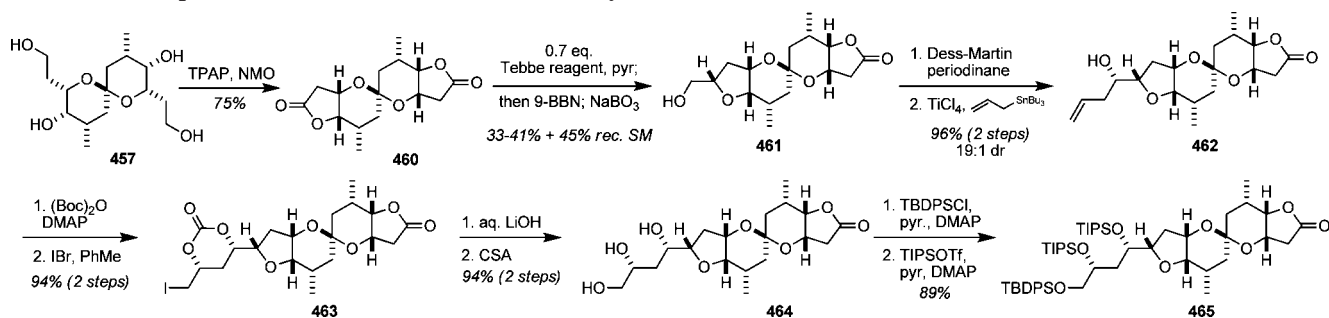
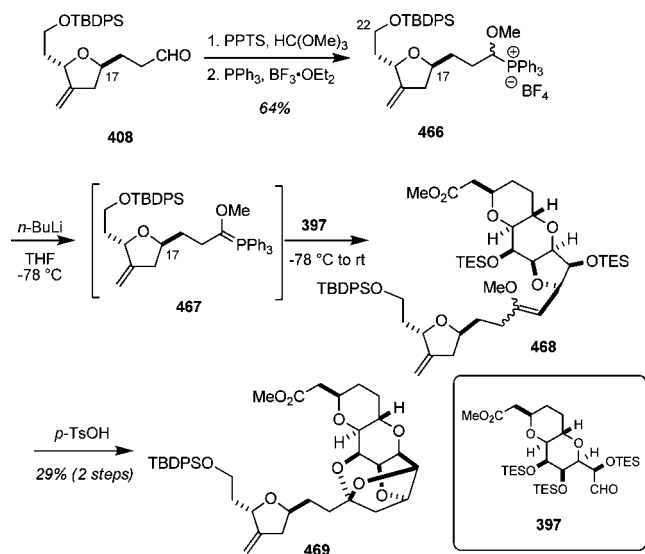
dropyran) **449** with absolute stereochemical control in high yield. Five additional steps were then required to convert **449** to **450**.

7.4. Synthesis of the C38–C54 Subunit<sup>113,114</sup>

In a similar vein to both Hirata/Yonemitsu and Salomon, Burke has designed an efficient construction of the ~C38–C54 domain by exploiting the local  $C_2$ -symmetry about the C44 spiroketal carbon. The sequence commenced with the known (*S*)-epoxide **451** (derived from (*S*)-malic acid), which was opened with the tetramethylethylenediamine (TMEDA) complex of lithium acetylide (Scheme 45). The crude alkyne was isomerized with potassium *tert*-butoxide to give **452**. Subsequent reduction with LAH provided the *E*-allylic alcohol as a single diastereomer, and exposure of the allylic alcohol to Johnson orthoester Claisen conditions smoothly furnished **453**. Claisen self-condensation was then carried out by treating **453** with LHMDS, and the resulting  $\beta$ -ketoester was decarboxylated under Krapcho conditions<sup>115</sup> to give the  $C_2$  symmetric ketone **454**. Asymmetric dihydroxylation with AD-mix- $\alpha$  to effect a stereoselective dihydroxylation and acid-catalyzed spiroketalization of the resultant tetraol yielded a 1.1:1.0 mixture of the  $C_2$  symmetric 1,7-dioxaspiro[5.5]undecane **455** and the isomeric, undesired 1,6-dioxaspiro[4.5]decane **456**. The mixture was debenzylated and equilibrated under acidic conditions to a more favorable mixture of the desired **457**, along with **458** and **459** (5:2:1). Fortunately, after separation the undesired products **458** and **459** were easily recycled to produce more **457** by re-exposure to the equilibrating conditions.

Selective oxidation of the primary alcohol groups of tetraol **457** (presumably via oxidation of the intermediate five-membered hemiacetals) was achieved with tetrapropylammonium perruthenate (TPAP)/*N*-methylmorpholine-*N*-oxide (NMO), forming the  $C_2$ -symmetric bis(lactone) **460** (Scheme 46). To avoid forming a statistical mixture of starting material and mono- and difunctionalized products, **460** was partially olefinated with 0.7 equiv of the Tebbe reagent. Subsequent hydroboration/oxidation gave **461** as an approximately 1:1 mixture with the starting material **460**. Alcohol **461** was then oxidized to the aldehyde and allylated under chelation-controlled conditions with titanium(IV) chloride and allyl-

## Scheme 46. Completion of the Burke C38–C54 Domain Synthesis

Scheme 47. The  $\alpha$ -Alkoxyphosphorane Approach to the C1–C22 Domain

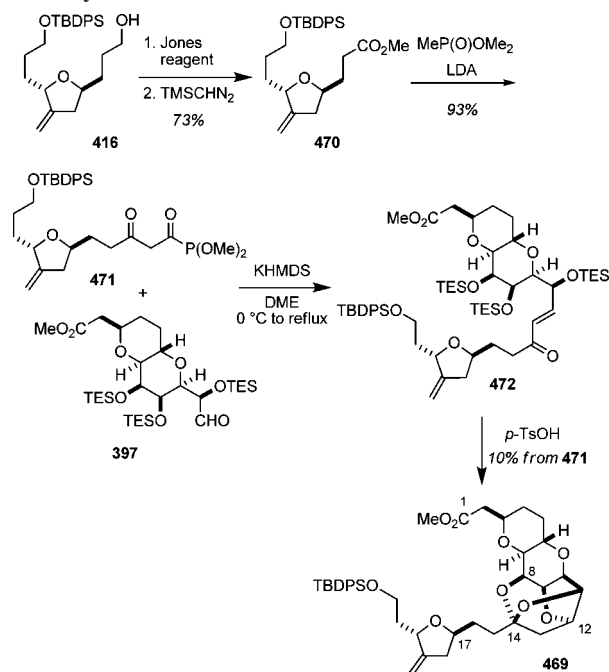
tributylstannane to give the homoallylic alcohol **462** as a single diastereoisomer. Conversion to the corresponding BOC carbonate, and subsequent treatment with iodine monobromide afforded the iodocarbonate **463** with excellent diastereoselectivity (>18:1). In four further steps, **463** was converted into the fully functionalized C38–C54 segment **465**.

## 7.5. Subunit Couplings

The Burke group has also reported studies into the coupling of the C1–C14 and C14–C22 fragments.<sup>116</sup> The first method used for joining the C14–C22 and C1–C13 fragments was a Wittig coupling/ketalization strategy, which relied on the preparation of a C14–C22 fragment with a phosphonium salt at the C14 terminus. Toward this end, aldehyde **408** was first treated with PPTS to provide the dimethyl acetal in high yield. Subsequent exposure to triphenylphosphine in the presence of boron trifluoride etherate provided the triphenylphosphonium tetrafluoroborate salt **466** (Scheme 47). Given the moisture sensitivity and the isolation difficulties **466** presented, it was treated without delay (in base-washed glassware) with *n*-butyllithium at  $-78$  °C to generate the ( $\alpha$ -methoxyalkyl)triphenylphosphorane **467**. Addition of **397** to the reaction mixture followed by slow warming provided **468**, which ketalized on treatment with *p*-toluenesulfonic acid to provide the complete C1–C22 domain, **469**, in a two-step yield of 29%.

The second method used to construct the C1–C22 segment involved a Horner–Wadsworth–Emmons coupling between **397** and **471** (Scheme 48). To prepare  $\beta$ -ketophosphonate **471**, alcohol **416** was oxidized with freshly prepared Jones

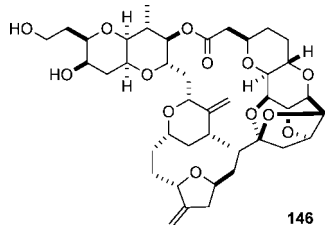
## Scheme 48. Burke's Horner–Wadsworth–Emmons Strategy for the Synthesis of the C1–C22 Domain



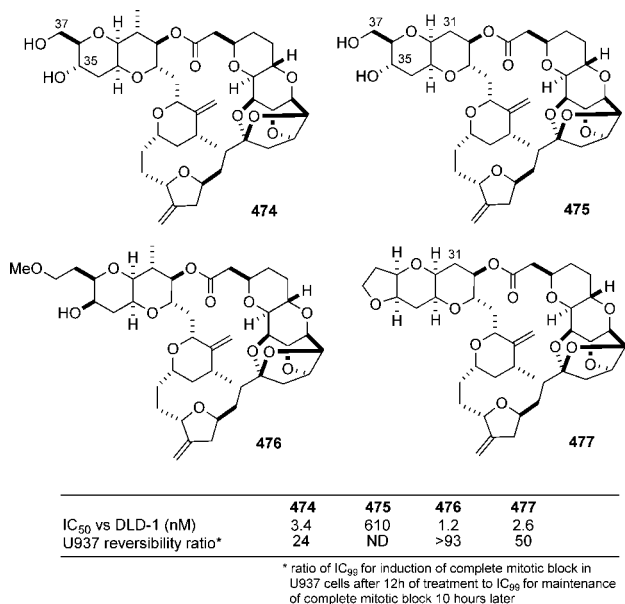
reagent and esterified with trimethylsilyldiazomethane to provide **470**. Addition of lithio(dimethyl)methylphosphonate to **470** then yielded the  $\beta$ -ketophosphonate **471**. Horner–Wadsworth–Emmons reaction of **397** and **471** with KHMDS as base proceeded to form enone **472** along with an unknown product that could not be separated. Thus, the enone was carried on crude into the Michael addition/ketalization sequence to provide **469** in 10% yield over these steps.

## 8. The Discovery and Development of E7389

In 1992 samples of synthetic halichondrin B and several intermediates were provided by the Kishi group to the Eisai Research Institute with a goal of evaluating *in vitro* and *in vivo* activity. In a remarkable discovery, the macrocyclic macrolactone diol shown in Figure 13 (**146**) was found to be within an order of magnitude as potent as the parent halichondrin B against DLD-1 human colon cancer cells ( $IC_{50}$  for **146** = 4.6 nM).<sup>117</sup> Further study showed that halichondrin B and **146** both blocked cell cycle progression at the G2/M phase, both caused microtubule destabilization, and both had similar profiles in the 60-cell-lines screen at the National Cancer Institute. Armed with this information, the stage was set to develop a potential halichondrin-derived therapeutic.



**Figure 13.** The right-hand macrolactone diol (**146**) of halichondrin B.



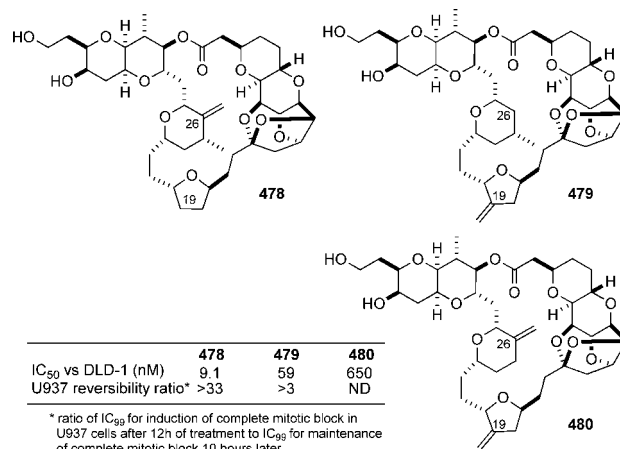
**Figure 14.** Selected SAR in the ~C30–C38 domain.

### 8.1. Preliminary SAR Studies

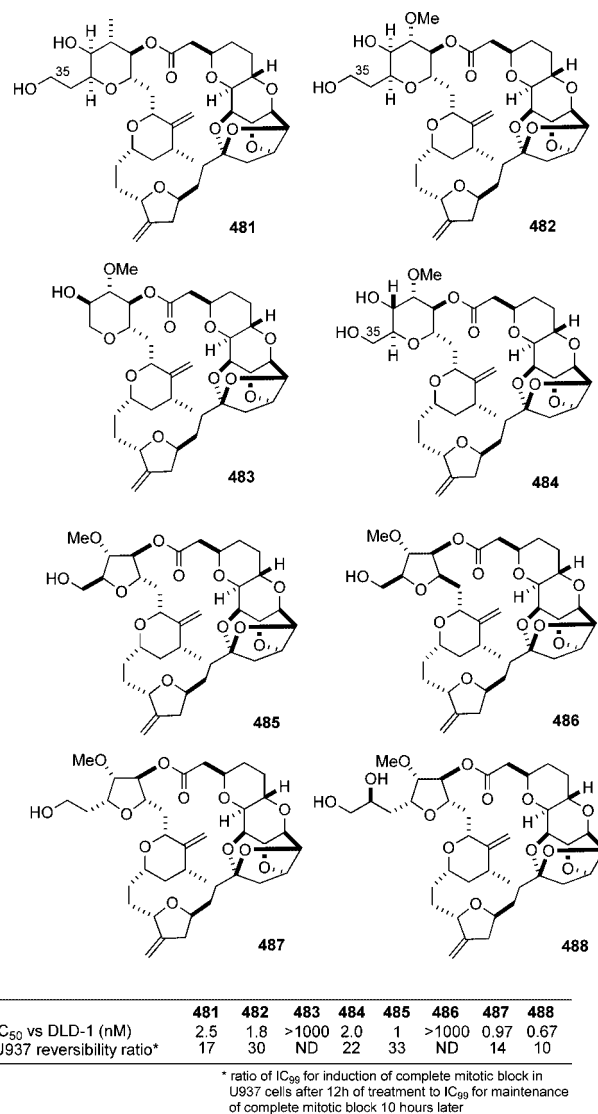
One of the initial hurdles to overcome was the observation that **146** was not active *in vivo* in a LOX human melanoma xenograft model. Flow cytometry revealed that the problem was related to reversibility of action of **146**, a feature that was not found with the natural product. For example, halichondrin B was able to maintain a complete mitotic block 10 h after drug washout at levels of 10 nM, whereas **146** was ineffective even at levels as high as 1 μM. To facilitate the evaluation of compounds under conditions that would be relevant to *in vivo* efficacy, ERI developed an in-house proprietary cell-based assay to evaluate compounds. A number of analogues of **146** that were modified in the terminal C30–C38 region were subsequently evaluated, and although the ability to inhibit cell growth was relatively uniform, the ability to cause an irreversible complete mitotic block was very sensitive to structure changes.<sup>118</sup> For example, among the compounds shown in Figure 14, diol **474** was the first compound able to maintain a reasonable degree of complete mitotic block. Although many compounds prepared as part of SAR around this region of the molecule displayed good potency, there were some exceptions, as can be seen with compound **475**, in which the C31 methyl group has been removed, resulting in an approximately 130-fold decrease in potency relative to **474**.

Other studies evaluated the effect of deletion of functionality in the C19–C26 domain. As can be seen in Figure 15, changes in this region were permissible, although at some penalty to either potency or reversibility.

A significant step forward came with the discovery that the C29–C36 pyranopyran domain could be replaced by



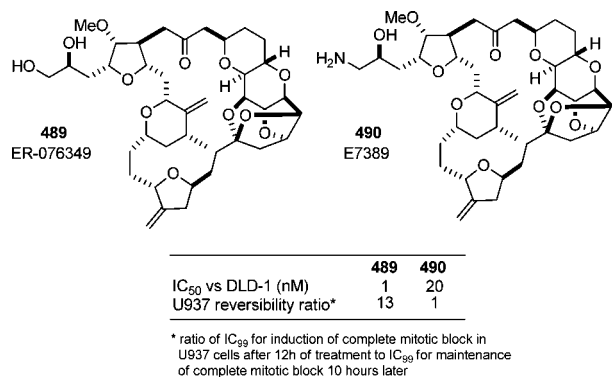
**Figure 15.** SAR in the C19–C26 domain.



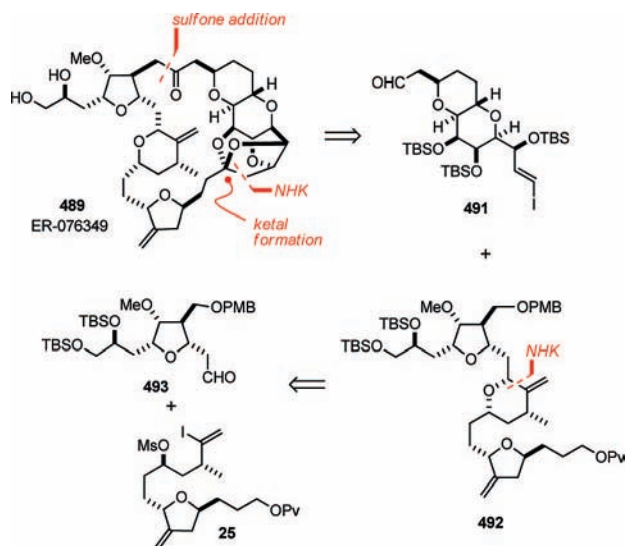
**Figure 16.** Tetrahydropyran and tetrahydrofuran analogues.

monocyclic pyran and furan derivatives.<sup>119</sup> A large number of compounds were evaluated in this series, and some examples are shown in Figure 16.

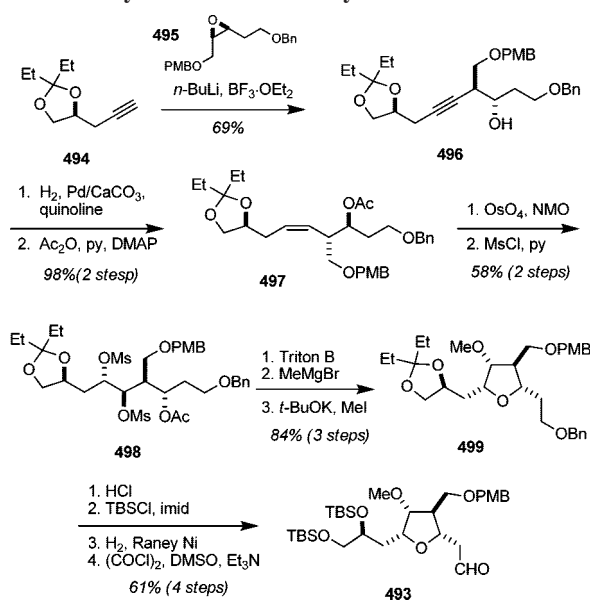
Compounds **481** and **488** were tested in the LOX melanoma xenograft model, and neither showed any efficacy. A number of possible explanations for this were possible, but ultimately the question of the stability of the macrolactone



**Figure 17.** Eisai's lead compounds: ER-076349, **489**, and E7389, **490**.



**Scheme 49.** Synthesis of the Aldehyde **493**



**Figure 18.** An overview of the synthesis strategy for ER-076349.

in these tetrahydropyran and tetrahydrofuran analogues toward nonspecific esterases present in mouse serum became of concern. Attention turned to the preparation of nonhydrolyzable isosteres for the ester such as ketone, ether, and amide functionalities. Among these the most promising in terms of *in vitro* activity was the ketone, and two compounds rose to prominence: the diol **489** (ER-076349) and the amino alcohol **490** (E7389, previously ER-086526) (Figure 17).

ER-076349 exhibited activity *in vivo* in xenograft models against a variety of cancers including MDA-MB435 breast carcinoma, COLO-205 colon carcinoma, LOX melanoma, and NIH:OVCAR-3 ovarian carcinoma. There was no evidence of toxicity at the doses tested.<sup>120</sup> Subsequent SAR from ER-076349 led to a variety of compounds [see the next section for details], and the lead compound to emerge from these studies was E7389. Although slightly less potent than ER-076349, E7389 has the important characteristic of having a U937 reversibility ratio of 1.

## 8.2. Synthesis and SAR of ER-076349, E7389, and Analogues

The Eisai synthesis of both ER-076349 and E7389 employs much of the technology laid down in Kishi's studies. Against this backdrop, an analysis of ER-076349, from which E7389 can be readily obtained, led to three key fragments **491**, **493**, and the ubiquitous **25** (Figure 18).

The sequence to construct the C27–C35 aldehyde **493**, began with a regioselective opening of epoxide **495** with the acetylide derived from acetylene **494** (Scheme 49). Partial reduction of the alkyne under Lindlar conditions and acylation provided *cis*-olefin **497**. Dihydroxylation then afforded an 8:1 mixture of diastereomeric alcohols, which were converted to the corresponding mesylates, whereupon separation was possible. Treatment of mesylate **498** with Triton B resulted in deacetylation and formation of the tetrahydrofuran ring. Subsequent desulfonation with methylmagnesium bromide, and methylation of the alcohol gave **499**. In four further steps, the C27–C35 aldehyde **493** was obtained.

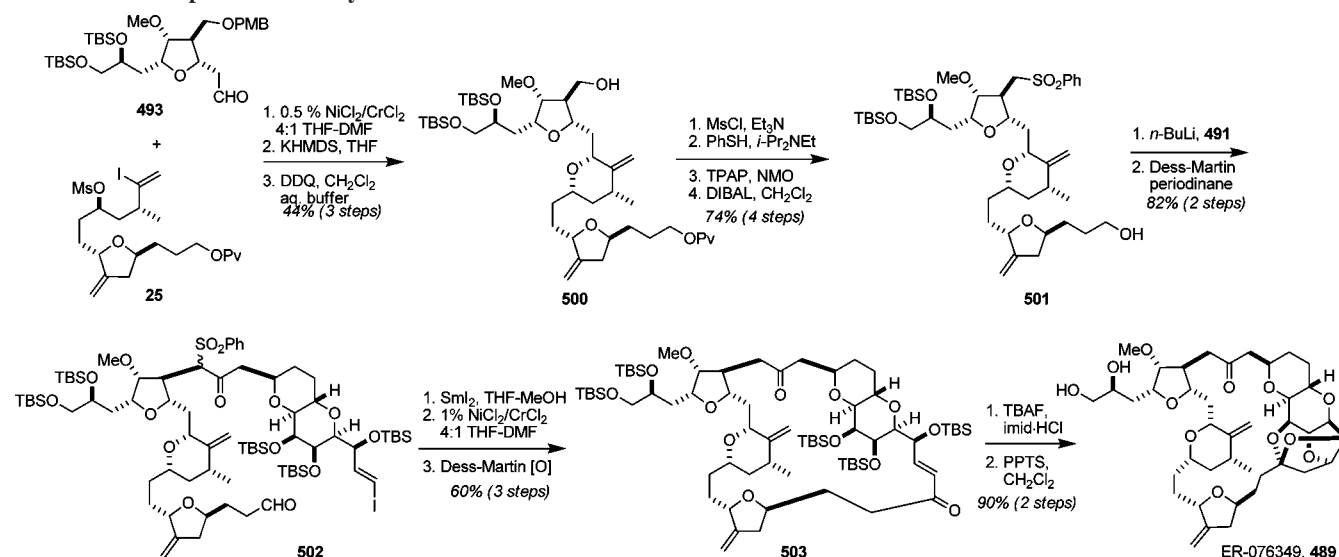
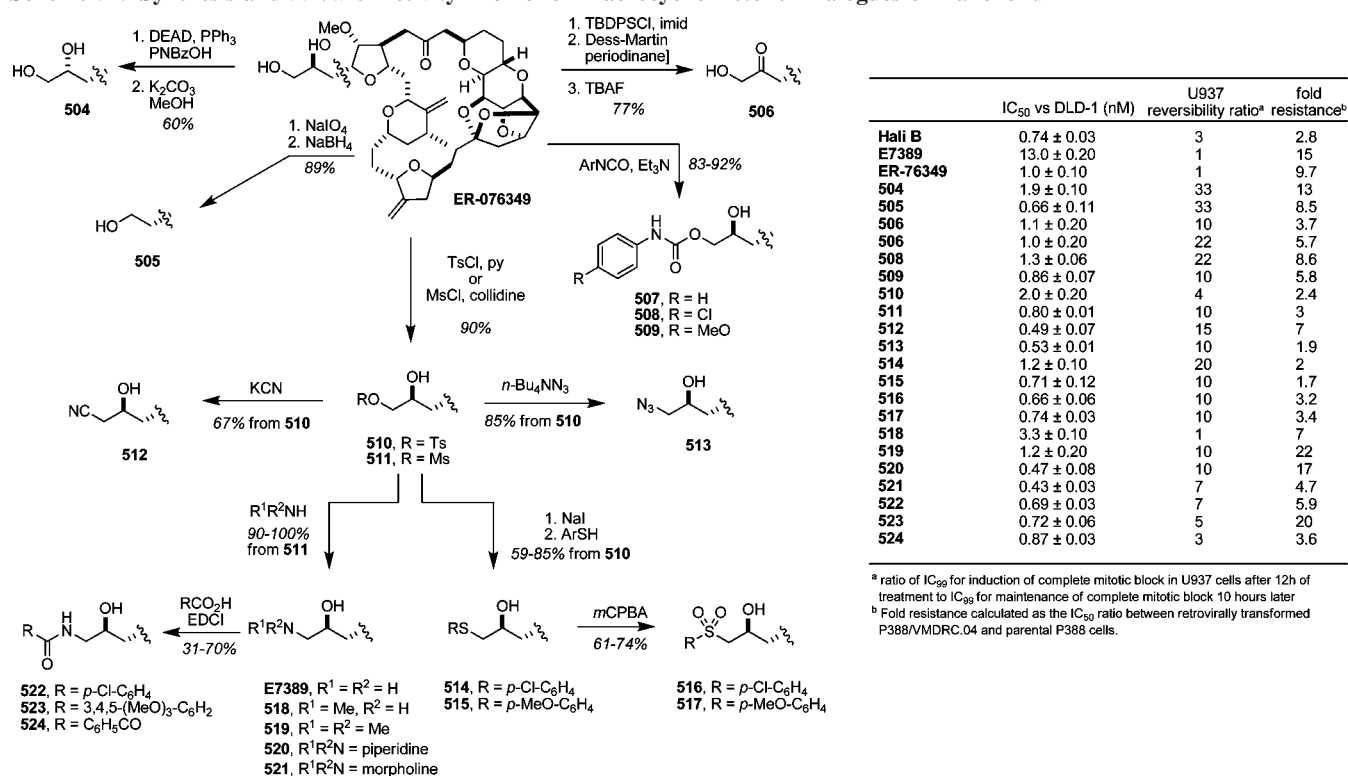
Nozaki–Hiyama–Kishi coupling of aldehyde **493** with vinyl iodide **25** and subsequent base-induced cyclization provided a 3:1 mixture of C27 diastereomers favoring the desired product (Scheme 50). The PMB ether was then removed to yield **500**, at which point the diastereomers were separable. Alcohol **500** was converted to sulfone **501** in a four-step protocol, and subsequent reaction of lithiated **501** with aldehyde **491** and oxidation gave **502**. Samarium(II) iodide was then used to mediate desulfonation, and a Nozaki–Hiyama–Kishi macrocyclization and subsequent allylic alcohol oxidation gave enone **503**. Lastly, exposure of **503** to TBAF buffered with imidazole hydrochloride and then PPTS provided the ER-076349. The synthesis is approximately 35 steps longest linear sequence from commercial materials, and its use to prepare material for preclinical, and possibly clinical, use stands as testament to the power of organic synthesis and the talents of scientists at the Eisai Research Institute.

With ER-076349 in hand, the C34/C35 vicinal diol was used as a handle for subsequent derivatization. As shown in Scheme 51, an array of analogues were synthesized using standard transformations.

Each of the compounds shown in Scheme 51 was evaluated for (i) cell growth inhibitory activity against DLD-1 human colon cancer cells under continuous exposure conditions, (ii) the ability to maintain a complete mitotic block 10 h after drug washout, and (iii) susceptibility to P-glycoprotein mediated drug efflux using murine P388/VMDRC.04 cells. As can be seen, the compounds in this



## Scheme 50. Completion of the Synthesis of ER-076349

Scheme 51. Synthesis and *in Vitro* Activity Profile for Macrocyclic Ketone Analogues of Halichondrin B

series displayed almost uniformly excellent activity and, in many cases, displayed single-digit reversibility ratios. All substrates were subject to P-glycoprotein mediated drug efflux, although in some cases the fold resistance was only on the order of 2-fold. On the basis of a combination of favorable features, E7389 was selected for development as a potential anticancer chemotherapeutic agent, with the name eribulin (or eribulin mesylate for the corresponding methanesulfonate salt).<sup>121</sup>

## 8.3. Preclinical Development

As was noted in the previous section, eribulin displayed good potency, and when compared with ER-076349, vincristine, and paclitaxel for antiproliferative activity against eight cell lines, an average IC<sub>50</sub> value of 1.8 ± 1.1 nM was

obtained. This compared very favorably with ER-076349 (IC<sub>50</sub> = 0.45 ± 0.09 nM) and was more potent than vincristine and paclitaxel (IC<sub>50</sub> = 3.2 ± 0.7 and 7.3 ± 1.9 nM, respectively). A number of mouse xenograft models and dosing were used to evaluate eribulin's efficacy, and highly encouraging results were obtained. In MDA-MB-435 xenograft studies, treatment led to tumor regression with no evidence of toxicity based on body weight loss or water consumption. Dosing regimens at 0.25, 0.5, and 1 mg/kg were all either equally efficacious or superior to paclitaxel (dosed at the maximal tolerated dose of 25 mg/kg). Similar results were obtained with COLO 205 colon carcinoma, LOX melanoma, and NIH:OVCAR-3 ovarian cancer xenografts.<sup>119</sup> Toxicity studies *in vitro* showed no cytotoxicity at 1 μM eribulin in quiescent IMR-90 human fibroblasts.

The mode of action of eribulin has also been studied. Treatment of U937 human histiocytic lymphoma cells with eribulin resulted in arrest of cells in the G2/M phase. There were no effects on cells in the G1 and S phases, and cells in these phases became progressively depleted upon prolonged exposure to eribulin. There was marked mitotic spindle disruption, and a biotinylated compound related to eribulin was used to demonstrate that tubulin binding occurs.<sup>119</sup> In more recent studies, the exact nature of the interaction with tubulin has been further investigated.<sup>122</sup> Eribulin neither destabilizes nor shortens microtubules. It acts by blocking microtubule growth, which results in G2/M arrest because the microtubules are not long enough to reach the kinetochores. Molecular modeling suggests that eribulin binds in a cleft between the  $\alpha$ -subunit and  $\beta$ -subunit of tubulin, and it is thought that this blocks or slows nucleotide growth.

#### 8.4. Progress toward the Clinic: Current Status of E7389

The first trial of eribulin in humans was with 40 patients with refractory or advanced solid tumors. Eribulin was administered intravenously at 0.25–2/mg<sup>2</sup> on days 1, 7, and 15 of a 28-day cycle. Among these patients, two showed partial responses, three had mixed response, and 12 had stable disease for a median 4 month period. Similar data was obtained in several other phase I trials. Initial phase II clinical trials for breast cancer and non-small-cell lung cancer (NSCLC) involved a large subject group (~100 each), and the overall response rate for breast cancer was 15%. The NSCLC group had a slightly lowered response rates (~10%). A number of patients suffered neutropenia and fatigue, and ~40% complained of peripheral neuropathy, all common side effects with tubulin-active agents. Recently, eribulin has demonstrated activity in a heavily pretreated population of women with locally advanced or metastatic breast cancer. Subjects had received an anthracycline, a taxane, and capecitabine as prior therapy and were refractory to their last chemotherapy regimen. The overall response rate was 10–15%, and there were manageable peripheral neuropathy symptoms. Both the preclinical and clinical features of E7389 have been recently reviewed in detail.<sup>123</sup>

In light of these encouraging trials, further phase II and phase III clinical trials are ongoing in Europe, Japan, and the USA. Eisai has indicated that it plans to file an NDA with the FDA for eribulin as third-line treatment for breast cancer in 2009–2010.<sup>124</sup>

#### 9. Concluding Comments

The efforts invested early on in the halichondrin story by the isolation and structure elucidation groups of Uemura, Pettit and Blunt, and Munro provided the impetus for synthetic studies. In arguably the most high profile example of the power of contemporary organic synthesis to provide a remarkably complex natural product for further study, the Kishi group's commitment to the problem of the total synthesis of the halichondrins then provided material that has allowed the E7389 story to unfold to the point where there is realistic potential for clinical application. As a final concluding comment, we would note that despite the discovery and synthesis of a number of simplified analogues, most notably E7389, synthetic studies aimed at the synthesis of the halichondrins and halichondrin subunits remain an important goal for contemporary synthesis. Aside from

opportunities to develop new methods and strategies, synthesis remains the only viable method for the supply of these compounds, and developments in the synthesis arena will undoubtedly impact the future biology and medicine of these important molecules.

#### 10. References

- (1) Norcross, R. D.; Paterson, I. *Chem. Rev.* **1995**, *95*, 2041.
- (2) Hart, J. B.; Lill, R. E.; Hickford, S. J. H.; Blunt, J. W.; Munro, M. H. G. *Drugs Sea* **2000**, 134.
- (3) Yu, M. J.; Kishi, Y.; Littlefield, B. A. In *Anticancer Agents from Natural Products*; Cragg, G. M., Kingston, D. G. I., Newman, D. J., Eds.; CRC Press: Boca Raton, FL, 2005.
- (4) Choi, H.-W.; Demeke, D.; Kang, F.-A.; Kishi, Y.; Nakajima, K.; Nowak, P.; Wan, Z.-K.; Xie, C. *Pure Appl. Chem.* **2003**, *75*, 1.
- (5) Tachibana, K.; Scheuer, P. J.; Tsukitani, Y.; Kikuchi, H.; Van Engen, D.; Clardy, J.; Gopichand, Y.; Schmitz, F. J. *J. Am. Chem. Soc.* **1981**, *103*, 2469.
- (6) Murakami, Y.; Oshima, Y.; Yasumoto, T. *Nippon Suisan Gakkaishi* **1982**, *48*, 69.
- (7) Uemura, D.; Takahashi, K.; Yamamoto, T.; Katayama, C.; Tanaka, J.; Okumura, Y.; Hirata, Y. *J. Am. Chem. Soc.* **1985**, *107*, 4796.
- (8) Hirata, Y.; Uemura, D. *Pure Appl. Chem.* **1986**, *58*, 701.
- (9) (a) Munro, M. H. G.; Blunt, J. W. Personal communication. (b) Lake, R. J. Internal Report, University of Canterbury, February 26, 1988.
- (10) Litaudon, M.; Hart, J. B.; Blunt, J. W.; Lake, R. J.; Munro, M. H. G. *Tetrahedron Lett.* **1994**, *35*, 9435.
- (11) (a) Litaudon, M.; Hickford, S. J. H.; Lill, R. E.; Lake, R. J.; Blunt, J. W.; Munro, M. H. G. *J. Org. Chem.* **1997**, *62*, 1868. (b) Blunt and Munro have also described 53-methoxyneoisohomohalichondrin B, which has been observed to convert to isohomohalichondrin B in solution in an NMR tube, presumably via acetal hydrolysis. They have suggested that it is an artifact of isolation. See ref 2.
- (12) Pettit, G. R.; Herald, C. L.; Boyd, M. R.; Leet, J. E.; Dufresne, C.; Doubek, D. L.; Schmidt, J. M.; Cerny, R. L.; Hooper, J. N. A.; Rutzler, K. C. *J. Med. Chem.* **1991**, *34*, 3339.
- (13) (a) Pettit, G. R.; Tan, R.; Gao, F.; Williams, M. D.; Doubek, D. L.; Boyd, M. R.; Schmidt, J. M.; Chapuis, J. C.; Hamel, E.; Bai, R.; Hooper, J. N. A.; Tackett, L. P. *J. Org. Chem.* **1993**, *58*, 2538. (b) Pettit, G. R.; Gao, F.; Doubek, D. L.; Boyd, M. R.; Hamel, E.; Bai, R.; Schmidt, J. M.; Tackett, L. P.; Rutzler, K. *Gazz. Chim. Ital.* **1993**, *123*, 371. (c) Pettit, G. R.; Ichihara, Y.; Wurzel, G.; Williams, M. D.; Schmidt, J. M.; Chapuis, J.-C. *J. Chem. Soc., Chem. Commun.* **1995**, 3, 383.
- (14) Bai, R.; Paull, K. D.; Herald, C. L.; Malspeis, L.; Pettit, G. R.; Hamel, E. *J. Biol. Chem.* **1991**, *266*, 15882.
- (15) Munro, M. H. G.; Blunt, J. W.; Dumdei, E. J.; Hickford, S. J. H.; Lill, R. E.; Li, S.; Battershill, C. N.; Duckworth, A. R. *Prog. Ind. Microbiol.* **1999**, *35*, 155.
- (16) Aicher, T. D.; Buszek, K. R.; Fang, F. G.; Forsyth, C. J.; Jung, S. H.; Kishi, Y.; Matelich, M. C.; Scola, P. M.; Spero, D. M.; Yoon, S. K. *J. Am. Chem. Soc.* **1992**, *114*, 3162.
- (17) Takai, K.; Kimura, K.; Kuroda, T.; Hiyama, T.; Nozaki, H. *Tetrahedron Lett.* **1983**, *24*, 5281.
- (18) (a) Jin, H.; Uenishi, J.; Christ, W. J.; Kishi, Y. *J. Am. Chem. Soc.* **1986**, *108*, 5644. (b) Kishi, Y. *Pure Appl. Chem.* **1992**, *64*, 343.
- (19) Aicher, T. D.; Kishi, Y. *Tetrahedron Lett.* **1987**, *28*, 3463.
- (20) (a) Omura, K.; Sharma, A. K.; Swern, D. *J. Org. Chem.* **1976**, *41*, 957. (b) Omura, K.; Swern, D. *Tetrahedron* **1978**, *34*, 1651.
- (21) Mancuso, A. J.; Huang, S.-L.; Swern, D. *J. Org. Chem.* **1978**, *43*, 2480.
- (22) Stamos, D. P. Studies towards a practical synthesis of the c.1-c.38 segment of halichondrin b (stereodifferentiation), Ph.D. Thesis, Harvard University, Cambridge, MA, 1997.
- (23) (a) Dess, D. B.; Martin, J. C. *J. Org. Chem.* **1983**, *48*, 4155. (b) Dess, D. B.; Martin, J. C. *J. Am. Chem. Soc.* **1991**, *113*, 7277.
- (24) Mahoney, W. S.; Brestensky, D. M.; Stryker, J. M. *J. Am. Chem. Soc.* **1988**, *110*, 291.
- (25) Aicher, T. D.; Buszek, K. R.; Fang, F. G.; Forsyth, C. J.; Jung, S. H.; Kishi, Y.; Scola, P. M. *Tetrahedron Lett.* **1992**, *33*, 1549.
- (26) Buszek, K. R.; Fang, F. G.; Forsyth, C. J.; Jung, S. H.; Kishi, Y.; Scola, P. M.; Yoon, S. K. *Tetrahedron Lett.* **1992**, *33*, 1553.
- (27) Vekemans, J. A. J. M.; Boerekamp, J.; Godefroi, E. F.; Chittenden, G. J. *F. Recl. Trav. Chim. Pays-Bas* **1986**, *104*, 266.
- (28) Yamaguchi, M.; Hirao, I. *Tetrahedron Lett.* **1983**, *24*, 391.
- (29) (a) Sharpless, K. B.; Michaelson, R. C. *J. Am. Chem. Soc.* **1973**, *95*, 6136. (b) Tanaka, S.; Yamamoto, H.; Nozaki, H.; Sharpless, K. B.; Michaelson, R. C.; Cutting, J. D. *J. Am. Chem. Soc.* **1974**, *96*, 5254.
- (30) Fang, F. G.; Kishi, Y.; Matelich, M. C.; Scola, P. M. *Tetrahedron Lett.* **1992**, *33*, 1557.

- (31) Oikawa, Y.; Yoshioka, T.; Yonemitsu, O. *Tetrahedron Lett.* **1982**, *23*, 885.
- (32) Inanaga, J.; Hirata, K.; Saeki, H.; Katsuki, T.; Yamaguchi, M. *Bull. Chem. Soc. Jpn.* **1979**, *52*, 1989.
- (33) Duan, J. J.; Kishi, Y. *Tetrahedron Lett.* **1993**, *34*, 7541.
- (34) Corey, E. J.; Suggs, J. W. *Tetrahedron Lett.* **1975**, *16*, 2647.
- (35) Stamos, D. P.; Kishi, Y. *Tetrahedron Lett.* **1996**, *37*, 8643.
- (36) Kolb, H. C.; VanNieuwenhze, M. S.; Sharpless, K. B. *Chem. Rev.* **1994**, *94*, 2483.
- (37) Stamos, D. P.; Sheng, C.; Chen, S. S.; Kishi, Y. *Tetrahedron Lett.* **1997**, *38*, 6355.
- (38) Stamos, D. P.; Chen, S. S.; Kishi, Y. *J. Org. Chem.* **1997**, *62*, 7552.
- (39) Blanchette, M. A.; Choy, W.; Davis, J. T.; Essensfeld, A. P.; Masamune, S.; Roush, W. R.; Sakai, T. *Tetrahedron Lett.* **1984**, *25*, 2183.
- (40) (a) Itsuno, S.; Nakano, M.; Miyazaki, K.; Masuda, H.; Ito, K.; Hirao, A.; Nakahama, S. *J. Chem. Soc., Perkin Trans. 1* **1985**, *10*, 2039. (b) Corey, E. J.; Bakshi, R. K.; Shibata, S.; Chen, C. P.; Singh, V. K. *J. Am. Chem. Soc.* **1987**, *109*, 7925. (c) Corey, E. J.; Bakshi, R. K.; Shibata, S. *J. Am. Chem. Soc.* **1987**, *109*, 5551.
- (41) (a) Fuerstner, A.; Shi, N. *J. Am. Chem. Soc.* **1996**, *118*, 12349. (b) Fuerstner, A.; Shi, N. *J. Am. Chem. Soc.* **1996**, *118*, 2533.
- (42) Namba, K.; Jun, H.-S.; Kishi, Y. *J. Am. Chem. Soc.* **2004**, *126*, 7770.
- (43) Kaburagi, Y.; Kishi, Y. *Org. Lett.* **2007**, *9*, 723.
- (44) (a) Namba, K.; Kishi, Y. *J. Am. Chem. Soc.* **2005**, *127*, 15382. (b) Choi, H.-w.; Nakajima, K.; Demeke, D.; Kang, F.-A.; Jun, H.-S.; Wan, Z.-K.; Kishi, Y. *Org. Lett.* **2002**, *4*, 4435. (c) Wan, Z.-K.; Choi, H.-w.; Kang, F.-A.; Nakajima, K.; Demeke, D.; Kishi, Y. *Org. Lett.* **2002**, *4*, 4431. (d) Zhang, Z.; Huang, J.; Ma, B.; Kishi, Y. *Org. Lett.* **2008**, *10*, 3073. (e) Namba, K.; Cui, S.; Wang, J.; Kishi, Y. *Org. Lett.* **2005**, *7*, 5417. (f) Namba, K.; Kishi, Y. *Org. Lett.* **2004**, *6*, 5031. (g) Kurosu, M.; Lin, M.-H.; Kishi, Y. *J. Am. Chem. Soc.* **2004**, *126*, 12248. (h) Namba, K.; Wang, J.; Cui, S.; Kishi, Y. *Org. Lett.* **2005**, *7*, 5421.
- (45) Jackson, K. L.; Henderson, J. A.; Motoyoshi, H.; Phillips, A. J. *Angew. Chem., Int. Ed.* **2009**, *48*, 2346.
- (46) Davies, H. M. L.; Ahmed, G.; Churchill, M. R. *J. Am. Chem. Soc.* **1996**, *118*, 10774.
- (47) Scholl, M.; Ding, S.; Lee, C. W.; Grubbs, R. H. *Org. Lett.* **1999**, *1*, 953.
- (48) Jackson, K. L.; Henderson, J. A.; Morris, J. C.; Motoyoshi, H.; Phillips, A. J. *Tetrahedron Lett.* **2008**, *49*, 2939.
- (49) Kobayashi, Y.; Kusakabe, M.; Kitano, Y.; Sato, F. *J. Org. Chem.* **1988**, *53*, 1586.
- (50) Grieco, P. A.; Oguri, T.; Yokoyama, Y. *Tetrahedron Lett.* **1978**, *19*, 419.
- (51) (a) Roskamp, E. J.; Johnson, C. R. *J. Am. Chem. Soc.* **1986**, *108*, 6062. (b) Pirrung, M. C.; Werner, J. A. *J. Am. Chem. Soc.* **1986**, *108*, 6060.
- (52) Namba, K.; Kishi, Y. *Org. Lett.* **2004**, *6*, 5031.
- (53) Henderson, J. A.; Jackson, K. L.; Phillips, A. J. *Org. Lett.* **2007**, *9*, 5299.
- (54) Ho, T.-L.; Sapp, S. G. *Synth. Commun.* **1983**, *13*, 267.
- (55) Um, J. M.; Houk, K. N.; Phillips, A. J. *Org. Lett.* **2008**, *10*, 3769.
- (56) Aicher, T. D.; Buszek, K. R.; Fang, F. G.; Forsyth, C. J.; Jung, S. H.; Kishi, Y.; Matelich, M. C.; Scolia, P. M.; Spero, D. M.; Yoon, S. K. *J. Am. Chem. Soc.* **1992**, *114*, 3162.
- (57) Stewart, I. C.; Douglas, C. J.; Grubbs, R. H. *Org. Lett.* **2008**, *10*, 441.
- (58) Kaburagi, Y.; Kishi, Y. *Org. Lett.* **2007**, *9*, 723.
- (59) Holmquist, C. R.; Roskamp, E. J. *Tetrahedron Lett.* **1992**, *33*, 1131.
- (60) Horita, K.; Hachiya, S.; Nagasawa, M.; Hikota, M.; Yonemitsu, O. *Synlett* **1994**, *1*, 38.
- (61) Roush, W. R.; Brown, R. J. *J. Org. Chem.* **1982**, *47*, 1371.
- (62) Horita, K.; Hachiya, S.-I.; Yamazaki, T.; Naitou, T.; Uenishi, J. i.; Yonemitsu, O. *Chem. Pharm. Bull.* **1997**, *45*, 1265.
- (63) Horita, K.; Nagasawa, M.; Hachiya, S.; Yonemitsu, O. *Synlett* **1994**, *1*, 40.
- (64) Horita, K.; Nagasawa, M.; Sakurai, Y.; Yonemitsu, O. *Chem. Pharm. Bull.* **1998**, *46*, 1199.
- (65) (a) Saito, S.; Ishikawa, T.; Kuroda, A.; Koga, K.; Moriwake, T. *Tetrahedron* **1992**, *48*, 4067. (b) Saito, S.; Hasegawa, T.; Inaba, M.; Nishida, R.; Fujii, T.; Nomizu, S.; Moriwake, T. *Chem. Lett.* **1984**, *8*, 1389.
- (66) Mori, Y.; Kuhara, M.; Takeuchi, A.; Suzuki, M. *Tetrahedron Lett.* **1988**, *29*, 5419.
- (67) Horita, K.; Sakurai, Y.; Nagasawa, M.; Hachiya, S.; Yonemitsu, O. *Synlett* **1994**, *1*, 43.
- (68) Horita, K.; Sakurai, Y.; Nagasawa, M.; Yonemitsu, O. *Chem. Pharm. Bull.* **1997**, *45*, 1558.
- (69) Horita, K.; Sakurai, Y.; Hachiya, S.-i.; Nagasawa, M.; Yonemitsu, O. *Chem. Pharm. Bull.* **1994**, *42*, 683.
- (70) Still, W. C.; Gennari, C. *Tetrahedron Lett.* **1983**, *24*, 4405.
- (71) Christensen, B. G.; Strachan, R. G.; Trenner, N. R.; Arison, B. H.; Hirschmann, R. F.; Chemerda, J. M. *J. Am. Chem. Soc.* **1960**, *82*, 3995.
- (72) (a) Lewis, M. D.; Cha, J. K.; Kishi, Y. *J. Am. Chem. Soc.* **1982**, *104*, 4976. (b) Kozikowski, A. P.; Sorgi, K. L.; Wang, B. C.; Xu, Z. B. *Tetrahedron Lett.* **1983**, *24*, 1563. (c) Hosomi, A.; Sakata, Y.; Sakurai, H. *Tetrahedron Lett.* **1984**, *25*, 2383. (d) Giannis, A.; Sandhoff, K. *Tetrahedron Lett.* **1985**, *26*, 1479.
- (73) Horita, K.; Nishibe, S.; Yonemitsu, O. *Phytochem. Phytopharm.* **2000**, *386*.
- (74) Horita, K.; Sakurai, Y.; Nagasawa, M.; Maeno, K.; Hachiya, S.; Yonemitsu, O. *Synlett* **1994**, *1*, 46.
- (75) Horita, K.; Hachiya, S.-i.; Ogihara, K.; Yoshida, Y.; Nagasawa, M.; Yonemitsu, O. *Heterocycles* **1996**, *42*, 99.
- (76) Hanessian, S.; Sumi, K. *Synthesis* **1991**, *12*, 1083.
- (77) Chen, K. M.; Hardtmann, G. E.; Prasad, K.; Repic, O.; Shapiro, M. J. *Tetrahedron Lett.* **1987**, *28*, 155.
- (78) Horita, K.; Nagasawa, M.; Hachiya, S.-I.; Sakurai, Y.; Yamazaki, T.; Uenishi, J. i.; Yonemitsu, O. *Tetrahedron Lett.* **1997**, *38*, 8965.
- (79) (a) Lindgren, B. O.; Nilsson, T. *Acta Chem. Scand.* **1973**, *27*, 888. (b) Bal, B. S.; Childers, W. E., Jr.; Pinnick, H. W. *Tetrahedron* **1981**, *37*, 2091.
- (80) Horita, K.; Hachiya, S.-i.; Ogihara, K.; Yoshida, Y.; Nagasawa, M.; Yonemitsu, O. *Heterocycles* **1996**, *42*, 99.
- (81) Cooper, A. J.; Salomon, R. G. *Tetrahedron Lett.* **1990**, *31*, 3813.
- (82) (a) Jacobsen, E. N.; Marko, I.; Mungall, W. S.; Schroeder, G.; Sharpless, K. B. *J. Am. Chem. Soc.* **1988**, *110*, 1968. (b) Wai, J. S. M.; Marko, I.; Svendsen, J. S.; Finn, M. G.; Jacobsen, E. N.; Sharpless, K. B. *J. Am. Chem. Soc.* **1989**, *111*, 1123.
- (83) (a) Gao, Y.; Sharpless, K. B. *J. Am. Chem. Soc.* **1988**, *110*, 7538. (b) Kim, B. M.; Sharpless, K. B. *Tetrahedron Lett.* **1989**, *30*, 655.
- (84) Mukaiyama, T.; Kobayashi, S.; Shoda, S. *Chem. Lett.* **1984**, *9*, 1529.
- (85) Cooper, A. J.; Pan, W.; Salomon, R. G. *Tetrahedron Lett.* **1993**, *34*, 8193.
- (86) Barton, D. H. R.; McCombie, S. W. *J. Chem. Soc., Perkin Trans 1* **1975**, *16*, 1574.
- (87) Kim, S.; Salomon, R. G. *Tetrahedron Lett.* **1989**, *30*, 6279.
- (88) DiFranco, E.; Ravikumar, V. T.; Salomon, R. G. *Tetrahedron Lett.* **1993**, *34*, 3247.
- (89) Matsuzawa, S.; Horiguchi, Y.; Nakamura, E.; Kuwajima, I. *Tetrahedron* **1989**, *45*, 349.
- (90) (a) Burke, S. D.; Jung, K. W.; Phillips, J. R.; Perri, R. E. *Tetrahedron Lett.* **1994**, *35*, 703. (b) Burke, S. D.; Jung, K. W.; Lambert, W. T.; Phillips, J. R.; Klovning, J. J. *J. Org. Chem.* **2000**, *65*, 4070.
- (91) Masamune, S.; Ma, P.; Okumoto, H.; Ellingboe, J. W.; Ito, Y. *J. Org. Chem.* **1984**, *49*, 2834.
- (92) (a) Shing, T. K. M.; Tsui, H. C.; Zhou, Z. H.; Mak, T. C. W. *J. Chem. Soc., Perkin Trans. 1* **1992**, *7*, 887. (b) Shing, T. K. M.; Tsui, H. C.; Zhou, Z. H. *J. Chem. Soc., Chem. Commun.* **1992**, *11*, 810.
- (93) Iida, H.; Yamazaki, N.; Kibayashi, C. *J. Org. Chem.* **1986**, *51*, 3769.
- (94) For related examples see: (a) Gilchrist, T. L.; Stanford, J. E. *J. Chem. Soc., Perkin Trans. 1* **1987**, *1*, 225. (b) Schoenen, F. J.; Porco, J. A., Jr.; Schreiber, S. L.; VanDuyne, G. D.; Clardy, J. *Tetrahedron Lett.* **1989**, *30*, 3765. (c) Sisti, A. J.; Vitale, A. C. *J. Org. Chem.* **1972**, *37*, 4090.
- (95) Lambert, W. T.; Burke, S. D. *Org. Lett.* **2003**, *5*, 515.
- (96) (a) Criegee, R.; Banciu, A.; Keul, H. *Chem. Ber.* **1975**, *108*, 1642. (b) Schreiber, S. L.; Claus, R. E.; Reagan, J. *Tetrahedron Lett.* **1982**, *23*, 3867.
- (97) Rodriguez, A.; Nomen, M.; Spur, B. W.; Godfroid, J. J. *Tetrahedron Lett.* **1999**, *40*, 5161.
- (98) Jiang, L.; Burke, S. D. *Org. Lett.* **2002**, *4*, 3411.
- (99) Trost, B. M.; Van Vranken, D. L. *Angew. Chem., Int. Ed. Engl.* **1992**, *31*, 228.
- (100) Baudry, D.; Ephritikhine, M.; Felkin, H. *Nouv. J. Chim.* **1978**, *2*, 355.
- (101) Jiang, L.; Martinelli, J. R.; Burke, S. D. *J. Org. Chem.* **2003**, *68*, 1150.
- (102) Burke, S. D.; Buchanan, J. L.; Rovin, J. D. *Tetrahedron Lett.* **1991**, *32*, 3961.
- (103) Gao, Y.; Klunder, J. M.; Hanson, R. M.; Masamune, H.; Ko, S. Y.; Sharpless, K. B. *J. Am. Chem. Soc.* **1987**, *109*, 5765.
- (104) Burke, S. D.; Zhang, G.; Buchanan, J. L. *Tetrahedron Lett.* **1995**, *36*, 7023.
- (105) Steglich, W.; Hoefle, G. *Angew. Chem., Int. Ed. Engl.* **1969**, *8*, 981.
- (106) Broekema, R. *J. Recl. Trav. Chim. Pay-Bas.* **1975**, *94*, 209.
- (107) Fuji, K.; Kawabata, T.; Kujita, E. *Chem. Pharm. Bull.* **1980**, *28*, 3662.
- (108) Ito, Y.; Hirao, T.; Saegusa, T. *J. Org. Chem.* **1978**, *43*, 1011.
- (109) Burke, S. D.; Quinn, K. J.; Chen, V. J. *J. Org. Chem.* **1998**, *63*, 8626.
- (110) Evans, D. A.; Ennis, M. D.; Mathre, D. J. *J. Am. Chem. Soc.* **1982**, *104*, 1737.
- (111) Keller, V. A.; Kim, I.; Burke, S. D. *Org. Lett.* **2005**, *7*, 737.

- (112) Cha, J. K.; Christ, W. J.; Kishi, Y. *Tetrahedron* **1984**, *40*, 2247.
- (113) Burke, S. D.; Austad, B. C.; Hart, A. C. *J. Org. Chem.* **1998**, *63*, 6770.
- (114) Austad, B. C.; Hart, A. C.; Burke, S. D. *Tetrahedron* **2002**, *58*, 2011.
- (115) Krapcho, A. P.; Weimaster, J. F. *J. Org. Chem.* **1980**, *45*, 4105.
- (116) Lambert, W. T.; Hanson, G. H.; Benayoud, F.; Burke, S. D. *J. Org. Chem.* **2005**, *70*, 9382.
- (117) Kishi, Y.; Fang, F. G.; Forsyth, C. J.; Scola, P. M.; Yoon, S. K. Halichondrins and related compounds, US Patent, 5,338,865, 1995.
- (118) Wang, Y.; Habgood, G. J.; Christ, W. J.; Kishi, Y.; Littlefield, B. A.; Yu, M. J. *Bioorg. Med. Chem. Lett.* **2000**, *10*, 1029.
- (119) Seletsky, B. M.; Wang, Y.; Hawkins, L. D.; Palme, M. H.; Habgood, G. J.; DiPietro, L. V.; Towle, M. J.; Salvato, K. A.; Wels, B. F.; Aalfs, K. K.; Kishi, Y.; Littlefield, B. A.; Yu, M. J. *Bioorg. Med. Chem. Lett.* **2004**, *14*, 5547.
- (120) Towle, M. J.; Salvato, K. A.; Budrow, J.; Wels, B. F.; Kuznetsov, G.; Aalfs, K. K.; Welsh, S.; Zheng, W.; Seletsky, B. M.; Palme, M. H.; Habgood, G. J.; Singer, L. A.; DiPietro, L. V.; Wang, Y.; Chen, J. J.; Quincy, D. A.; Davis, A.; Yoshimatsu, K.; Kishi, Y.; Yu, M. J.; Littlefield, B. A. *Cancer Res.* **2001**, *61*, 1013.
- (121) Kishi has recently described a study aimed towards selective aminolysis of oxiranes in the context of E7389 synthesis: Kaburagi, Y.; Kishi, Y. *Tetrahedron Lett.* **2007**, *48*, 8967.
- (122) Dabydeen, D. A.; Burnett, J. C.; Bai, R.; Verdier-Pinard, P.; Hickford, S. J. H.; Pettit, G. R.; Blunt, J. W.; Munro, M. H. G.; Gussio, R.; Hamel, E. *Mol. Pharmacol.* **2006**, *70*, 1866.
- (123) Newman, S. *Curr. Opin. Invest. Drugs* **2007**, *8*, 1057.
- (124) <http://www.reuters.com/article/pressRelease/idUS55316+01-Feb-2008+PRN20080201>. Retrieved May 12, 2009.

CR900016W